EDITORS:
T.J. SULLIVAN, M.J.N. PRIESTLEY,
G.M. CALVI

A Model Code for the Displacement-Based Seismic Design of Structures

DBD12

This publication has been developed to provide guidance as to how the direct displacement-based design methodology can be codified. It is intended for insertion within the seismic requirements of a code, establishing how design forces can be obtained using a Direct Displacement-Based Design (DDBD) approach. The document has currently been prepared with reference to several clauses of Eurocode 8. This document is presented in a traditional "Code + Commentary" format, on a split two-column page. The commentary aims to generally clarify the code requirements and indicate references where the background and further discussion on the requirements can be found.

The document is a revised version of the draft model code DBD09. The bulk of the text and requirements in this code have been developed from the recommendations provided in the book on DDBD by Priestley et al. (2007) and from research carried out following that publication, including developments made by Linea IV of the RELUIS project (www.reluis.it).

Currently the model code has been prepared for a wide range of building structures and bridges. However, the model code does not yet cover all structural systems and materials. In addition, a number of novel recommendations have been proposed that are preliminary in nature because of the limited amount of experimental or analytical data on which they are based. Future versions of this document will therefore look to refine the current recommendations and extend the guidelines to encompass a more complete range of structural systems.
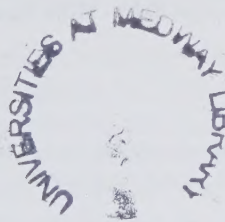
A Model Code for the Displacement-Based Seismic Design of Structures
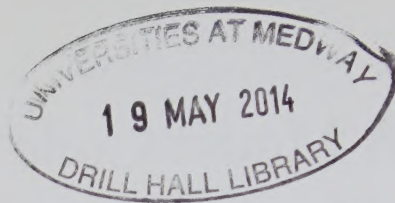
DBD12

(SUPERSEEDS THE DRAFT MODEL CODE DBD09)

Editors: T.J. Sullivan, M.J.N. Priestley, G.M. Calvi

April, 2012

PREFACE

This model code is designed to provide guidance as to how the direct displacement-based design methodology can be codified. It is intended for insertion within the seismic requirements of a code, establishing how design forces can be obtained using a Direct Displacement-Based Design (**DDBD**) approach. The document has currently been drafted with reference to several clauses of Eurocode 8. The text is presented in a traditional "Code + Commentary" format, on a split two-column page. The commentary aims to generally clarify the code requirements and indicate references where the background and further discussion on the requirements can be found.

This document is a revised version of DBD09, the draft model code for displacement-based design issued for public enquiry in May 2009. The bulk of the text and requirements in this code have been developed from the recommendations provided in the book on DDBD by Priestley et al. (2007) and from the work carried out by the various research units of a 3-year Italian research initiative into the displacement-based design and assessment of structures as part of the RELUIS (*Rete dei Laboratori Universitari di Ingegneria Sismica*) project (research line IV). The revisions included in this version of the model code include the reorganisation of the clauses into what we trust is a more suitable order, the insertion of more figures aimed at clarifying the code requirements, the modification of some clauses and equations in the light of recent research findings, and the correction of minor typos in the text and equations.

In this revised version of the model code two different expressions are proposed for the scaling of elastic displacement spectra for different levels of elastic damping. The first (Eq.1.2) corresponds to that included in the draft version of the Eurocode 8, whereas the second (Eq.1.4a) is in the current version of the Eurocode 8 and was also included in the draft version of this model code. The reason that the older damping reduction expression has been re-introduced in this version of the model code is that a given equivalent viscous damping expression (see Section 7) should be used in conjunction with the damping modifier expression (Eq.1.2 or 1.4a) that best matches the characteristics of the ground motions used to develop the (calibrated) equivalent viscous damping expression. This finding has been made by Pennucci et al. (2011) and is discussed in more detail in Annex 2. The implication of this finding is that the two-step process of calculating first an equivalent viscous damping value and then a displacement reduction factor could be simplified and condensed into a single step in which effective-period inelastic displacement spectra are constructed as a function of ductility using displacement-

reductions factors. This possibility is discussed further in Pennucci et al. (2011). Future revisions of the model code may therefore move away from the equivalent viscous damping approach to a displacement reduction factor methodology. However, given that most engineers have become familiar with the equivalent viscous damping approach, this version of the model code has maintained the approach and has aimed to ensure that equivalent viscous damping expressions (Section 7) are paired with the correct damping modified expression (Section 1). Nevertheless, designers should be aware that future versions of the model code are likely to substitute the equivalent viscous damping approach with spectral displacement-reduction factors.

Currently the model code has been prepared for a specific range of building structures and bridges. Given the limited range of structures that could be considered to date, the model code does not yet cover all structural systems and materials. In addition, a number of recommendations have been proposed that are preliminary in nature because of the limited amount of experimental or analytical data on which they are based. Future versions of this document will look to refine the current recommendations and extend the guidelines to encompass a more complete range of structural systems.

With the above in mind, readers are kindly invited to send their suggestions for future editions of the model code to the editors at the address below. We thank you in advance for your contributions.

Tim Sullivan   Nigel Priestley   Gian Michele Calvi

C/O EUCENTRE: Via Ferrata 1, Pavia, 27100, Italy

Pavia, Italy, February 2012

CONTRIBUTORS

A large number of people have contributed to this work and their efforts are greatly appreciated. The editors wish to express their gratitude to all those people who provided feedback and editorial suggestions for improvement of the model code. Special thanks go to Alberto Lago for his careful proof-reading of the document. In addition, the editors thank the people listed below who either participated in Research Line IV of the RELUIS 2005-2008 project or provided contributions on the technical content of the Model Code:

Principles, General Aspects, Actions

Nigel Priestley	ROSE School, IUSS Pavia, Pavia, Italy
Gian Michele Calvi	IUSS Pavia, Pavia, Italy
Tim Sullivan	University of Pavia, Italy
Katrin Beyer	École polytechnique fédérale de Lausanne, Switzerland
Alberto Lago	ROSE School, IUSS Pavia, Pavia, Italy
Domenico Pennucci	ROSE School, IUSS Pavia, Pavia, Italy
Jorge Riviera	ROSE School, IUSS Pavia, Pavia, Italy

Design Seismicity

Enzo Faccioli	Politecnico di Milano, Italy
Roberto Paolucci	Politecnico di Milano, Italy
Carlo Cauzzi	Politecnico di Milano, Italy
Manuela Villani	ROSE School, IUSS Pavia, Pavia, Italy

RC Frame Structures

Andrea Benedetti	University of Bologna, Italy
Luca Landi	University of Bologna, Italy
Daniele Malavolta	University of Bologna, Italy

RC Wall and Frame-Wall Structures

Ferdinando Laudiero	University of Ferrara, Italy
Nerio Rullini	University of Ferrara, Italy
Michele Rizzato	University of Ferrara, Italy

Pre-Cast Concrete Structures

Paolo Riva	University of Bergamo, Italy
Andrea Belleri	University of Bergamo, Italy

Masonry Structures

Guido Magenes	University of Pavia, Italy
Andrea Penna	University of Pavia, Italy
Francesco Graziotti	University of Pavia, Italy
Luigi Gambarotta	University of Genova, Italy
Antonio Brencich	University of Genova, Italy

Steel Structures

Gaetano Della Corte	University of Napoli Federico II, Italy

Composite Steel-Concrete Structures

Luigi di Sarno	University of Napoli, Italy

Timber Structures

Paolo Zanon	University of Trento, Italy
Maurizio Piazza	University of Trento, Italy
Daniele Zonta	University of Trento, Italy
Cristiano Loss	University of Trento, Italy

Bridge Structures

Lorenza Petrini	Politecnico di Milano, Italy
Ricardo Alejandro Zapata Montoya	ROSE School, IUSS Pavia, Pavia, Italy
Oguz Bahadir Sadan	Politecnico di Milano, Italy
Juan Camilo Ortiz Restrepo	ROSE School, IUSS Pavia, Pavia, Italy
Adhikari Gopal	ROSE School, IUSS Pavia, Pavia, Italy
Claudio Maggi	(formerly) University of Pavia, Italy

Isolated Structures

Donatello Cardone	University of Basilicata, Italy
Mauro Dolce	Dipartimento della Protezione Civile, Italy
Giuseppe Palermo	University of Basilicata, Italy
Giuseppe Gesualdi	University of Basilicata, Italy

Foundation Structures

Roberto Paolucci	Politecnico di Milano, Italy
Claudio di Prisco	Politecnico di Milano, Italy
Mauro Vecchiotti	Politecnico di Milano, Italy
Raffaele Figini	Politecnico di Milano, Italy
Lorenza Petrini	Politecnico di Milano, Italy

Retaining Structures

Vincenzo Pane	University of Perugia, Italy
Manuela Cecconi	University of Perugia, Italy
Sara Vecchietti	University of Perugia, Italy

TABLE OF CONTENTS

NOMENCLATURE

The following nomenclature is used in this model code:

a	constant for steel brace ductility capacity from Tremblay (2002) model
a_t	constant used in the equivalent viscous damping evaluation of timber systems with annular bolted joints
A	member cross section area
A_{core}	cross section area of the core of a BRB
A_v	section shear area
b	constant for steel brace ductility capacity from Tremblay (2002) model
C	constant to account for P-delta effects when setting the design base shear strength
C_1	fixity coefficient 1 for a bridge pier
$C_{1,T}$	period dependent mid-height moment coefficient for cantilever walls
C_2	fixity coefficient 2 for a bridge pier
$C_{2,T}$	period dependent shear magnification constant for cantilever walls
C_3	fixity coefficient 3 for a bridge pier
$C_{3,T}$	period dependent shear magnification constant for cantilever walls of dual systems
$C_{d,i}$	viscous damper constant at level i (Eq.8.3)
C_F	floor restrain constant (Eq.C6.4)
C_P	pier fixity coefficient
d_{bl}	diameter of longitudinal reinforcement bars
d	embedment depth of a retaining wall
D_d	target displacement of isolation device/system
e	length of a steel link within an EBF structure
e_R	stiffness eccentricity relative to the direction of excitation (Eq.C5.2)
E	elastic modulus of the structural material
E_c	elastic modulus of concrete
E_s	elastic modulus of steel
EFA	expected floor acceleration at the development of peak storey drifts
f_y	characteristic yield stress of structural material
f_{ye}	expected yield stress of structural material
f_{yh}	yield stress of transverse confining reinforcement
f'_c	characteristic concrete compressive strength.
f'_{cc}	confined concrete compressive strength as per Mander (1988) model
f'_{ce}	expected concrete compressive strength
f'_m	characteristic masonry compressive strength
f'_{me}	expected masonry compressive strength
f_u	ultimate material strength
F_D	maximum force (occurring at zero displacement) expected in a viscous damper
F_{el}	elastic force in an isolation device at the design displacement
F_{FR}	friction force of sliding bearings at the design displacement
F_i	equivalent lateral design force at level i

F_s	force of the isolation system at the design displacement D_d
$F_{u,k}$	ultimate shear capacity of a single dowel in a bolted timber joint
F_v	shear flexibility coefficient for coupling beams
g	acceleration due to gravity
G	shear modulus of structural material
G/G_{max}	soil modulus ratio
h	excavation height of a retaining wall
h_1	height of level 1
h_b	depth of beam section
$h_{b,x}$	depth of beam section in bay x of a frame
h_{CB}	depth of coupling beam
h_{cp}	clear height of masonry pier
h_{col}	column height
h_i	height of level i
h_p	strain-hardening ratio of steel braces
h_s	storey height (distance between centres of consecutive floors)
H	total height of a retaining wall, including the buried portion of the wall
H_{cf}	height of contra-flexure in RC walls.
H/D	pier height to section depth ratio
H_e	effective height of the equivalent SDOF structure.
H_n	total building height
H_{pier}	height of bridge pier
I	second moment of inertia
I_{cr}	cracked second moment of inertia of a concrete section
I_{gr}	gross second moment of inertia of a concrete section
I_r	ratio between the isolation system effective period (T_{IS}) and the period (T_{fb}) of the structure without isolation (fixed base)
I_{deck}	second moment of inertia of the deck of a bridge
I_p	soil plasticity index (used in Fig.C7.6)
I_{pier}	second moment of inertia of the pier of a bridge
I_{ss}	second moment of inertia of the bridge superstructure (deck)
$J_{R,\mu}$	effective torsional stiffness defined (Eq.C5.3)
k	equivalent lateral force redistribution constant
k_c	normalized column strain
$k_{c,d}$	normalized column strain at the design state
$k_{c,y}$	normalized column strain at the yield state
k_{cr}	factor representing stiffness reduction due to cracking in the case of concrete floor systems
K_e	design effective stiffness of the equivalent SDOF system
$K_{e,max}$	maximum required effective stiffness of the equivalent SDOF system
k_{Xi}	elastic stiffness value of wall i in the global X direction (Section C5.8)
k_{Zi}	elastic stiffness value of wall i in the global Z direction (Section C5.8)
l	wall height used in evaluation of equivalent viscous damping of retaining wall systems
L_{br}	node-to-node length of a brace
L	length (span) of a portal frame structure
L_b	length of beams (between column centrelines) of a frame structure
$L_{b,x}$	length of beams (between column centrelines) of bay x of a frame structure
L_{CB}	length of coupling beam
L_{CBcc}	length of coupling beam measured between wall centres (see Fig.C6.4)
L_{core}	length of the core of a BRB
L_d	length of bridge deck between abutment points
L_e	effective length of a bracing element
L_{dia}	total length of floor diaphragm measured perpendicular to the direction of excitation

$L_{dia,c}$ maximum clear length of floor diaphragm segment between vertical lateral load resisting systems
L_i, A_i length and area of the i-th tapering of a BRB
L_p plastic hinge length
L_{sp} length of strain penetration
L_w length of structural wall
m_i seismic mass at point i in the structure
m_e effective mass of the equivalent SDOF system
$m_{as,i}$ mass of layer i of the active soil wedge of a soil retaining wall system
$m_{ps,i}$ mass of layer i of the passive soil wedge of a soil retaining wall system
$m_{w,i}$ mass of layer i of a soil retaining wall system
m_{xs} mass of the "x" ("active" or "passive") component of a soil retaining wall system
M_1 overturning resistance of structure 1 forming part of a combined structural system
M_2 overturning resistance of structure 2 forming part of a combined structural system
$M_b{}^o$ design moment at bottom of column associated with overstrength of adjoining beams or of column itself (at base level)
M_B expected base flexural strength of cantilever RC wall
M_{CB}/M_{total} ratio of overturning resistance provided by coupling beams to total overturning resistance.
$M_{C,D}$ required dependable flexural strength of RC columns in dual system structures
M_{CE} 1st mode design moment of RC columns (obtained from DBD procedure)
M_{frame} total overturning resistance offered by a frame structure.
M_{fr}/M_{total} ratio of frame overturning resistance to total overturning resistance.
M_n overturning resistance of structure n forming part of a combined structural system
$M^o{}_{0.5H}$ capacity design moment at mid-height of cantilever RC wall
M_p plastic flexural resistance of a steel link section forming part of an EBF structure
$M_t{}^o$ design moment at top of column associated with overstrength of adjoining beams
M_{total} total overturning resistance of a structural system
M_x overturning resistance offered by bay x of a frame structure.
n total number of storeys in building
n_b number of bays in a frame
n_{piers} number of piers restraining bridge deck lateral movements
N total number of building storeys
$N_{b,R}$ buckling strength for axial compression

P total gravity load expected to act on structure during earthquake
P_i total gravity load expected to act on level i of structure during earthquake
p pitch between two dowels of a timber joint
p_u ultimate bearing capacity of soil
PGA   Peak ground acceleration
PFA   Peak floor acceleration
q design gravity load on a timber portal frame for the seismic combination
q_{lim} ultimate gravity load for a timber portal frame
r external radius of an annular timber joint
r_g radius of gyration of steel brace section
r_Δ force-displacement post-yielding stiffness ratio
R_ξ response spectrum modification factor
$R_{\xi,0}$ response spectrum modification factor in the short period range
$R_{\xi,L}$ response spectrum modification factor in the long period range
$S_{CD,i}$ capacity design action for location i of the structure
$S_{1D,i}$ 1st mode design action for location i of the structure (for capacity design combination)
$S_{2,i}$ 2nd mode action for location i of the structure
$S_{3,i}$ 3rd mode action for location i of the structure

$S_{n,i}$	n^{th} mode action for location i of the structure
S_{CP}	dependable strength of capacity protected elements
T_e	effective period of the equivalent SDOF system
T_i	initial period of structure
T_C	corner period of spectral acceleration plateau
T_D	corner period of displacement spectrum (refer Fig. 1.1)
t	total number of tapered sections of a BRB
t_i	thickness of soil layer i
V_1	design base shear of structure 1 within a combined structural system
V_2	design base shear of structure 2 within a combined structural system
V_{Base}	design base shear of structure
V_B	design shear at base of RC wall
V_B^o	capacity design shear at base of RC wall
V_{CBi}	design shear in the coupling beams at level i.
$V_{C,D}$	required dependable shear strength of RC columns in dual system structures
V_{CE}	1st mode design shear of RC columns (obtained from DBD procedure)
V_{di}	design shear force (associated with LS design displacement profile) of level i
V_E	seismic design shear force in RC columns associated with 1st mode response
$V_{E,base}$	seismic design shear force at base of RC columns associated with 1st mode response
V_n	design base shear of structure n within a combined structural system
V_N	characteristic shear resistance of a structural element
V_n^o	capacity design shear at top of RC wall in dual system structure
V_p	plastic shear resistance of a steel link section forming part of an EBF structure
x	distance from abutment to point of interest along bridge deck
x_i	distance to level i
x_{i+1}	distance to level $i+1$
x_{CP-CM}	distance (measured on-plan) between the critical point and the centre of mass
$(x_i - e_{RX})$	distance, measured along the global X axis, of element i from centre of stiffness (Section C5.8)
z_i	distance from the buried end of a retaining wall to point i
$(z_i - e_{RZ})$	distance, measured along the global Z axis, of element i from centre of stiffness (Section C5.8)
Z	factor used to account for the number of storeys in setting the lateral force distribution of base isolated frame buildings
α	velocity power factor for viscous dampers
α_Δ	inverted V-brace frame displaced shape parameter
α_a	inclination of the active soil wedge behind a retaining wall
α_i	brace angle at the ith storey of an inverted V-brace frame
α_p	inclination of the passive soil wedge in front of a retaining wall
β	inverted V-brace frame displaced shape parameter
β_1	parameter used in the equivalent viscous damping of base isolated systems
β_2	parameter used in the equivalent viscous damping of base isolated systems
β_c	coupling factor for coupled wall structures
β_t	ratio between the depth of timber section and radius of annular bolted joint.
β_F	ratio of frame overturning resistance to total overturning resistance in a frame-wall structure
δ	retaining wall roughness
δ_c	displaced shape component at the critical element of the structure associated with the inelastic first mode response
$\delta_{d,i}$	fundamental mode damper displacement demand at level i
δ_i	displaced shape component at position i in the structure associated with the inelastic first mode response

$\delta_{u,k}$	characteristic value of the ultimate sliding deformation of dowel
$\Delta_{0.05}$	5% damped spectral displacement demand
Δ_1	equivalent SDOF system displacement of structure 1 forming part of a combined structural system
Δ_2	equivalent SDOF system displacement of structure 2 forming part of a combined structural system
Δ_n	equivalent SDOF system displacement of structure n forming part of a combined structural system
Δ_c	displacement of critical element in the structure
Δ_{centre}	peak displacement at the (on-plan) centre of mass of the building
Δ_{CP}	peak displacement at the (on plan) critical point of the building
$\Delta_{D,0.05}$	5% damped spectral displacement demand for SDOF of period T_D
$\Delta_{D,el}$	elastic spectral displacement demand at period T_D
$\Delta_{D,\xi}$	spectral displacement demand at period T_D for the design value of equivalent viscous damping
Δ_d	the equivalent SDOF characteristic or "design" displacement to be used for design
$\Delta_{d,ss}$	equivalent SDOF design displacement of the "x" (where x can be the "active" or "passive") part of a soil retaining wall system
Δ_i	displacement of level i (represents the design displacement for fundamental mode)
$\Delta_{i,ls}$	displacement of level i for the design limit state
$\Delta_{i,y}$	displacement of level i at structural yield (in frame-wall structures refers to wall yield, in steel braced frame structures it refers to compression brace buckling)
$\Delta_{i,p}$	displacement at level i due to inelastic deformations of plastic hinges
Δ_j	displacement component of timber portal structures due to joint deformations
$\Delta_{j,0}$	displacement component of timber portal structures due to joint deformations with gravity load effects neglected
Δ_{max}	maximum displacement at the top of a retaining wall
$\Delta_{N,y}$	displacement of level N at yield of Inverted V-brace system
Δ_f	equivalent SDOF displacement due to deformations of the foundations
Δ_s	elastic deformation of timber frame (excluding joint deformations)
Δ_{st}	equivalent SDOF displacement due to deformations of the structure (assuming rigid foundations)
Δ_y	yield displacement
$\overline{\varepsilon}$	normalized tension brace strain
ε_y	material yield strain
$\varepsilon_{c,i}$	axial strain in columns at the ith storey
$\varepsilon_{c,i,y}$	axial strain in columns at the ith storey at frame yield state
$\varepsilon_{c,dc}$	concrete compressive strain for damage control limit state
ε_{ls}	limit state strain of longitudinal reinforcement
ε_{su}	ultimate strain of longitudinal reinforcement
ξ, ξ_{eq}	equivalent viscous damping
ξ_0	elastic viscous damping component
ξ_1	equivalent viscous damping of structure 1 forming part of a combined structural system
ξ_2	equivalent viscous damping of structure 2 forming part of a combined structural system
ξ_n	equivalent viscous damping of structure n forming part of a combined structural system
ξ_{sys}	equivalent viscous damping of a combined structural system
ξ_{CBi}	equivalent viscous damping of coupling beam at level i
ξ_{as}	equivalent viscous damping of the active soil wedge of a retaining wall system
ξ_{ps}	equivalent viscous damping of the passive soil wedge of a retaining wall system
ξ_d	design value of equivalent viscous damping
ξ_f	equivalent viscous damping offered by foundation system
ξ_{pier}	equivalent viscous damping of pier

ξ_w	equivalent viscous damping of the wall forming part of a retaining wall system
ξ_{st}	equivalent viscous damping offered by structural system (assuming fixed foundations)
ϕ	soil friction angle
ϕ_d	dowel diameter for timber joints
ϕ^o	overstrength factor used in capacity design
ϕ_{ls}	curvature of structural section at design limit state
ϕ_s	material strength reduction factor used to determine dependable shear strength
ϕ_{yCB}	yield curvature of coupling beam section
ϕ_{yW}	yield curvature of structural wall section
γ	soil unit volume weight
$\gamma_{ls,link}$	limit state chord rotation of an EBF link
$\gamma_{p,link}$	plastic chord rotation of an EBF link
γ_s	soil shear strain
γ_t	ratio of timber portal length to section depth (at main joint)
$\gamma_{y,link}$	yield chord rotation of an EBF link
$\theta_{br,i,y}$	brace contribution to the ith storey angle of inverted V-brace system at yield state
θ_c	drift ratio limit for the performance level being considered
$\theta_{col,i}$	column contribution to the ith storey angle of inverted V-brace system
$\theta_{col,i,y}$	column contribution to the ith storey angle of inverted V-brace system at frame yield state
θ_i	storey drift ratio at the ith storey
$\theta_r{}'$	residual (also referred to as permanent) drift ratio
$\theta_{CB,ls}$	coupling beam drift limit for the limit state being considered
θ_N	torsional rotation of floor at peak displacement response
θ_p	design plastic rotation
θ_{pCW}	design plastic rotation of wall for coupled-wall structures
$\theta_{P-\Delta,i}$	P-delta stability coefficient (Eq.5.9) for storey i
θ_{pFW}	design plastic rotation of wall for frame-wall structures
$\theta_{y,CBi}$	storey drift at yield of coupling beams at level i
$\theta_{i,y}$	storey drift at yield of structure at level i
θ_y	yield drift of a structure
$\chi_{br} = \dfrac{N_{b,R}}{f_y A}$	normalized buckling strength for axial compression brace
$\chi_{br,i}$	normalized buckling strength for axial compression brace at the ith storey
χ_c	normalized buckling strength ratio for column
Λ	ratio of the elastic force in the isolation device to the friction force of sliding bearings, at the design displacement
λ	ratio of the pre-stressing resistance to the resistance of dissipating devices within a hybrid system
$\overline{\lambda}$	non dimensional slenderness of an element
$\mu = \Delta_d/\Delta_y$	displacement ductility
μ_f	steel brace ductility capacity
μ_{CBi}	ductility demand of coupling beams at level i
μ_d	design ductility
$\mu_{\Delta i}$	displacement ductility demand of wall i (Section C5.8)
ρ_v	volumetric ratio of transverse reinforcement hoops or spirals
ρ	ratio of axial strain in column to column buckling strain
$\nu_{b,max}$	maximum mid-span deformation of beams within inverted V-brace systems

ω dynamic amplification factor used for higher modes in capacity design force estimates

ω_f dynamic amplification factor for flexure

$\omega_{f,c}$ dynamic amplification factor for flexure in frame structures from level 1 to $\frac{3}{4} H_n$

ω_v dynamic amplification factor for shear

ω_θ design drift reduction factor to account for higher mode effects on drifts

ABBREVIATIONS

The following abbreviations are used in this model code:

BRB   Buckling Restrained Brace
CP   Critical Point
CM   Centre of Mass (on-plan, for torsion considerations)
DDBD   Direct Displacement-Based Design
EC8   Eurocode 8 (CEN 2004a)
EQ   Earthquake
EVD   Equivalent Viscous Damping
FPB   Friction Pendulum Bearings
FSB   Flat Sliding Bearings
HDRB   High-Damping Rubber Bearings
IS   Isolation System
LDRB   Low-Damping Rubber Bearings
LRB   Lead-Rubber Bearings
MDOF   Multi-Degree of Freedom
MRF   Moment Resisting Frame
NLTH   Non-Linear Time-History
SDOF   Single Degree of Freedom
SMA   Shape Memory Alloy

CODE

1. DESIGN SEISMICITY

1.1 General: Structures shall be designed such that performance criteria defined in Section 2 are met for the levels of seismic intensity specified in this section for the designated seismic zone.

1.2 Seismic Zone Considerations: For structures in Zone A (moderate to high seismicity) performance criteria for Levels 1, 2 and 3 intensity shall be met. For structures in Zone B (low seismicity) performance criteria for Level 3 intensity shall be met.

1.3 Design Intensity Levels: The defined probability of exceedence for a given intensity level depends on the structural occupancy usage and damage consequences, as defined in Table 1.1.

Table 1.1: Design Intensity (Probability of Exceedence) per Structural Category and Performance Level

| Importance Class* | Earthquake Design Intensity | | |
	Level 1 No Damage	Level 2 Repairable Damage	Level 3 No Collapse
I	Not Required	50% in 50 years	10% in 50 years
II	50% in 50 years	10% in 50 years	2% in 50 years
III	20% in 50 years	4% in 50 years	1% in 50 years
IV	10% in 50 years	2% in 50 years	1% in 50 years

refer EC8.1 T4.3 for importance class definitions

1.4 Elastic Design Displacement Spectrum: Design intensity for a specified level shall be expressed in terms of an elastic displacement spectrum corresponding to an elastic damping ratio of $\xi = 0.05$, characterized by a "corner" period T_D with corresponding displacement demand $\Delta_{D,0.05}$, as shown in Fig.1.1. Values of T_D, and $\Delta_{D,0.05}$ shall be based on local seismicity and the specified probability of exceedence.

COMMENTARY

C1 Two seismic zones are specified. Zone A is representative of reasonably high seismicity, where serviceability (Level 1 EQ) and damage control (Level 2 EQ) considerations are expected to govern the design, despite the fact that the level 3 seismic hazard is of greater intensity than level 2. However, as higher mode effects tend to be intensity dependent (see Priestley et al. 2007) capacity design actions should be evaluated for level 3 intensity.

In Zone B earthquakes are rare. However, at very long return periods, significant seismic intensity may occur. For these structures it appears to be inappropriate to design for serviceability or damage criteria, and the single requirement is that the building must not collapse with no loss of life under the Level 3 earthquake. More onerous performance criteria may be adopted at the discretion of the engineer or client.

Table 1.1 lists tentative suggestions for seismic risk for the three categories of earthquake, and different occupancy levels given different importance classes in EC8 part 1. Recent earthquakes have highlighted that the damage caused by more unlikely earthquakes than those indicated in Table 1.1 has not been considered acceptable by the communities affected. Thus, it may be that future codes will require seismic design to lower probabilities of exceedence than those indicated in Table 1.1. However, what should be deemed as "acceptable risk" is likely to vary from region to region and also with time. Consequently, it is recommended that risk levels be agreed with clients and it is anticipated that the risk levels indicated in Table 1.1 be revised as research in the area develops.

Note also that the Class I structures are those of minor importance to society and therefore it is not envisaged that a serviceability performance level be investigated.

Bridge structures should be designed for importance class III, unless more specific risk criteria are agreed with the client.

C1.4 Values of the corner period T_D and elastic displacement $\Delta_{D,0.05}$ at long periods will have to be specified geographically, in much the same
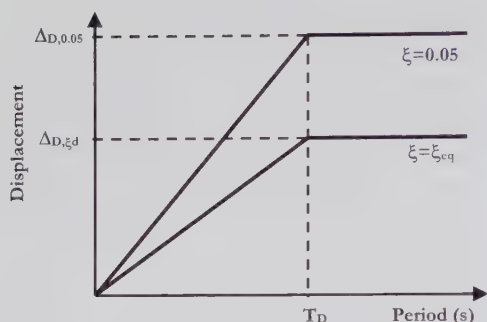
<div style="columns:2">

CODE

Figure 1.1 Design Displacement Spectra

1.5 Damped Design Displacement Spectrum: The basic elastic displacement spectra defined for the site shall be modified to account for the effects of energy dissipation by multiplying the displacement ordinates with a response spectrum modification factor, R_ξ in accordance with Eq. (1.1).

$$\Delta_\xi = R_\xi \Delta_{0.05} \qquad \qquad .(1.1)$$

1.5.1 Modification Factor for the Design of Structures Responding Inelastically: For the seismic design of structures expected to respond inelastically the equivalent viscous damping dependent modification factor to be used in Eq.(1.1) shall be obtained from Eq.(1.2) for sites where near-field effects are not expected, and from Eq.(1.3) for near-field sites where forward directivity is possible:

$$R_\xi = (0.07/(0.02+\xi))^{0.5} \qquad (1.2)$$

$$R_\xi = (0.07/(0.02+\xi))^{0.25} \qquad (1.3)$$

where the equivalent viscous damping for the structure, ξ, shall be obtained in accordance with the requirements of Section 7.

1.5.2 Modification Factor for the Design of Highly Damped Structures Responding Elastically: For the seismic design of highly damped structures responding principally elastically and for base-isolation systems covered by Cl.7.16, the modification factor, R_ξ, to be used in Eq.(1.1) shall be obtained considering the

COMMENTARY

way that the national annex specifies the local variation of PGA.

The design displacement elastic spectra shown in Fig.1.1 disregard the non-linear variation in displacements that would correspond to the EC8 acceleration design spectrum in the range $0 \leq T \leq T_C$. The linearly increasing displacement trend corresponds to the T^{-1} decreasing branch between T_C and T_D of the EC8 acceleration spectrum; and this trend is extended from $T = 0$ up to a corner period, T_D, typically in the range of 1.5 to 7.5 seconds, beyond which the displacement remains constant. As such, the present displacement spectrum should not be used for back-calculating the acceleration spectrum at short periods. Research by Faccioli et al. (2004) suggests that the corner period should be both magnitude and distance dependent.

C1.5 The DDBD approach utilises the elastic displacement response spectrum for design. In order to account for the effects of energy dissipation and/or non-linear structural response, the spectrum is reduced by the response spectrum modification factor R_ξ. The R_ξ factor is set as a function of an equivalent viscous damping value which is typically a function of the displacement ductility demand. As such, the equivalent viscous damping approach is essentially providing a simplified means of identifying inelastic displacement spectra (associated with the effective period as defined in Cl.5.4). Section 7 of this document provides expressions for the equivalent viscous damping of different structural systems for use with the relevant modification factor expression.

Modification factors are specified separately for structures responding inelastically (Cl.1.5.1) as opposed to highly damped structures responding elastically (Cl.1.5.2). This recommendation is made because historically there has been some uncertainty as to the correct formulation for the reduction of spectral displacements with equivalent viscous damping. The values suggested by Eq.(1.4) match the EC8 expression for damping reduction factors and correspond to the findings of Faccioli and Villani (2009) for a study on elastic spectral displacement variations in Italy. However, as has been demonstrated

</div>

CODE

local seismicity and earthquake characteristics. In lieu of a specific study, Eq.(1.4) can be used for sites where near-field effects are not expected.

$$R_{\xi 0} = \left(0.10/(0.05 + \xi)\right)^{0.5} \tag{1.4a}$$

$$R_{\xi L} = \frac{1}{18}\left[(1 - R_{\xi 0})T + 25R_{\xi 0} - 7\right] \tag{1.4b}$$

where R_{ξ} is equal to $R_{\xi 0}$ for periods of up to 7s and $R_{\xi L}$ for periods between 7s and 25s.

COMMENTARY

through numerous NLTH analyses, the most recent of which have been conducted by Pennucci et al. (2011), improved displacement estimates are obtained for structures responding inelastically when the equivalent viscous damping expressions within Section 7 are combined with the damping modification factor expression given in Cl.1.5.1. Further discussion of this is provided in the Preface and in Annex 2.

It is recognised that energy dissipation does not reduce seismic response as effectively when structures are subject to near-field earthquakes or where directivity is possible. As such, Eq.(1.3) has been proposed by Priestley et al. (2007) to allow for near field effects. However, there is only limited evidence (Bommer and Mendis 2005) for the scaling magnitude indicated and therefore future research on near-field effects on spectral displacements is required.

CODE

2. PERFORMANCE CRITERIA

2.1 General: Structural performance under the specified design intensities shall be defined by drift and strain limits as defined in Sections 2.2 to 2.5.

2.2 Maximum Drifts: The maximum drifts shall be limited to values reported in Table 2.1. The drift refers to the racking that develops between two structural levels. The drift ratio, θ, is defined by Eq. 2.1

$$\theta_i = \left(\Delta_{i+1} - \Delta_i\right)/\left(x_{i+1} + x_i\right) \qquad (2.1)$$

where Δ_i and Δ_{i+1} are the maximum displacements of levels i and i+1 respectively and $(x_{i+1} - x_i)$ is the distance between levels.

Table 2.1: Storey Drift Limits for Non-Structural Elements at Different Design Performance Levels

Drift Limit	Level 1 No Damage	Level 2 Repairable Damage	Level 3 No Collapse
Buildings with brittle non-structural elements*	0.004+	0.025	No Limit
Buildings with ductile non-structural elements*	0.007+	0.025	No Limit
Buildings with non-structural elements detailed to sustain building displacements*	0.010+	0.025	No Limit

+ *For the design of base isolated buildings, the performance Level 1 drift limits for fixed-base buildings shall be used for all design intensity levels.*
* *Shear design of flat slab systems should account for design drifts shown, or lower drift limits should be adopted.*

COMMENTARY

C2. The design displacement for the structure may be controlled by material strain limits, by drift limits, which are typically used to control damage to non-structural components of the building, or by any other deformation quantity that is appropriate for the structure being designed. Table 2.2 provides residual drift limits which may also constrain the design. The strain limits relate to the deformations permitted at well detailed plastic-hinge zones. Capacity design requirements of Section 9 must also be satisfied to ensure unwanted plastic mechanisms do not develop.

C2.2 Drift limits are intended to ensure that under Level 1 (serviceability) intensity only insignificant damage can be expected, and any necessary repairs can be carried out without affecting normal operations. Under Level 2 (damage-control) intensity, damage should be economically repairable. No non-structural drift limits are specified for Level 3 (collapse prevention) intensity, for which the performance criterion is to require no collapse. However, high drifts will imply significant P-Δ effects which must be included in the design (see requirements in Section 8 and refer to Priestley et al. 2007).
Since brittle elements, such as masonry infill, exhibit damage at drift limits significantly different from other non-structural materials, lower serviceability drift limits are specified. Element-specific drift limits could be defined in the future to encourage manufacturers to identify and improve the deformation capacity of non-structural elements.

Table 2.1 requires that base-isolated buildings satisfy serviceability deformation limits at all design intensity levels. The intention of this requirement is to take advantage of the fact that deformation demands on non-structural elements can be well limited via base isolation, even for intense seismic events. Note that base-isolated buildings will undergo high displacements at the isolation level and all lifelines and non-structural elements (including services) that cross the isolation level shall be detailed to safely accommodate the displacements of the isolation system.

CODE

2.3 Residual Drifts: Residual drifts should be limited to values reported in Table 2.2. The residual drift limits shall be maintained for retaining structures. The residual drift ratio, θ_r, is defined as the relative residual displacement of one structural level with respect to the other. The residual drift should consider the residual rotation of underlying foundation systems.

Table 2.2: Residual/Permanent Drift Limits

System	Level 1 No Damage	Level 2 Repairable Damage	Level 3 No Collapse
Building Structures	0.002	0.005	No Limit
Bridge Structures	0.002	0.014	No Limit
Retaining Walls distant from Structures*	0.005	0.010	No Limit

* Sliding deformations of retaining walls shall also be limited to ensure functionality of the retained system.

COMMENTARY

C2.3 Residual drifts limits are provided since residual deformations have been observed to render a structure un-operational or un-safe or unacceptable for occupants. Residual drift limits are provided for both earthquake events with intensity level 1 and 2. The drift limit for the level 1 event is intended to ensure that the structure does not appear deformed by users and remains operational. The drift limits provided for both buildings and bridges for the level 2 event, are intended to ensure that the structure does not need straightening as part of structural repairs.

Guidance on the design to residual drift limits is rather limited but is developing. McCormick et al. (2008) report on findings made in Japan on both physiological and psychological effects of residual drifts on occupants of buildings. They concluded that residual drifts of 0.5% are generally perceivable by occupants and residuals in the order of 1.0% cause occupants discomfort. Moreover, they concluded that in Japan it was generally less expensive to rebuild a structure than to repair it when residual drifts exceed 0.5%. These findings have prompted the specification of 0.5% for the "repairable damage" limit state. However, a less conservative limit could be adopted if agreed with building owners. The low limit of 0.2% has been set for the serviceability limit state in building structures in an effort to ensure that doors, windows and the like will be able to open and close following a Level 1 event.

Additional research is required to ensure that the drift limits do provide the intended performance. As such, the values indicated in T.2.2 for building and bridge structures are preliminary values that can be used by designers but will not currently be imposed as a requirement until more definitive residual-displacement design procedures are available. The importance of further research in this area is apparent from the observation that the indicated level 2 drift limit may be critical for steel structures and the like.

Until better guidance is available, the residual drift limits for retaining structures should be limited by assuming that the peak drift will equal the residual drift. However, improved residual deformation limits are required for retaining structures since both sliding and overturning can be important depending on the purpose of the retaining system.

CODE

2.4 Maximum Strains: The maximum strains shall be limited for different performance levels to the values in Table 2.3 for structural elements.

Table 2.3: Strain Limits for Plastic Hinges of Structural Elements

Material	Level 1 No Damage	Level 2 Repairable Damage	Level 3 No Collapse
Concrete comp. strain	0.004	Eq.(2.2) <0.02	1.5Eq.(2.2) < 0.03
Re-bar tension strain	0.015	$0.6\varepsilon_{su}$ <0.05	$0.9\varepsilon_{su}$ <0.08
Structural Steel Strain - Class 1 Sections, Flexural Plastic Hinges	0.010	No limit*	No limit*
Structural Steel strain - Class 2+ & 3 Sections, Flexural Plastic Hinges	ε_y	ε_y	ε_y
Steel Brace Strain (see Eq. 2.3)	$\chi_{br}\varepsilon_y$	$0.25\mu_i\varepsilon_y$	$0.5\mu_i\varepsilon_y$
Reinforced Masonry comp. strain	0.003	Eq.(2.2) <0.01	1.5Eq.(2.2) <0.015
Timber tension strain	$0.75\varepsilon_t$	$0.75\varepsilon_t$	$0.75\varepsilon_y$
Dowels of timber joints	δ_y	$0.67\delta_u$	δ_u
Isolated Structures	As per Section 2.4.3		

* However, requirements of Cl.5.6 of EC3 1.1 shall be satisfied.
+ Higher strain limits may be used for Class 2 sections if the values are supported by adequate experimental data.

Table 2.4 sets maximum soil-shear strains for soil-structure systems.

Table 2.4: Soil Strain Limits for Soil-Structure Systems

System	Level 1 No Damage	Level 2 Repairable Damage	Level 3 No Collapse
Soil strain, γ_s	γ_s such that $G/G_{max} \geq 0.80$	γ_s such that $G/G_{max} \geq 0.30$	γ_s such that $G/G_{max} \geq 0.20$
Retaining Walls Distant from Structures	γ_s such that $G/G_{max} \geq 0.40$	γ_s such that $G/G_{max} \geq 0.30$	γ_s such that $G/G_{max} \geq 0.20$

COMMENTARY

C2.4 Strain limits have been set such that under Level 1 (serviceability) performance level only insignificant damage can be expected, and any necessary repairs can be carried out without affecting normal operations. For Level 2 (damage-control), damage should be economically repairable. For Level 3 (near-collapse), the building should not collapse, though repair may not be economically worthwhile.

Strain limits for class 1 structural steel at the repairable damage and no-collapse limit states have been removed in this version of the model code, in line with the recommendations of EC3 part 1 (CEN 2005) but designers are required to satisfy the requirements of Cl.5.6 of EC3 part 1. In light of this, it is expected that serviceability, or drift (peak or residual) limits will govern the seismic design of steel structures with class 1 flexural plastic hinges. The yield strain is specified as a limit for class 2 and 3 sections as the development of large inelastic deformations cannot be guaranteed due to the potential for local inelastic buckling of steel flanges of both beams and columns. Limits are not specified for Class 4 sections but if such sections are included in a structure their design should ensure the sections remain elastic and stable, in accordance with normal gravity load design verifications.

Timber strains are required to remain well within fracture strain values, since tensile failure of timber is brittle. This does not mean, however, that timber structures must respond to earthquakes within the elastic range. The appropriate design philosophy is to design timber structures with ductile connections using a capacity design approach to avoid timber failure. As such, Table 2.3 also includes deformation limits for the dowels of timber joints. The yield and ultimate deformation capacity of the dowels should be calculated in accordance with Eurocode 5 (CEN 2004b).

C.Table 2.4: Soil strain limits refer to the maximum shear strain, induced by earthquake shaking, of the soil within the vicinity of the soil-structure interface. These are set in relation to an acceptable reduction of effective shear modulus of the soil that can be deduced based on available curves from the literature (see Kramer, 1996).

CODE

COMMENTARY

The limits proposed in Table 2.4 refer to the soil-foundation interface, and do not suppose that engineers can control the soil strains imposed by the passage of seismic waves. As such, the G/G_{max} limits should be considered equivalent to limits in the allowable reduction in foundation stiffness, although the relation between G and K is not linear and the direct specification of foundation stiffness reduction limits might be deemed more appropriate in the future (see Sullivan et al. (2010) for further discussion). The level 1 limit has been set to minimise residual deformations of soil in the serviceability limit state. Levels 2 and 3 have been both set to avoid large nonlinear soil deformations during and after earthquake shaking, which may lead to collapse of the foundation system. The seismic liquefaction potential at the site should be assessed as well. If the specified limits are not met, soil improvement actions should be carried out.

2.4.1 For confined concrete and confined masonry, the damage control limit strain in compression is:

The effect that the consequent reduction in foundation stiffness has on system response must also be assessed (see 6.1).

$$\varepsilon_{c,dc} = 0.004 + 1.4 \frac{\rho_v f_{yh} \varepsilon_{su}}{f'_{cc}} \qquad (2.2)$$

C2.4.1 The confined concrete compressive strain limit of Eq.(2.2) is based on the Mander model. See Mander et al. (1988) for details.

2.4.2 For traditional structural steel braces, the axial ductility capacity can be given by Eq.(2.3):

$$\mu_F = a + b\bar{\lambda} \qquad (2.3)$$

where the constant a shall be taken as 2.4, the constant b shall be taken as 8.3, and the non-dimensional slenderness ratio is given by:

$$\bar{\lambda} = \frac{L_e}{r_g} \sqrt{\frac{f_y}{\pi^2 E}} \qquad (2.4)$$

For Buckling-Restrained Braces, refer to cyclic deformation limits provided by manufacturer.

2.4.3 In Base-Isolated structures, the structural elements of the substructure and the superstructure shall be designed to remain within the elastic range. As a consequence, maximum acceptable material strains for the structure above and below the isolation level should satisfy the performance level 1 criteria shown in Table 2.3, for all earthquake design intensities considered.

C2.4.2 Considering data from a collection of experimental results, Tremblay (2002) proposed that the ductility available in the last deformation excursion before failure may be given by Eq.(2.3) for the case of cold-formed rectangular hollow section (RHS) braces. The use of Eq. (2.3) for hot rolled RHS or circular tubes is conservative since the ductility at fracture is expected to be larger for such sections in comparison to cold formed RHS braces. Data for other cross section shapes should be collected in the future.

Note that Tremblay defines μ_f as the sum of the positive and negative deformation, divided by the yield deformation. Therefore, the factor of one half of μ_f adopted within Table 2.3 for Level 3 earthquake intensities is specified assuming a symmetric displacement history, which should represent a conservative hypothesis, justified also with consideration of the dispersion obtained in Tremblay cyclic test results. Future work may suggest an alternative factor is appropriate.

CODE

2.5 Maximum Chord Rotations for Structural Elements: The chord rotations of structural elements for which material drift limits have not been specified in Table 2.3 shall be limited for different performance levels to values substantiated through proper numerical analyses or experimental testing. In-lieu of such data, the values reported in Table 2.5 may be adopted.

Table 2.5: Chord Rotation Limits for Structural Elements at Different Design Performance Levels

Chord Rotation Limit	Level 1 No Damage	Level 2 Repairable Damage	Level 3 No Collapse
Framed timber walls+	0.010	0.020	0.030
Short links in EBF structures	$\gamma_{y,link}$	$\gamma_{y,link} +$ 0.08	$\gamma_{y,link} +$ 0.10
Long links in EBF structures°	$\gamma_{y,link}$	$\gamma_{y,link} +$ 0.02	$\gamma_{y,link} +$ 0.025
RC Bridge Piers*	θ_y	0.03	0.04
Isolated Bridges	$2\theta_y/3$	$2\theta_y/3$	θ_y
Vertical Masonry Elements (Piers)			
Autoclaved Aerated Concrete	0.001S _F	0.003S 0.005F	0.005S 0.006F
Calcium Silicate**	0.001S _ F	0.002S 0.008F	0.002S 0.010F
Perforated Clay Blockst	0.001S _ F	0.002S 0.014F	0.003S 0.020F
Double-leaf undressed stone	0.001S _ F	0.004S 0.006F	0.006S 0.008F
Horizontal Masonry Elements (Spandrels)			
Spandrels with Lintel Beams (all masonry types)	0.0015	0.020	No limit
Spandrels Composite with RC slabs	0.004	0.008	0.010

+ *For brittle claddings, must also satisfy limits in Table 2.1.*
° *Limits valid for long links located centrally and shall not be used for links adjacent to columns.*
* *Optional – see commentary.* $\theta_y = pier yield drift.$
** *With unfilled head joints.*
† *Limits are for perforated clay blocks with vertical holes (<45% gross area). The limits for flexural mechanisms are based on data obtained only for clay blocks with unfilled head-joints.*
S *Limit valid for elements expected to form shear type mechanism.*
F *Limit valid for elements expected to form a flexural or hybrid (mixed flexure-shear) type mechanism..*

COMMENTARY

C2.5 Chord rotation limits are proposed for a series of structural elements in this section recognising that for these structural elements it is more convenient to design to a chord rotation limit than material strain limits. The aim has been to set conservative rotation limits in Table 2.5 and designers could undertake proper numerical analyses (e.g. moment-curvature analyses for RC sections) to justify alternative limits.

The chord rotation is defined as the relative translational displacement of the element between points of contraflexure, divided by the contraflexure length, as illustrated in Fig. C2.1.

$$\text{Chord rotation} = \Delta_{CF}/L_{CF}$$
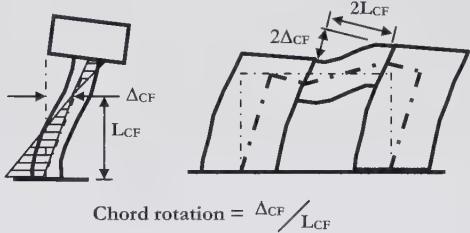
Fig. C2.1: Definition of the chord rotation referred to in Table 2.5.

Chord rotation limits have been set for nailed timber framed wall systems, rather than strain limits in order to simplify the design procedure. To this extent, note that the chord rotation limits indicated in Table 2.5 are not intended to substitute specific code drift limits for non-structural elements and the chord rotation limits of Table 2.5 should be considered together with the storey drift limits of Table 2.1 and Table 2.2. Folz and Filiatrault (2001) indicated ultimate storey drift limits for timber-framed walls in order of 2% to 4%. Considering these values, the lower bound value of 2% has been incorporated as the damage control limit, and the median value of 3% has been set as the collapse limit. Future research should better quantify these limits. A chord rotation limit of 1.0% is indicated for walls covered with deformable claddings such as plywood and fibre-board. In the event that brittle claddings are used on the timber framing, the drift limits of Table 2.1 shall be used. Full-scale shake table tests of a two-storey wood-framed building showed cracking of stucco and gypsum wallboard occurred at a storey drift of around 0.5% (Christovasilis et al. 2007).

CODE

COMMENTARY

The deformation limits proposed for masonry elements should be considered as preliminary. The limits proposed for masonry vertical elements stem from Magenes et al. (2008 a,b,c, 2011a), Ötes et al. (2003), Penna et al. (2008), and Galasco et al. (2010). Tomaževič (2007) proposes damage measure based on in-scale shaking table tests. The limits proposed for horizontal (spandrel) elements stem from studies on the deformation capacity of spandrel elements conducted by Gattesco et al. (2008), Dazio et al. (2010), Beyer et al. (2010), Magenes et al. (2011b), and Graziotti et al. (2011).

The in-plane deformation capacity for a spandrel at the collapse limit state is considered unlimited if a lintel (that is well connected to the adjacent piers) is provided to support the spandrel and out-of-plane excitations are not excessive.

The bridge pier yield drift values, θ_y, indicated in Table 2.5 can be determined using section yield curvature values together with an estimate of the curvature distribution in the structure at yield. For yield drift values of common structural systems refer to the equations included within this code and the expressions provided by Priestley et al. (2007).

The chord rotation limits indicated for links of steel EBF structures align with the recommendations of Englehart and Popov (1989). Short links are defined as those with length, e, less than $1.6M_p/V_p$, whereas long links are defined as those with length, e, greater than $3.0M_p/V_p$. The yield rotation of the links, θ_{yL}, should be calculated considering both shear and flexural deformations of the link.

Optional chord rotation limits are specified for RC bridge piers to enable designers to set design displacements without prior knowledge of the damage control or ultimate section curvature values. Such curvature values require knowledge of the reinforcement content and axial load ratio which are not typically known at the start of the design procedure. The chord rotation values indicated are expected to provide conservative estimates of the actual inelastic deformation capacity of the piers. End conditions should be considered carefully when computing target displacements from the chord rotation limits.

CODE

COMMENTARY

For isolated bridge systems, the isolation system should be designed such that the piers and deck remain elastic. As a consequence, the deformations of the piers and deck should be less than the elastic limit. For the serviceability and damage control performance levels it is recommended that elastic behaviour be assured by designing for 2/3 the chord rotation at yield of the piers (θ_y).

CODE	COMMENTARY

3. DESIGN MATERIAL STRENGTHS

3.1 Design Material Strengths for Plastic Hinge Regions:
The following material properties shall be used, in lieu of more accurate data, to determine the required strength of plastic hinge actions through the Direct DBD approach:

- Concrete compression: $f'_{ce} = 1.3 f'_c$
- Masonry compression: $f'_{me} = 1.2 f'_m$
- Steel reinforcement: $f_{ye} = 1.1 f_y$
- Structural steel:
  $f_{ye} = 1.1 f_y$ for S 355 & S 450
  $f_{ye} = 1.15 f_y$ for S 275
  $f_{ye} = 1.2 f_y$ for S 235

The following material properties shall be used, in lieu of more accurate data, to determine the maximum feasible strength (overstrength) of plastic hinge regions for capacity design:

- Concrete compression: $f'_{co} = 1.7 f'_c$
- Masonry compression: $f'_{mo} = 1.7 f'_m$
- Steel reinforcement: $f_{yo} = 1.3 f_y$
- Structural steel:
  $f_{yo} = 1.3 f_y$ for S 355 & S 450
  $f_{yo} = 1.35 f_y$ for S 275
  $f_{yo} = 1.4 f_y$ for S 235

3.2 Design Material Strengths for Capacity-Protected Members or Regions of Members:
Characteristic material strengths, without amplification, shall be used for capacity-protected members or regions of members.

C3. In selecting material strengths for seismic design, consideration must be given to the implications of underestimating or overestimating the material strengths.

C3.1 Expected material strengths are greater than characteristic strengths commonly used to provide suitable protection for load-factor resistant gravity load design. However, expected material strengths are appropriate for plastic hinge design since the actual strengths will be developed during ductile design earthquake events. Providing less or more strength to the hinge regions will change the probability that a given limit state is exceeded, and can also affect the capacity design actions.

For details of the European steel grade S 235 to S 450, see EN 10025-2:2004 (CEN 2004c).

C3.2 In order to ensure that the intended plastic mechanism develops, characteristic material strengths should be used for the design against all actions except the design actions in the plastic hinge zones.

CODE

COMMENTARY

4. MATERIAL STRENGTH REDUCTION FACTORS

4.1 Provision of Strength to Plastic Hinges: No material strength-reduction factors are applied for the action providing ductility.

4.2 Provision of Strength for Capacity-Protected Actions: Normal material strength-reduction factors are applied in line with Eurocode provisions.

C4. In line with the comments provided in C3.1 and C3.2, strength reduction factors should be used in providing resistance against all design actions, except the design action of the plastic hinge zones (for which strength reduction factors should not be applied).

C4.1 Care should be exercised when interpreting Cl.4.1 which applies only to the design action strength at plastic hinge zones. For example, for a flexural RC plastic hinge, material strength reduction factors need not be applied when designing plastic hinge flexural capacity. However, material strength reduction factors should be applied when designing shear capacity for the same plastic hinge region.

CODE

COMMENTARY

5. FUNDAMENTAL DESIGN APPROACH

Consideration of the following aspects shall be included in the seismic design:

- Selection of locations of intended plastic hinges to ensure a satisfactory mechanism of inelastic deformation.
- Appropriate combination of gravity and seismic effects.
- Protection in accordance with capacity design principles of members and actions required to remain within the elastic range of response.
- Strength requirements for wind and other non-seismic load cases and the impact these requirements may have for capacity design.

C5. As with traditional seismic design, displacement-based design relies on the selection of suitable inelastic mechanisms to ensure adequate deformation capacity. As suitable mechanisms are dependent on the structural form being considered, and in the interests of brevity, specific requirements for plastic hinge locations are not made here. It is required, however, that the designer has identified an intended plastic mechanism and that capacity design is followed to ensure that such a mechanism will develop.

In evaluating the gravity loads to combine with seismic forces, the designer should consider the changes in stiffness that occur at peak seismic response and the limited forces that can be applied to plastic hinge regions. This will often mean that the effects of gravity on the design moments of plastic hinges will be relatively small and may be ignored. See Priestley, Calvi & Kowalsky (2007) for further details and guidance.

The DDBD approach uses an equivalent SDOF system (sometimes termed a *Substitute Structure* as per Gulken & Sozen (1974) and Shibata & Sozen (1976)) to characterise the structure at the design deformation level. The fundamental equations used to characterise the equivalent SDOF system are presented in this chapter.

5.1 Displacement-Based Design Base Shear:

The design base shear force used to set the strength of plastic hinge regions of the intended plastic mechanism shall be determined for an equivalent SDOF structure in accordance with Eq.(5.1):

$$V_{Base} = K_e \Delta_d + V_{P-\Delta} \leq 2.5 R_\xi . PGA . m_e + V_{P-\Delta} \quad (5.1)$$

where the characteristic displacement, Δ_d, shall be set in accordance with Section 5.2, the effective stiffness, K_e, shall be obtained in accordance with Section 5.3, the effective mass, m_e, shall be obtained in accordance with Section 5.5 and the P-delta base shear component, $V_{P-\Delta}$, shall be obtained in accordance with Section 5.6.

C5.1 The design base shear is obtained as the product of the equivalent SDOF system effective stiffness and design displacement. In order to account for P-delta effects, this base shear is increased in accordance with Section 5.6 to ensure that the effective stiffness acting at peak response ensures that the design displacement level is not exceeded.

A limit on the required base shear is imposed on Eq.(5.1) as a function of the PGA in order to account for the non-linear variation of the displacement spectrum at short periods which has been conservatively taken as linear in Fig. 1.1. The ratio of 2.5PGA is intended to represent the plateau level of acceleration in the elastic design response spectrum and should be set with due consideration of local site (soil) conditions.

CODE

5.2 Characteristic Displacement: The characteristic displacement (also referred to as the design displacement) to be used for design shall be found from Eq.(5.2):

$$\Delta_d = \frac{\sum_{i=1}^{n}\left(m_i \Delta_i^2\right)}{\sum_{i=1}^{n}\left(m_i \Delta_i\right)} \tag{5.2}$$

where the seismic mass, m_i shall be set in accordance with subsections 5.5.1 to 5.5.3, and the fundamental mode displacement, Δ_i, of the mass at point i, shall be found as:

$$\Delta_i = \omega_\theta \Delta_{i,ls} - \theta_{N,i}.x_{CP-CM} \tag{5.3}$$

where $\Delta_{i,ls}$ is the displacement of point i at the development of the deformation limit state, obtained for different structural typologies in accordance with Section 6. The term $\theta_{N,i}.x_{CP-CM}$ shall be set to account for torsional response in accordance with Section 5.8. The higher mode reduction factor, ω_θ, shall be set in accordance with the requirements of Section 5.9.

5.3 Effective Stiffness: The effective stiffness of the equivalent SDOF structure shall be obtained from Eq.(5.4):

$$K_e = 4\pi^2 m_e / T_e^2 \tag{5.4}$$

where the effective period, T_e, shall be obtained in accordance with Section 5.4 and the effective mass, m_e, shall be obtained in accordance with Section 5.5.

For structures with effective period greater than T_D, the value of effective stiffness obtained from Eq.(5.4) need not exceed $K_{e,max}$ given by Eq.(5.5).

$$K_{e,max} = 4\pi^2 m_e / T_e^2 \frac{\Delta_{D,\xi d}}{\Delta_d} \tag{5.5}$$

COMMENTARY

C5.2 The characteristic displacement (also often referred to as the design displacement) is the displacement of the equivalent SDOF system that will ensure the structural and non-structural deformation limits are not exceeded. The displacement is that associated with the on-plan centre of mass of the structure.

Buildings with mass, stiffness, or strength eccentricity can be expected to twist during an earthquake, such that the displacements of different points on the same level, i, will differ. As such, in Eq.(5.3) the term $\theta_{N,i}.x_{CP-CM}$ is used to account for torsion-induced differences in displacement between the critical point (on-plan) of a structure and the centre-of-mass. For guidance on setting $\theta_{N,i}.x_{CP-CM}$ see Section 5.8.

Section 6 provides guidelines for specification of the displacement profile, $\Delta_{i,ls}$, at development of the performance limit state. As DDBD is an effective 1st mode approach, if deformations due to higher mode effects are expected to be significant, then the 1st mode design displacement profile should be set lower than the limit state displacement profile using the reduction factor, ω_θ, as shown. Guidance on the specification of the higher mode reduction factor is provided in Section 5.9.

C5.3 Eq.(5.4) is found from simple inversion of the equation for the period of a SDOF oscillator. The limit set on the effective stiffness, $K_{e,max}$, recognises, in an approximate fashion, that the displacement demands on the fundamental mode of long-period structures are limited by the ground motion spectral displacement demands.

C.5.4 The required effective period is the period possessing a spectral displacement demand at the design damping level equal to the equivalent SDOF characteristic (design) displacement. It can be found directly through Eq.s(5.4) to (5.6) or by entering the damped design spectrum with the characteristic displacement, as shown in Fig. C5.1(a).

CODE

5.4 Effective Response Period: The effective period of the SDOF structure shall be obtained from Eq.(5.6)

$$T_e = \frac{\Delta_d}{\Delta_{D,\xi}} \cdot T_D \qquad (5.6)$$

where $\Delta_{D,\xi}$ is obtained by scaling the 5% damped spectral displacement component at T_D by Eq.(1.1).

COMMENTARY

(a)

(b)
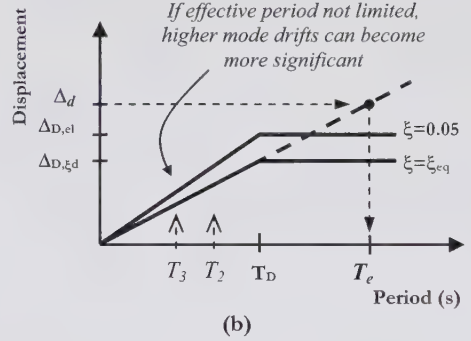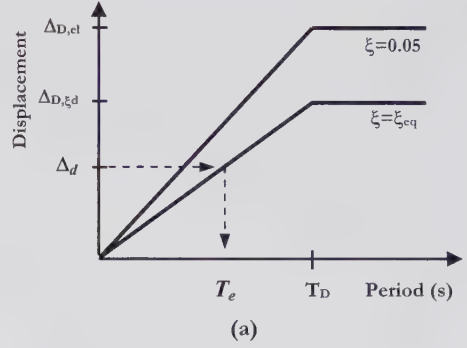
Fig. C5.1: Identification of the effective period from the damped design displacement spectrum for (a) typical case in which $T_e < T_D$, and (b) case in which $T_e > T_D$.

In the event that Δ_d is greater than $\Delta_{D,\xi d}$, an acceptable solution can lie at long periods and in such cases it is recommended that Eq.s (5.4) to (5.6) be applied instead of the graphical approach, in order to limit the effective period and thereby limit disproportionally large higher mode deformations (see Fig.C5.1(b)).

5.5 Effective Mass: The effective mass of the equivalent SDOF structure shall be obtained from Eq.(5.7).

$$m_e = \sum_{i=1}^{n} (m_i \Delta_i) / \Delta_d \qquad (5.7)$$

where the seismic masses, m_i shall be established in accordance with subsections 5.5.1 to 5.5.3, and Δ_i shall be found from Eq.(5.3).

C5.5 The effective mass is the mass of the equivalent SDOF structure. It is needed to determine the required effective stiffness of the substitute structure.

CODE

5.5.1 Seismic Masses of Building Structures:
The seismic masses of building structures can typically be lumped at floor levels. The magnitude of the masses shall be taken as the mass associated with the un-factored self weight of the building, plus the mass of the imposed loads expected at the time of the design earthquake event.

5.5.2 Seismic Masses of Bridge Structures:
The seismic masses to be used in the seismic design of bridge structures shall be determined considering the weight of the main structure and the imposed loads expected at the time of the earthquake. The weight of the foundation structure shall also be included if significant foundation movements are anticipated.
Where the superstructure is supported on bearings or equipped with an isolation system (IS), the movements of the masses above and below the bearing/IS level shall be accounted for.

5.5.3 Seismic Masses of Retaining Structures:
The seismic masses to be used in the seismic design of soil retaining structures shall include the retaining structure, the active soil wedge behind the structure and the passive wedge, if any, in front of the structure.

COMMENTARY

C.5.5.2 The seismic masses of bridge structures can typically be lumped at the top of the bridge piers. The magnitude of the masses can be established on a tributary width basis using the un-factored self weight of the bridge deck together with the mass of the imposed loads expected at the time of the design earthquake event plus one-third the mass of the piers. Note that traffic loads may be excluded from the mass calculation because the vehicles are not rigidly connected to the bridge deck. If foundation movements are significant then the foundation mass should also be considered in defining the system masses.
For bridges with tall piers that possess a height to section depth ratio, H/D, greater than 10, additional masses up the height of the pier should be included (refer Priestley et al. 2007 and Adhikari, 2007).

C5.5.3 Cecconi et al. (2007) recommend that the effective mass of retaining wall systems be determined considering the soil volume that is displaced as part of the whole system (soil - structure) mechanism. The system can be discretised, as indicated in Fig. C5.2, into i soil layers of thickness t_i, such that:

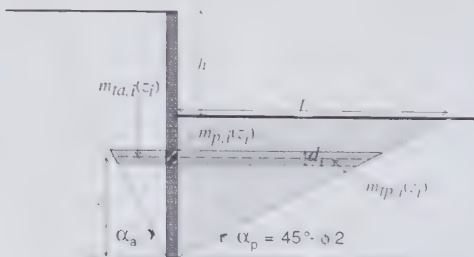$$m_i = m_{as.i} + m_{ps.i} + m_{w.i} \qquad (C5.1)$$

Fig. C5.2: Mass components of a cantilever diaphragm retaining wall system (Cecconi et al. 2007)

More detailed but preliminary recommendations for the DDBD of cantilever diaphragm retaining wall systems, developed by Cecconi et al. (2007), are included in Annex 3.

CODE

5.6 Allowance for P-delta Effects: P-delta effects shall be accounted for in design through inclusion of a P-delta base shear component, $V_{P-\Delta}$, calculated in accordance with Eq. (5.8):

$$V_{P-\Delta} = C \frac{\sum_{i=1}^{n} P_i \Delta_i}{H_e} \qquad (5.8)$$

where the effective height, H_e, shall be obtained according to Section 5.7, and the P-delta constant, C, shall be obtained from rational analyses or can be taken as:

$C=0.0$ for structures with $m_e g / K_e H_e < 0.05$.

$C=0.5$ for concrete structures and any systems possessing thinner hysteretic loops similar to the Takeda or Flag-Shape models.

$C=1.0$ for steel structures and systems with large hysteretic loops similar to the bi-linear, elasto-plastic or Ramberg-Osgood models, with large residual displacements.

In addition, the P-delta stability coefficient, determined in accordance with Eq. (5.9), shall not exceed 0.30.

$$\theta_{P-\Delta,i} = \frac{P_i (\Delta_i - \Delta_{i-1})}{V_{,i} (h_i - h_{i-1})} \qquad (5.9)$$

5.7 Effective Height: The effective height of buildings (and similar structures) shall be determined according to Eq. (5.10).

$$H_e = \sum_{i=1}^{n} (m_i \Delta_i h_i) / \sum_{i=1}^{n} (m_i \Delta_i) \qquad (5.10)$$

COMMENTARY

C5.6 The treatment of P-delta effects in DDBD is relatively straightforward, and is illustrated in Fig. C5.2 below. As the design displacement profile is set as a design target, the overturning moments caused by the displaced gravity loads can be calculated directly, as is done in the numerator of Eq.(5.8). When these P-delta moments are significant, it is the stiffness corresponding to the degraded strength and the design displacement (see K_e in Fig. C5.3) that should match the required stiffness. Hence, Eq.(5.8) defines the increment in base shear that will provide the necessary effective stiffness. As explained by Priestley et al. (2007), the full increment of stiffness would be too conservative for some hysteretic types and as such, the P-delta constant has been introduced into Eq.(5.8).
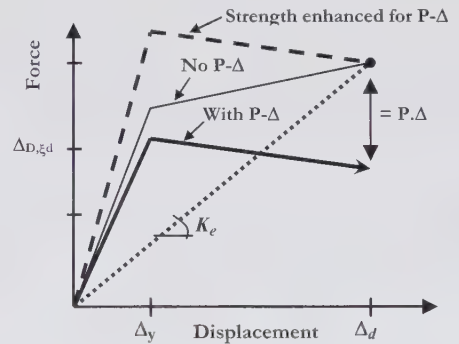
Fig. C5.3: Accounting for P-delta effects with strength enhancement (adapted from Priestley et al. 2007).

The P-delta stability coefficient indicated in Eq.(5.9) should be evaluated for each level of a building and the maximum value checked against the limit of 0.30. The limit of 0.30 is intended to reduce the probability of dynamic instability.

C5.7 The effective height is the height of the equivalent SDOF system. It is needed for the evaluation of P-delta effects and for the calculation of system ductility demands in order to set the equivalent viscous damping of certain structural systems in Chapter 7.

CODE

5.8 Allowance for Torsional Response: The torsionally induced in-plan difference between the peak displacement of the critical point in the structure, $\Delta_{CP,i}$, and the peak displacement of the centre of mass, $\Delta_{CM,i}$, at location i, shown in Eq.(5.3) as $\theta_{N,i}.x_{CP-CM}$, shall be defined by Eq.(5.11):

$$\theta_{Ni}.x_{CP-CM} = \Delta_{CP,i} - \Delta_{CM,i} \qquad (5.11)$$

and shall be obtained from rational analyses. For structures possessing a strength eccentricity, as defined in Section 5.8.1, equal to zero, the term $(\Delta_{CP,i}-\Delta_{CM,i})$ in Eq.(5.11) may be obtained from elastic analyses.

5.8.1 Strength Eccentricity: The strength eccentricity shall be taken as the distance between the centre of strength and the centre of mass, measured normal to the direction of excitation considered. The centre of strength is defined as the centre of the lateral strength of all primary seismic members. To minimise twist in the inelastic range, the member strengths should be distributed such that the strength eccentricity is minimised.

COMMENTARY

C5.8 The Direct DBD procedure controls the displacements of the centre of mass. As torsion can affect the displacements of a structure away from the centre of mass, Eq.(5.3) includes a torsional rotation component that aims to account for twist by adjusting the centre-of-mass deformations of the structure. Torsion is affected by both elastic stiffness eccentricities and by strength eccentricities in the inelastic range. As pointed out by Priestley et al. (2007), the torsionally induced difference in peak displacements proposed in Eq.(5.11) may act to either decrease or increase the design displacement, since the difference in displacements $(\Delta_{CP}-\Delta_{CM})$ may be positive or negative, as illustrated in Fig. C5.4. The critical point (on plan) will typically correspond to a point at the perimeter of the building but may be at an internal point (the location of a lateral load resisting system) particularly if the critical design displacement profile is governed by material strain limits.

The use of rational analysis to establish the twist at peak response must account for the redistribution in effective stiffness that occurs as a plastic mechanism forms in the structure. One could consider the use of NLTH analyses to obtain accurate estimates of the likely twist, with an initial design undertaken using an estimated value for the twist and with the characteristics of the lateral load resisting system set so as to minimise the strength and stiffness eccentricity. Alternatively, Priestley et al. (2007) and Beyer et al. (2008) present an approach that estimates the twist at peak response according to:

$$\theta_N = \frac{V_{Base}.e_R}{J_{R,\mu}} \qquad (C5.2)$$

where e_R is the stiffness eccentricity relative to the direction of excitation and $J_{R,\mu}$ is an effective torsional stiffness defined by Eq.(C5.3):

$$J_{R,\mu} = \sum_1^n \frac{k_{Zi}}{\mu_{\Delta i}}(x_i - e_{RX})^2 + \sum_1^n k_{Xi}(z_i - e_{RZ})^2$$

$$\qquad (C5.3)$$

where k_{Xi} and k_{Zi} are, respectively, the elastic stiffness values of wall i in the global X and Z

CODE

COMMENTARY

(a)

(b)
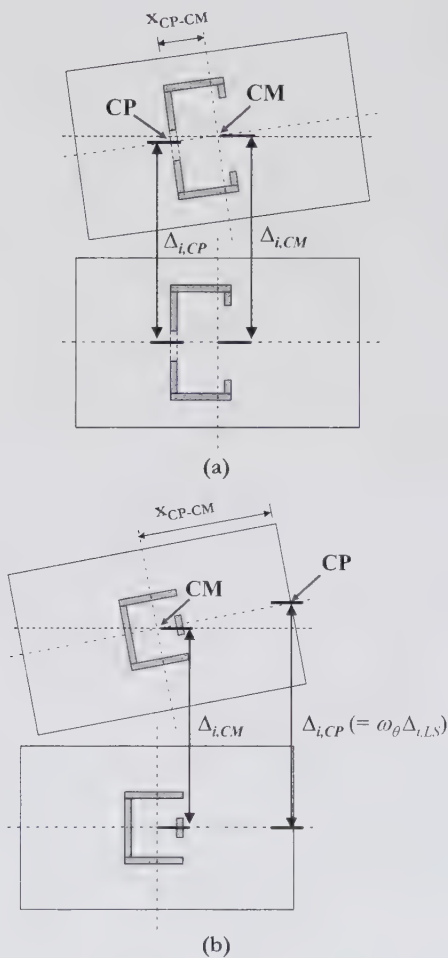
Fig. C5.4: Twisting translational response of buildings (plan view) for two scenarios: (a) Critical point (CP) defined by strain limits in coupling beam, and (b) Critical point (CP) defined by maximum non-structural drift demands.

directions, $\mu_{\Delta i}$ is the ductility demand of wall i in the Z direction, $(x_i - e_{RX})$ and $(z_i - e_{RZ})$ are distances, measured along the X and Z axes respectively, of element i from the centre of stiffness in the X and Z directions. See Priestley et al. (2007) or Beyer et al. (2008) for further details.

The approach of Priestley et al. (2007) and Beyer

CODE

COMMENTARY

et al. (2008) can be considered semi-empirical since it does not explicitly account for torsional inertia and assumes the rotation should be calculated using the stiffness eccentricity (as per Eq.(C5.2)) but that the differences in on-plan floor displacements caused by the twist should be calculated using eccentricities relative to the centre of strength.

Beyer et al. (2008) report that the displacements of the perimeter of a structure are typically not greater than 10% the centre of mass displacements when the strength eccentricity is zero. This highlights the fact that when the strength eccentricity is minimised, the twist in the non-linear range of response is minimised. Hilje et al. (2010) show that the twist is likely to be a function of the ductility demand, with the stiffness eccentricity influencing the twist at low ductility demands and the strength eccentricity influencing the twist at high ductility demands. With these points in mind, Cl.5.8 permits the term $(\Delta_{CP,i}-\Delta_{CM,i})$ to be calculated from elastic analyses if the strength eccentricity is zero. This could require an iterative design procedure in which the rotation is at first estimated in order to determine a set of design forces for the elastic analyses.

5.9 Higher Mode Reduction Factor: The higher mode reduction factor, ω_θ, required for calculation of the design displacement profile in accordance with Eq. (5.3), shall be defined by rational analyses or, for building structures, from the curves presented in Fig. 5.1.

The curves of Fig. 5.1 distinguish between buildings in which plastic hinges form at the base of the main lateral resisting system only (e.g. cantilever wall buildings) and buildings in which plastic hinges form up the height of the main lateral resisting system (e.g. frame structures). For systems in which the equivalent SDOF overturning resistance offered by base hinging is of similar magnitude to that offered by upper level hinging (e.g. dual frame-wall buildings and coupled wall structures) higher mode factors may be interpolated between the curves of Fig. 5.1.

C5.9: The Direct DBD procedure controls the displacements of the first mode of vibration. Higher modes of vibration can increase the deformations of a structure, above those caused by first mode response. However, for typical regular structural typologies, higher modes do not affect the storey displacements greatly and therefore in the DDBD procedure, a simplified means of accounting for deformations due to higher modes is proposed here.

For structures sensitive to higher mode effects, the fundamental mode design displacement profile is set equal to the limit state deformation profile reduced by the factor, ω_θ, as per Eq.(5.3). In this way, when the higher mode deformations add to the fundamental mode deformations, the performance limits are still maintained. This is illustrated in Fig. C5.5.

CODE
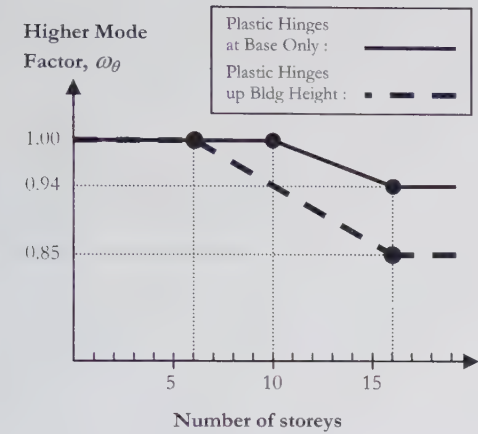
Fig. 5.1: Higher mode factors for use in Eq.(5.1).

For bridge structures, the higher mode factor shall be defined by rational analyses, or, in-lieu of such analyses, a value of $\omega_\theta = 0.94$ may be adopted for the transverse response direction and a value of $\omega_\theta = 1.0$ may be adopted for the longitudinal response direction.

COMMENTARY
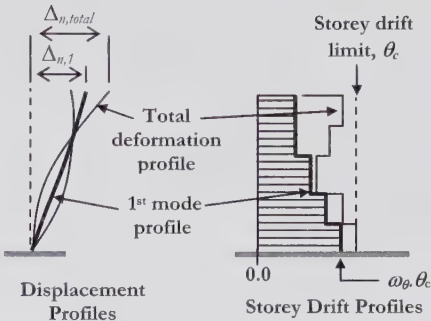
Fig. C5.5: Use of higher mode factor, ω_θ, to set reduced 1st mode displacement levels.

The curves for the higher mode factors presented in Fig.5.1 have been set to approximately align with the empirical expressions developed by Pettinga & Priestley (2005), Sullivan et al. (2006), and Smyrou et al. (2008). Some simplified analytical expressions for the higher mode deformations of inelastic RC walls have been developed by Pennucci et al. (2011) and such alternative approaches will be considered for future revisions of the model code. Note that the curves are aimed at predicting higher mode contributions during inelastic response and for elastic response, modal analysis would be more accurate.

For regular bridges of short span between abutments the factor can typically be taken equal to 1.0. Modal response spectrum analysis can be utilised to estimate displacement contributions due to higher modes at potentially critical pier locations. The ω_θ factor can then be set as $\omega_\theta = (1-\Delta_{high}/\Delta_c)$, where Δ_{high} is the displacement at the critical pier due to higher mode response. Alternatively, design can be done by estimating the ω_θ factor as 0.94, but note that this is a very approximate value and for bridges in which higher modes may significantly affect the displaced shape, it is recommended that non-linear time-history analyses be used to verify the bridge performance.

CODE

6. DESIGN DISPLACEMENT PROFILE

The limit state design displacement profile shall be set by the most critical deformation limit defined in Chapter 2, and shall be determined in accordance with the requirements of this chapter. The guidelines provided in this chapter for the displaced shapes of building structures, are for vertically regular building systems of up to 20-storeys in height possessing stiff floor diaphragms. Vertically regular building systems are defined as those that conform to the regularity requirements of EC8 part 1 Section 4.2.3.3. For vertically irregular systems, design displacement profiles must be established using accepted principles of structural mechanics, an iterative design-analysis approach, or via experimental data.

For systems with floor diaphragms that may possess some flexibility, the impact of diaphragm flexibility on the design displacement profile shall be accounted for in line with Section 6.15.

6.1 Foundation Displacements: The effect of foundation movements on the design displacement profile for the structural system being designed shall be considered. Assessment can be made at the end of the DDBD process when design actions on the foundations are obtained.

If foundation deformations are deemed significant, the limit state design displacement profile, $\Delta_{i,ls}$, in Eq.(5.2) shall be substituted by the displacement profile that accounts for SSI, $\Delta_{i,ls,SSI}$, defined by Eq.(6.1).

$$\Delta_{i,ls,SSI} = \Delta_{i,st} + \Delta_{i,f} \qquad (6.1)$$

where, $\Delta_{i,f}$ is the displacement of point i due to foundation deformations and $\Delta_{i,st}$ is the displacement of point i due to structural deformation.

COMMENTARY

C6. Direct displacement–based seismic design relies on determination of a displacement profile at the specified performance level, in order to identify the characteristics of the equivalent SDOF model corresponding to the inelastic first mode response. Typically, the limit state design displacement will be controlled by either a non-structural drift limit or a strain limit of the structural material.

Displaced shape expressions of various structural types have been obtained through NLTH analyses of regular structural systems in which it was assumed that floors act as rigid-diaphragms in-plane, being fully flexible out-of-plane. For vertically irregular systems an iterative design and non-linear analysis procedure may be needed in order to identify how stiffness and strength distributions affect the inelastic displacement profile.

Most expressions for the displaced shape in this Chapter specify the displacement profile at development of the performance limit state and are denoted by $\Delta_{i,ls}$. As DDBD is an effective 1st mode approach, if deformations due to higher mode effects are expected to be significant (see Section 5.9), then the 1st mode design displacement profile should be set lower than the limit state displacement profile using the factor, ω_θ, as stated earlier in Section 5.2.

C6.1 Soil-structure interaction (SSI) can significantly affect the response of a structure and should be considered within the design. Eq.(6.1) provides the basic expression for the design displacement profile with account for SSI. Values of $\Delta_{i,st}$ may be considered equivalent to the $\Delta_{i,ls}$ values given in Sections 6.2 to 6.14 except that the design displacement profiles must account for the impact of foundation movements on the deformations of the critical element. To this extent, foundation deformations may or may not lead to an increase in the allowable system displacement. For example, considering a RC wall structure, if wall ductility demands are critical then foundation rotations will permit a larger system displacement for the same structural ductility demand but if storey drift limits are critical, then foundation rotations will tend to increase storey drifts and hence the

CODE

COMMENTARY

system displacement should not change significantly.

In order to evaluate the role of the soil-foundation system an estimate of both the foundation deformations and damping is required. However, as the foundation stiffness and deformations may not be known until design forces from the overlying structure are obtained, an iterative design approach may be required as per Paolucci et al. (2009) in which curves for decay of rotational and translational stiffness and an increase in damping ratio as a function of the foundation deformation have been calibrated. Annex 5 provides guidance for the stiffness and damping of shallow foundation systems. Sullivan et al. (2010) also discuss how such information might be used for the DDBD of RC wall structures on shallow foundations.

6.2 Moment Resisting Frame Buildings: The design displacement profile, corresponding to the inelastic first mode shape at the design drift limit, established using the structural and non-structural deformation limits specified in Section 2, shall be determined by structural analysis or, when inelastic response is expected, by direct use of Eq.(6.2):

$$\Delta_{i.ls} = \theta_c h_i \cdot \frac{\left(4H_n - h_i\right)}{\left(4H_n - h_1\right)} \qquad (6.2)$$

For frame structures that are expected to respond elastically for the limit state under consideration, the displaced shape shall correspond to the fundamental mode shape obtained from eigen-value analyses.

C6.2 The design displacement profile of frames is somewhat dependent on the distribution of strength up the height of the building. The recommendations provided here require that the frames be detailed to develop a beam-sway mechanism (except at roof level). Building frames will normally be governed by code drift limitations, rather than material strain limits. Consequently the normal design approach will be to design for drifts, and subsequently check strain limits. The inelastic first mode shape of Eq. (6.2), depicted schematically in Fig. C6.1, has been obtained empirically through a large set of non-linear time-history analyses of regular frame structures of up to 20 storeys height. Refer Priestley et al. (2007) and Pettinga and Priestley (2005). When using Eq.(6.2) member strengths should be assigned to equilibrate the lateral force distribution specified in Section 8.1.
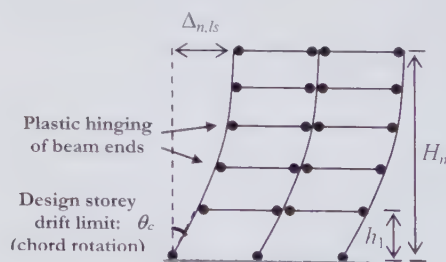

Fig. C6.1: Inelastic displaced shape of Eq.(6.2)

CODE

6.3 RC Cantilever Wall Buildings: The design displacement profile shall be defined by rational structural analysis, or, for walls with aspect ratio (H_n/L_w) greater than 3.0 expected to respond inelastically for the limit state being considered, by Eq.(6.3).

$$\Delta_{i,li} = \Delta_{yi} + \Delta_{pi} = \frac{\phi_{yW}}{2} h_i^2 \left(1 - \frac{h_i}{3H_n}\right) + \theta_p h_i \qquad (6.3)$$

where the yield curvature, ϕ_{yW}, can be obtained from sectional moment-curvature analysis or using the expressions provided in Annex 1.

For wall structures that are expected to respond elastically for the limit state under consideration, the displaced shape shall correspond to the fundamental mode shape obtained from eigen-value analyses or shall be approximated from Eq.(6.3) by setting the plastic rotation equal to zero and substituting the yield curvature with a lower, expected wall curvature value.

For wall structures with aspect ratio less that 3.0, shear deformations should be taken into account in definition of the design displacement profile.

6.3.1 Design Plastic Rotation, θ_p: In Eq.(6.3) the design plastic rotation, θ_p, shall be taken from Eq. (6.4).

$$\theta_p = \theta_c - \frac{\phi_{yW} H_n}{2} \leq \left(\phi_{ls} - \phi_{yW}\right)L_p \qquad (6.4)$$

COMMENTARY

An alternative means of obtaining the inelastic first mode shape is to undertake adaptive non-linear pushover analyses (see Antoniou and Pinho, 2004), displacing the structure out to the storey drift limit θ_c.

For DDBD at the serviceability (level 1) limit state it may often be the case that moment-resisting frames are expected to respond elastically. In such cases it is recommended that eigen-value analyses be used to identify the fundamental mode shape. Analysis models of RC frames should incorporate cracked section stiffness values set as a function of the member strength (see Priestley et al. (2007)). As such, in order to avoid an iterative design process, it is recommended that such serviceability limit states be checked after the member strengths required to satisfy level 2 or 3 design intensity levels have been identified.

C.6.3 The design displacement profile for RC wall structures should consider the elastic and inelastic deformations expected up the height of the structure. Cracking, reinforcement strain penetration, the tension shift, higher mode effects and other characteristics of reinforced concrete should be considered in establishing the likely displaced shape.

Priestley et al. (2007) provide Eq.s (6.3) to (6.5) as an approximate method for analytically determining the design displacement profile. The approach sums an elastic deformation profile with rigid-body rotation about the base associated with a plastic hinge rotation, as is illustrated in Fig. C6.2.

The yield displacement profile approximates the elastic curvature profile up the walls as being linear from the yield curvature at the base, to zero at the roof level (see Priestley et al. (2007) for discussion).

For walls with aspect ratio <3.0 shear deformations should be considered in setting the design displacement profile.

The limit state curvature, ϕ_{ls}, should be found from moment-curvature analyses. Note that for rectangular RC walls Priestley et al. (2007) propose $\phi_{ls} = 1.2\varepsilon_{s,ls}/L_w$.

CODE

where the plastic hinge length, L_p, can be taken as:

$$L_p = kH_n + 0.1L_W + L_{SP} \qquad (6.5)$$

where $k=0.15(f_u/f_y-1)\leq0.06$, and $L_{sp}=0.022f_y d_{bl}$.

6.4 Dual Frame-Wall Buildings: The design displacement profile shall be defined by rational analysis, or by Eq.(6.6):

$$\Delta_{i,ls} = \Delta_{iy} + \theta_{pFW} h_i \qquad (6.6)$$

6.4.1 Frame-Wall design plastic rotation: In Eq.(6.6) the design plastic rotation, θ_{pFW}, shall be taken from Eq. (6.7):

$$\theta_{pFW} = \theta_c - \frac{\phi_{yW} H_{CF}}{2} \leq (\phi_{ls} - \phi_y)L_p \qquad (6.7)$$

where H_{CF} is the height of the wall contraflexure point at the development of the design deformation and the plastic hinge length, L_p, shall be obtained substituting H_{CF} for H_n in Eq.(6.5).

For regular frame-wall structures with uniform beam strengths up the building height, the contra-flexure height may be related to the proportion of overturning resisted by the frames, $\beta_F = M_{fr}/M_{total}$, through Eq.(6.8) and Eq.(6.9):

$$\frac{H_{CF}}{H_n} = \frac{(\sqrt{9 - 8\beta_F} - 1)}{n^{0.25}} \qquad (6.8)$$

But if: $\left(\frac{(\sqrt{9-8\beta_F} - 1)}{n^{0.25}} \geq \frac{n-1}{n} \right)$

then: $$\frac{H_{CF}}{H_n} = 1.0 \qquad (6.9)$$

COMMENTARY
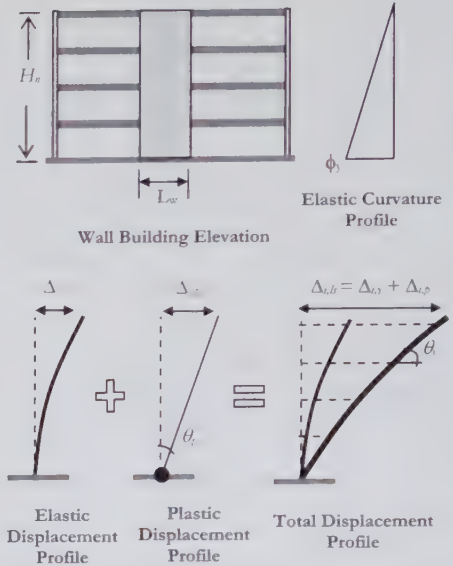
Fig. C6.2: Basis of design displaced shape for RC cantilever walls, as per Eq.(6.3).

C.6.4 In frame-wall systems the walls tend to restrict deformations of the lower floors and the frames restrict deformations over the upper floors (see Sullivan et al. 2006). As the proportion of overturning resistance provided to the frames increases, the walls will be subject to increased reverse bending over their upper storeys, with a contra-flexure point developing. The displaced shape of frame-wall structures has been found to be a function of the height to contra-flexure in the walls (Sullivan et al. 2004). The contra-flexure height can be found through knowledge of the frame and wall strength proportions (see Sullivan et al. 2006 and Priestley et al. 2007).

C.6.4.1 For regular frame-wall structures with uniform beam strengths up the building height (in which the walls resist difference between total demand and frame resistance), Eq.s (6.8) and (6.9) provide a reasonable approximation for the contraflexure height as a function of the overturning proportions. The expressions were developed by modifying the contraflexure height associated with a coupled uniform beams (refer Pennucci et al. 2011) to account for the discrete nature of low and medium rise structures. The

CODE

6.4.2 Frame-Wall Yield Displacement Profile:
In Eq.(6.6) the displacement profile at yielding of the walls shall be defined by:

for $h_i \leq H_{CF}$:

$$\Delta_{iy} = \phi_{yW}\left(\frac{h_i^2}{2} - \frac{h_i^3}{6H_{CF}}\right) \qquad (6.10)$$

for $h_i > H_{CF}$:

$$\Delta_{iy} = \phi_{yW}\left(\frac{H_{CF}h_i}{2} - \frac{H_{CF}^2}{6}\right) \qquad (6.11)$$

The wall yield curvature ϕ_{yW} shall be obtained from sectional moment-curvature analysis, experimental data, or from the expressions provided in Annex 1.

6.5 Coupled RC Wall Buildings:
The design displacement profile of coupled wall buildings shall be defined by rational analysis in which the degree of coupling is considered, or by Eq.(6.12).

$$\Delta_{i,ls} = \Delta_{iy} + \theta_{pCW}h_i \qquad (6.12)$$

where the yield deformation profile can be obtained as for a frame-wall structure using Section 6.4.2.

6.5.1 Coupled Wall Design Plastic Rotation:
In Eq.(6.12) the design plastic rotation, θ_{pCW}, shall be taken from Eq.(6.13).

$$\theta_{pCW} = \theta_c - \frac{\phi_{yW}H_{CF}}{2}$$

$$\leq \frac{\theta_{CB.ls}}{1 + L_{w,av}/L_{CB}} - \frac{\phi_{yW}H_{CF}}{2}$$

$$\leq \left(\phi_{lsW} - \phi_{yW}\right)L_p \qquad (6.13)$$

where $\theta_{CB.ls}$ is the coupling drift limit given in Section 6.5.2, H_{CF} is the height of the wall contraflexure point at the development of the

COMMENTARY

curves of more precise but also more complex expressions from Sullivan (2007) are shown in Fig. C6.3 below. Either these curves or Eq.s (6.8) and (6.9) can be used for design.
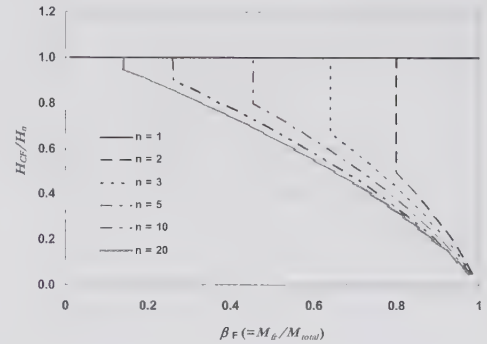
Fig. C6.3: Wall contraflexure height ratio for dual systems (adapted from Sullivan, 2007).

C.6.4.2 The yield displacement profiles indicated in Eq.s (6.10) and (6.11) as from Sullivan et al. (2006) approximate the elastic curvature profile in the walls as being linear from the yield curvature, at the base, to zero at, and above, the contra-flexure height.

C.6.5 The design displacement profile of coupled wall structures is similar to that of frame-wall structures.

C.6.5.1 Coupling beam deformations will often control the design deformation profile of coupled wall structures. As such, in addition to considering non-structural drift limits and base plastic hinge deformation limits, the coupling beam drift limit must be established, as per Section 6.5.2.
The different coupling beam length definitions used in Eq.s (6.13) and (6.14) are illustrated in Fig. C6.4.

CODE

design deformation, L_{CB} is the clear length of the coupling beams, and L_p is the plastic hinge length that can be obtained substituting H_{CF} for H_n in Eq.(6.5).

The contraflexure height, H_{CF}, shall be obtained from rational analysis or through substitution of β_c for β_F in Eq.s(6.8) and (6.9), where the degree of coupling, β_c is given by Eq.(6.14).

$$\beta_c = \frac{M_{CB,B}}{M_{total}} = \frac{L_{CBcc} \cdot \sum_{i=1}^{n} V_{CBi}}{M_{total}} \qquad (6.14)$$

where $M_{CB,B}$ is the overturning resisted by the coupling beams, M_{total} is the total overturning resistance, L_{CBcc} is the length of coupling beams measured between wall centres and V_{CBi} is the design shear in the coupling beam at level i of an n storey structure.

6.5.2 Coupling Beam Drift Limits: In Eq.(6.13) the coupling beam drift limit shall consider the deformation capacity of the coupling beams. This can be obtained as:

Conventional Coupling-Beam Reinforcement:

$$\theta_{CB,ls} = \frac{\varepsilon_{ls} 2L_{SP}}{0.75 h_{CB}} \qquad (6.15)$$

Diagonal Coupling-Beam Reinforcement:

$$\theta_{CB,ls} = \frac{\varepsilon_{ls}(0.5L_{CB} + L_{SP})}{0.75 h_{CB}} \qquad (6.16)$$

where the strain penetration length can be taken as $L_{sp}=0.022f_{ye}d_{bl}$ (f_{ye} in MPa).

6.6 Steel Concentrically Braced Frame Systems: Both the yielding and the limit state displacement profiles shall be defined by rational analyses.

6.7 Steel Eccentrically Braced Frame Systems: Both the yielding and the limit state displacement profiles shall be defined by rational analyses.

COMMENTARY

$$L_{w,av} = (L_{w1} + L_{w2})/2$$

Fig. C6.4: Length definitions used in Eq.s(6.13) and (6.14) for coupled wall systems.

In the case that coupling beams of equal strength are used up the building height, the coupling ratio can be related to the contraflexure height setting $\beta_c = \beta_F$ in Eq.s(6.8) and (6.9) or using Fig. C6.3.

C.6.5.2 Damage to coupling beams observed following numerous earthquakes has revealed that coupling beams with conventional reinforcement (i.e. with reinforcement arranged along the principle axes as in a typical RC beam) are only able to sustain limited storey drifts owing to the high deformation demands to which they are subjected to. With the introduction of diagonal reinforcing bars, as required in many international seismic codes, the deformation capacity can be significantly improved. The expressions shown here are taken from the recommendations of Priestley et al. (2007).

C.6.6 Research into the DDBD of steel concentrically braced frame (CBF) structures has been undertaken by Della Corte and Mazzolani (2009), Wijesundara (2010), and Akçelyan (2011) amongst others. However, as research in the area is on-going, this model code only specifies that rational analyses be used for their design. Preliminary guidelines are included in Annex 5.

C.6.7 Little work has been done on the DDBD of EBF systems and further research is required. Preliminary guidelines are provided in Annex 5.

CODE	COMMENTARY

6.8 Steel Buckling-Restrained Braced Frame Systems (BRB systems): Both the yielding and the design displacement profiles shall be defined by rational analysis.

Generally, the i-th storey drift angle can be decomposed into the summation of the contribution from braces, $\theta_{br,i}$, and the contribution from columns, $\theta_{col,i}$.

At yielding, the brace contribution to the i-th storey drift angle can be calculated as:

$$\theta_{br,i,y} = \frac{2\varepsilon_y / \gamma_i}{\sin 2\alpha_i} \tag{6.25}$$

in which γ_i is a function of the brace characteristics, quantified using Eq.(6.26).

$$\gamma = \frac{1}{\left(\dfrac{L_{core}}{L_{br}} + \displaystyle\sum_{i=1}^{t} \dfrac{A_{core}}{A_i} \dfrac{L_i}{L_{br}} \right)} \tag{6.26}$$

where t indicates the total number of tapered sections of the cross section of the BRB, L_i and A_i are the length and cross section area of the i-th tapering, L_{core} and A_{core} are length and cross section of the yielding core, L_{br} is the node-to-node length of the brace.

The column contribution can be calculated as:

$$\theta_{col,i} = \varepsilon_{c,iy} \left(\tan \alpha_i + \frac{2}{L_{br}} \sum_{i=1}^{n-1} h_i \right) \tag{6.27}$$

in which the axial strain in the columns ($\varepsilon_{c,i,y}$) can be assumed to be a fraction of the buckling value using the ρ factor:

$$\varepsilon_{c,y} = \rho \chi_{br,i} \varepsilon_y \text{ with } \rho < 1 \tag{6.28}$$

The limit state value of the i-th storey drift angle can subsequently be calculated as:

$$\theta_{i,ls} = \mu_d \theta_{br,i,y} + h_p \theta_{col,i,y} \tag{6.29}$$

in which μ_d is the design ductility and h_p is the expected strain hardening ratio of braces.

C6.8 The recommendations provided here for the displacement-based seismic design of steel BRB systems, stem from the work of Della Corte (2006).

BRB's are often constructed with an internal core that includes a number of tapered sections, intended to facilitate the capacity design protection of the brace connections. In this way inelastic response is expected to be concentrated in the critical (smaller) tapered section.

CODE

6.9 Unreinforced Masonry Buildings: The design displacement profile shall be defined by rational analysis, or, for buildings of up to three storeys in height, by the relevant form of Eq.(6.30) or Eq.(6.31).

For soft-storey mechanisms:

For $h_i < h_{ss}$:
$$\Delta_{i,ls} = 0.002 h_i \qquad (6.30a)$$

For $h_i \geq h_{ss}$:
$$\Delta_{i,ls} = 0.002 h_{ss-1} + \theta_c \left(h_{ss} - h_{ss-1} \right) \qquad (6.30b)$$

For distributed mechanisms:
$$\Delta_{i,ls} = \theta_c h_i \qquad (6.31)$$

where the critical design storey drift limit, θ_c, shall be determined by relating the chord rotation limits indicated in Table 2.4 to equivalent storey drift values.

COMMENTARY

C6.9 Various failure modes can develop in Masonry Structures (see, for example, Priestley et al. 2007) and there are many different types of masonry (stone, clay, concrete etc.) to consider. The deformation capacity of the masonry will depend on the type of masonry and the mechanism expected. Fig. C6.5 illustrates the displacement profiles associated with Eq.(6.30) and Eq.(6.31), which distinguish between masonry structures that will develop soft-storey mechanisms versus distributed mechanisms.
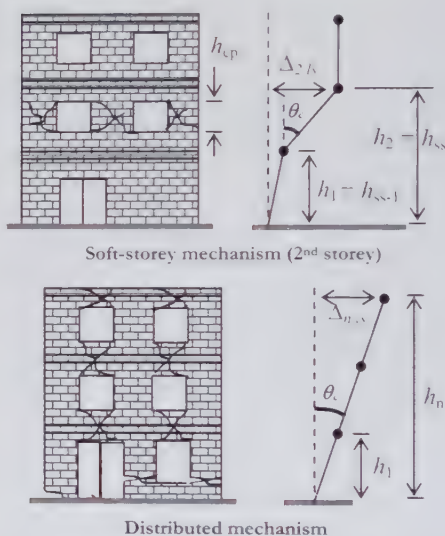

Soft-storey mechanism (2nd storey)

Distributed mechanism

Fig. C6.5: Displacement profile for Masonry Structures as per Eq.(6.30) (top) and Eq.(6.31) (bottom).

While for other construction materials a soft-storey mechanism can be avoided through good detailing, this is not always possible for masonry structures due to architectural requirements. In order to account for this in design, Eq.(6.30) permits masonry structures to be designed for a soft-storey mechanism, but note that this will typically require greater overall design base shear because of the lower displacement capacity that the system will possess.

Care is required in order to convert the chord rotation limits of Table 2.5 into equivalent storey drift values for use in Eq.(6.30) and Eq.(6.31). For example, considering the soft-storey mechanism in the upper part of Fig. C6.5,

CODE

6.10 Timber Buildings: The design displacement profile shall be defined by rational analysis. Expressions for the design displacements of some typical timber structural forms are provided in the following subsections.

6.10.1 Timber Portal Structures with Annular Bolted Joints: For SDOF timber portal structures with moment resisting joints formed of an annular arrangement of dowels, the design displacement of Eq.(5.2) can be directly obtained from:

$$\Delta_d = \Delta_j + \Delta_s \quad (6.32)$$

where Δ_j is the displacement due to rigid body rotation of columns as a consequence of joint deformations, and Δ_s is the elastic deformation of the portal, calculated assuming the joints to be rigid.

When gravity load effects are neglected, the joint deformation component Δ_j can be approximated using Eq.(6.33).

$$\Delta_{j,0} = \delta_{ls} \cdot \frac{\gamma_t \beta_t . h_{col} / L \cdot}{1 + \gamma_t \beta_t . L / h_{col}} \quad (6.33)$$

where δ_{ls} is the deformation limit of the dowel from Table 2.3; h_{col} is the height of the column and L the length of the portal frame; $\gamma_t = L/h_b$ is the ratio between the length of the portal and the depth h_b of the section; $\beta_t = h_b/r$ is the ratio between the depth of the section and the external radius r of the annular joint.

COMMENTARY

if the masonry piers have a clear height of h_{cp} and are set a chord rotation limit for the no-collapse limit state of θ_p (selected from Table 2.5 considering whether a flexure or shear-type mechanism is likely), then the storey drift limit θ_c would be $\theta_c = \theta_p . h_{cp}/(h_2-h_1)$.

Note also that the design displacement profiles indicated in Eq.(6.30) and Eq.(6.31) should be considered as preliminary since only a limited amount of experimental data was available to validate the expressions. Future research should aim to improve the expressions and account for different masonry types.

C6.10.1 Eq. (6.33) is that formulated by Zonta et al. (2006) for the ultimate limit state of annular bolted joints of the type shown in Fig. C6.6.
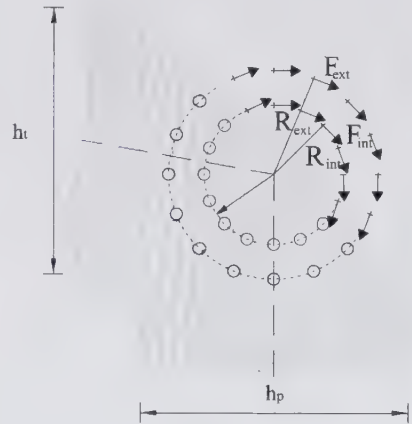

Fig. C6.6: Bolted annualar joint configuration considered by Zonta et al. (2006).

Eq.(6.33) has been generalized from the form proposed by Zonta et al. (2006) in order to permit consideration of different limit states through substitution of the dowel deformation limits indicated in Table 2.3 into Eq.(6.33). For simplicity, in formulating Eq.(6.33) Zonta et al. (2006) assume that all of the fasteners are located in a single circular pattern, of radius r and the connection is subject to both shear V and moment M. Zonta et al. (2006) further assume that the relation $M=VH$ holds for the portal and that the ultimate distribution of forces on dowels

CODE	COMMENTARY

CODE

To account for gravity load effects, the displacement from Eq.(6.33) is reduced as shown:

$$\Delta_t - \Delta_{t,u} \cdot \left(1 - \frac{q}{q_{\lim}}\right)$$

(6.34)

where q is the design gravity load for the seismic combination, and $q_{\lim}$ is the ultimate gravity load.

If a more precise model is not used, and second order effects can be neglected, $q_{\lim}$ can be taken as:

$$q_{\lim} = 24\pi \frac{F_{u,k}}{i(\gamma_t \beta_t)^2}$$

(6.35)

where p is the pitch between two dowels and $F_{u,k}$ is the ultimate characteristic shear capacity of a single dowel.

If a more precise model is not used, the following approximate expression of the elastic deformation of the portal, Δ_s, can be used:

$$\Delta_s \cong \frac{h_{col}}{2000}\gamma_t(\theta+1)$$

(6.36)

COMMENTARY

is proportional to that in the elastic state. Zonta et al. (2006) require that $\beta_t=h/r$ must be greater than 2 and is typically between 2.5 and 3. Furthermore, an approximate expression of β_t, proposed by Loss (2007), is:

$$\beta_t = 1/(0.5-4\phi\gamma_t/L)$$

(C6.1)

where ϕ is the diameter of the dowel.
The basis of Eq.(6.34) is detailed in Loss (2007).

The displacement component associated with the deformations of structural members, Δ_s, given by Eq.(6.36) is based on the elastic relation:

$$\Delta = \Delta + \Delta_{s,2} \frac{MH^2}{3EI_c} + \frac{M}{6EI_b}LH$$

(C6.2)

where E is the timber elastic modulus, and I_b and I_c are the moments of inertia of the beam and the column, respectively. Eq.(C6.2) depends on the member characteristics, but can be rearranged assuming some simplifications. If the portal is appropriately designed, the beam yielding moment $M_{R,c}$ should be greater than the joint ultimate resisting moment M_u such that $M_u=\alpha M_{R,c}$ where α is an over-strength factor.

Thus, Eq. C6.2 can be rewritten as:

$$\Delta_s = \frac{M}{3EI_b}\left(\frac{I_b}{I_c}H^2+\frac{HL}{2}\right)=\frac{HL}{3\alpha}\frac{M_{R,b}}{EI_b}\left(\frac{H}{L}\frac{I_b}{I_c}+\frac{1}{2}\right)$$
$$=\frac{HL}{3\alpha}\frac{2\varepsilon_y}{h}\left(\frac{I_b}{I_c}+\frac{\theta}{2}\right)=\frac{2}{3\alpha}\left(\theta\frac{I_b}{I_c}+\frac{1}{2}\right)H\gamma_t\varepsilon_y$$

(C6.3)

where ε_y is the yield strain of timber and $\theta=H/L$ is the aspect ratio of the portal. Reasonable values for yield strain and over-strength factor are $\varepsilon_y=0.002$ and $\alpha=1.2$-1.3, respectively. Note that for a typical warehouse building one might expect that $I_b/I_c \cong b_b/b_c=1.0$-0.5. Using the conservative value of $I_b/I_c=0.5$, the expression of Δ_s reduces to Eq.(6.36).

CODE

6.10.2 Timber Framed Wall Structures: The design displacement profile shall be defined by rational analysis, or by Eq.(6.37).

$$\Delta_{i.ls} = \theta_c h_i \qquad (6.37)$$

where θ_c is taken from Table 2.5 for the relevant design intensity level.

6.10.3 Pre-stressed Timber Structures: The design displacement profile of pre-stressed timber MRF structures shall be defined by rational analysis or by Eq.(6.2). The design displacement profile of pre-stressed timber wall structures shall be defined by rational analysis.

6.11 Bridge Structures:

6.11.1 Longitudinal Response: The design displacement profile shall be defined by rational analysis, or, for single deck bridges, by assuming that the deck translates as a rigid body. The design displacement shall then be limited by the critical pier or abutment member deformation.

COMMENTARY

C6.10.2 A linear displacement profile is proposed for timber-framed wall structures as it is anticipated that these structures do not exceed three to four storeys in height and are regular in elevation.
However, research by Moayed Alaee (2011) into the design of light-gauge steel-framed walls clad with timber panels has shown that at high intensity levels such systems will tend to develop soft-storey type displacement profiles. Nevertheless, if the drift limits in Table 2.5 are adopted, then it is expected that the linear profile will lead to acceptable seismic response.

C6.10.3 Section 6.10.3 refers to pre-stressed timber frame and wall structures with hybrid joints (see, for example, Palermo et al. 2006, Iqbal et al. 2008, Marriot 2009, Newcombe 2012). Newcombe (2012) found that the general design displacement profile for MRFs provided in Section 6.2 performs acceptably for pre-stressed timber frame systems. For pre-stressed timber wall systems, Newcombe (2012) found that a linear design displacement profile for pre-stressed timber walls is reasonable but that a non-linear design displacement profile (that considers shear and flexural deformations) would be more appropriate for the final design.

C6.11.1 It is typically assumed (see Priestley et al. 2007) that the deck is axially rigid, imposing the same displacement demands along the length of the bridge in the longitudinal direction. Note that this approximation may be inappropriate for the case of very long bridges.

C6.11.2 The displacement profile of bridges for response in the transverse direction of excitation can require an iterative design approach to establish accurately. However, if symmetrical piers are utilised, then it should be expected that the longitudinal design direction provides the critical design strength for the piers (refer Priestley et al. 2007).
In establishing the displaced shape in the transverse direction (represented in Eq.(6.38) by the δ_i and δ_c components), consideration should be given to the 1st mode force distribution

CODE

6.11.2 Transverse Response: The design displacement profile shall be defined by rational analysis, or for regular bridge types with stiff continuous decks using Eq.(6.38) and Table 6.1.

$$\Delta_{i,ls} = \delta_i \cdot \left(\frac{\Delta_c}{\delta_c}\right) \tag{6.38}$$

where δ_i is the inelastic first mode shape at point i, and δ_c is the inelastic first mode shape at point c, both of which are obtained from the relevant equation referenced in Table 6.1, and Δ_c is the displacement of the critical pier.

The decks shall be considered "stiff" if the ratio of their lateral sectional stiffness, EI_{deck}, to the pier sectional stiffness, EI_{pier}, satisfies Eq.(6.39).

$$\frac{48EI_{deck}}{C_p n_{piers} EI_{pier}} \left(\frac{H_{pier}}{L_d}\right)^3 \geq 0.02 \tag{6.39}$$

where H_{pier} can be taken as the average pier height, n_{piers} is the total number of piers, L_d is the length of the bridge deck between abutment points and C_p is a coefficient to account for pier fixity which can be taken equal to 3 for pinned-fixed piers and 12 for fixed-fixed piers.

Table 6.1: Transverse displacement shapes for regular continuous deck bridges

Pier Configuration		Abutment Type	Disp. Shape
Uniform	◿ⵔ	Pinned	Eq. 6.40
Uniform	ⵔ	Free	Eq. 6.41
Valley	◿ⵔ	Pinned	Eq. 6.40
Valley Ridge	ⵔ	Free	Eq. 6.42

$$\delta_i = \frac{16}{5L_d^4}\left(x^4 - 2L_d x^3 + L_d^3 x\right) \tag{6.40}$$

$$\delta_i = 1.0 \tag{6.41}$$

$$\delta_i = 1.5 - \frac{8}{5L_d^4}\left(x^4 - 2L_d x^3 + L_d^3 x\right) \tag{6.42}$$

COMMENTARY

expected at peak displacement response. For a bridge with lateral restraint at the abutments, part of the seismic inertia forces will be carried back by superstructure bending to the abutments, with the remainder being transmitted to the pier foundations by column bending. The superstructure lateral stiffness will normally be known at the start of the seismic design, but the effective stiffness of each pier will depend on its strength and ductility demand, and hence will not initially be known. This again implies that an iterative design approach will be needed.

The displacement profiles indicated in Table 6.1 and the deck stiffness limits are approximate expressions aimed at providing reasonable design strengths. For irregular bridge structures that do not match the configurations indicated in Table 6.1, it is recommended that non-linear time-history analyses be used to verify the seismic performance and finalise the design.

For guidance on the DDBD of cable-stayed bridges see Calvi et al. (2011). For guidance on the DDBD of RC arch-deck bridges, see Khan and Sullivan (2011).

CODE

6.12 Isolated Structures: The design displacement profile shall be defined by rational analysis. The displacement (D_d) of the seismic isolation system of buildings and bridges shall be properly selected, as a function of the type of isolation system utilized, the characteristics of the super- and sub-structure, the soil type and the earthquake design intensity (refer Table 1.1).

6.12.1 Base Isolated Buildings

For regular framed buildings with rigid diaphragms, the design displacement profile shall be defined by rational analyses or through the use of Eq.(6.43):

$$\Delta_{i,ls} = D_d + \theta_c h_i \qquad (6.43)$$

where D_d is target displacement of the isolation system, θ_c is the critical (minimum) design storey drift limit over the building height. The drift limit shall be set considering both non-structural limits (indicated in Table 2.1) and serviceability deformation limits for structural elements (level 1 of Table 2.3 and 2.5).

COMMENTARY

C6.12 Well designed isolated structures will ensure that deformations are principally concentrated at the isolation level.

The permissible displacement of an isolation system will depend greatly on the characteristics of the isolation system selected. Displacement ranges for different types of isolation device should be provided by manufacturers. Designers are encouraged to select isolation devices with large displacement capacity as this will generally lead to better performance in earthquakes of greater intensity. In addition to considering the maximum displacement capacity of an isolation device, designers can identify a minimum displacement demand on the isolation devices that will keep the accelerations experienced by the overlying superstructure low and ensure that seismic isolation is an effective structural solution. Cardone et al. (2010) provide guidance for the optimum selection of an isolation device's design displacement.

C6.12.1 The fundamental design requirement of base isolated buildings is that a serviceability performance level should be met for levels of seismic intensity specified in Table 1.1.

The limit state displacement profile indicated by Eq.(6.43) is illustrated in Fig.C6.7. The target displacement of the isolation system should be set large enough to significantly reduce acceleration and deformation demands on the overlying structure but small enough to satisfy deformation limits of the devices themselves (manufacturers should provide guidance on device deformation limits). Above the isolation level a linear displaced shape is set in proportion to the serviceability deformation limits of the overlying building. The structural displacements are added to the base level displacements of the isolation devices, as can be seen in Fig.C6.7. Cardone et al. (2009) report more refined expressions for the displaced shape of base isolated RC frame buildings. However, Eq.(6.43) is proposed here due to its general validity for a range of structural forms (including isolated RC wall buildings) and because the use of Eq.(6.43) in place of more refined expressions is not expected to lead to a significant loss of accuracy. With increased seismic intensity, significant increases in displacement demand should only
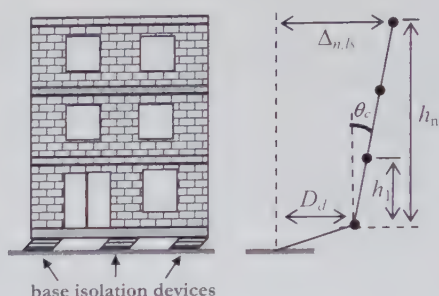
CODE

COMMENTARY

Fig. C6.7: Displacement profile for base-isolated buildings as per Eq.(6.42).

occur at the isolation level, with the overlying structure being effectively "isolated", remaining in the elastic range. This implies that the deformations of the overlying structure should be no greater than the non-structural drift limits or the elastic deformation capacity of the structure.

6.12.2 Isolated Bridges: The design displacement profile should be defined by assuming that the deck translates as a rigid body both in the longitudinal and transverse direction. The same approach should be followed for both continuous deck and simply supported deck bridges.

The design displacement amplitude of the deck in each direction shall be limited by the most critical of the isolation system design displacement, pier drift limit or deck joint deformation limits.

C6.12.2 The key aspect of the DDBD of bridges with seismic isolation is the definition of a uniform target displacement of the deck, which is assigned by the designer to accomplish given performance levels, expressed through limit values of the maximum isolation system displacement and of the pier drift.

The uniform translation of the deck is guaranteed by the selection of a suitable distribution of IS effective stiffnesses, which is determined by centring the centre of stiffness of the isolated pier systems with respect to the centre of mass of the bridge.

The DDBD of bridges with seismic isolation is based on the general performance objective that the full serviceability of the bridge should be maintained after the design earthquake. In order to satisfy this general requirement, the design must comply with the following criteria: (i) the seismic response of the superstructure (deck, movement joints, restrainers) and substructures (piers, abutments, foundations) must remain elastic, (ii) due to the critical role of its displacement capacity for the safety of the entire structure, the isolation system must be able to sustain a maximum horizontal displacement greater than that generated by the design earthquake, (iii) adequate clearance should be provided to the movement joints, in order to

CODE

COMMENTARY

accommodate the isolation system displacements, in both longitudinal and transverse direction, thus avoiding impacts between structural elements or damage to movement joints.

6.13 Structures with Added Damping: The design displacement profile for systems incorporating added damping devices shall be defined by rational analysis, taking into account the relative magnitude and distribution of damping forces.

C6.13 When evaluating the likely displacement profile of structures with added damping, a distinction should be made between linear and non-linear viscous dampers (see Fig.C6.8).
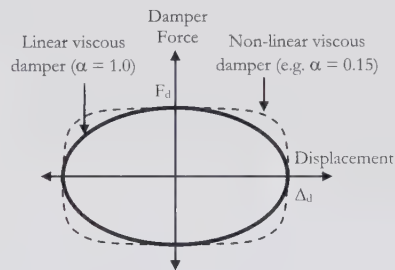

Fig. C6.8: Force-displacement response of linear and non-linear viscous dampers.

Research by Lago (2011) has indicated that for MRFs with linear viscous dampers located in diagonal braces at every storey of the building, the displaced shape is relatively insensitive to the distribution of damper properties. In contrast, it was found that the displaced shape can be altered significantly if dampers are located in an irregular manner (e.g. at single storey levels or over the top or bottom half of the building). For RC wall buildings Lago (2011) found that the displaced shape is relatively insensitive to the location of linear viscous dampers.

In the case that structures are fitted with non-linear viscous dampers (e.g. $\alpha = 0.15$) the damper hysteretic response approaches that of a friction slider with significant damping forces present close to peak displacement response. As a consequence, the displaced shape of both frame and wall structures at peak response can be significantly modified by the presence of non-linear viscous dampers. For information on the displaced shape of structures fitted with dampers, see Lago (2011).

<div style="display: flex;">
<div style="flex: 1;">

CODE

6.14 Retaining Structures:

6.14.1 Cantilever Diaphragm Walls: The design displacement profile shall be defined by rational analysis, or using Eq.(6.44):

$$\Delta_i = \theta_c \frac{1}{3H^3}\left(z_i^4 - 4Hz_i^3 + 6H^2z_i^2\right) \qquad (6.44)$$

or more simply through Eq.(6.45):

$$\Delta_i = \theta_c z_i \qquad (6.45)$$

In Eq.s (6.44) and (6.45), z_i is the distance from the buried end of the wall to point i, and H is the total height of the wall, including the embedment depth, d.

6.15 Floor Diaphragm Flexibility: In building structures, floor diaphragms shall be detailed to act as rigid diaphragms in-plane or the increase in storey drifts due to diaphragm flexibility shall be accounted for.

For flexible diaphragms, the additional storey drift, θ_{dia}, due to diaphragm deformations shall be defined through rational analysis.

</div>
<div style="flex: 1;">

COMMENTARY

C6.14.1 The approximate expression given by Eq.(6.45) implies a linear displacement profile leading to a maximum displacement at the top of the wall, Δ_{max}. Note that θ_c is conservatively assumed equal to the residual drift limit, θ_r, for cantilever retaining walls. Another plausible choice of the displacement pattern could be to use the 1st mode of vibration of a flexural-type cantilever beam. However, the effect of the difference in displacement profiles on the results has been found to be rather small (see Pane et al. 2007, and Vecchietti 2008).

C6.15 For normal well proportioned buildings, floors constructed with continuous reinforced concrete slabs will provide rigid diaphragm behaviour. However, flexible floor diaphragms have been observed (Nakaki 2000, Fleischman et al. 2002, Rivera 2009, Lavelle 2009) to increase storey drifts in building structures. For RC wall systems with flexible floors, increases in storey drift were observed by Rivera (2009) to typically be a maximum at the top and bottom storey of the buildings.

For interior floor segments (i.e. floor segments that span between two vertical lateral load resisting systems), the additional storey drift, θ_{dia}, due to diaphragm deformations can be approximated by:

$$\theta_{dia} = \frac{L_{dia,c}^2}{h_s 8k_{cr}} \frac{EFA.m_i g}{L_{dia}}\left[\frac{C_F L_{dia,c}^2}{48EI} + \frac{1}{GA}\right] \quad (C6.4)$$

where m_i is the seismic mass of storey i, g is the acceleration due to gravity, L_{dia} is the total length of the floor diaphragm measured perpendicular to the direction of excitation, $L_{dia,c}$ is the maximum clear length of the diaphragm segment between vertical lateral load resisting systems, E, G, I and A_r are the modulus of elasticity, shear modulus, second moment of inertia and shear area respectively of the floor diaphragm, h_s is the storey height (distance between floor centres) and k_{cr} is a factor to account for stiffness reductions due to cracking in the case of concrete floor systems. The term EFA refers to the expected floor acceleration at the development of peak storey drifts. The EFA should be defined through rational analysis or can be approximated

</div>
</div>

CODE

COMMENTARY

as 1.5 times the PGA for the site at the design intensity level under consideration.

For RC floors the value of k_{cr} can be obtained through sectional analysis or for solid RC floors from:

$$k_{cr} = \frac{I_{cr}}{I_{gr}} = 2.1\rho \frac{E_s}{E_c} \qquad (C6.5)$$

where ρ is the percentage of longitudinal reinforcement in the slab (area longitudinal reinforcement divided by section area), E_s is the reinforcing steel modulus of elasticity and E_c is the concrete modulus of elasticity.

The storey drift proposed by Eq.(C6.4) is based on the general equation for displacement of a simply supported beam subject to a uniform load, in line with the recommendations of Nakaki (2000) and Rivera (2009). The C_F constant is proposed to allow for different slab constraint conditions and adopts a value of $C_F = 5.0$ if the ends of the floor are free to rotate and a value of $C_F = 1.0$ if the ends of slab are free, as illustrated in Fig. C6.9.
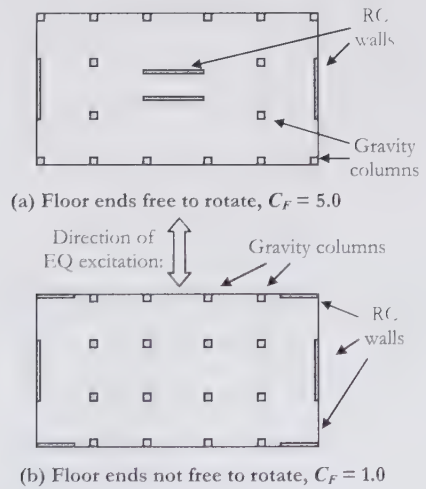

(a) Floor ends free to rotate, $C_F = 5.0$

(b) Floor ends not free to rotate, $C_F = 1.0$

Fig. C6.9: Example of structural layouts that would provide different floor restraint constants, C_F, for use in Eq. C6.4.

CODE	COMMENTARY

COMMENTARY

In order to provide a simplified means of predicting the storey drifts due to diaphragm flexibility, Eq.(C6.4) assumes that the first floor acceleration can be used to estimate the drift component for any given floor. Furthermore, rather than undertake a specific spectral analysis, it is proposed (in line with the findings of Rivera, 2009) that for RC wall structures the peak acceleration of the first floor can be assumed equal to the spectral acceleration plateau which is typically 2.5 times the PGA, and for frame structures a lower value of 80% the spectral plateau (i.e. 2.0 times the PGA) is suggested.

However, the use of the peak floor acceleration in Eq.(C6.4) is expected to be too conservative since the peak floor acceleration is not expected to occur at the same instant in time as the peak storey drifts. In addition, Eq.(C6.4) utilises a uniform acceleration profile along the length of the floor whereas it is expected that peak accelerations occur at floor mid-span and then reduce closer to the supports. As such, the EFA proposed for use in Eq.(C6.4) has been set at 1.5 times the PGA. Future research should better quantify what this acceleration should be. Refer to C9.3.7 for further discussion of floor diaphragm forces.

Depending on the location of lateral force resisting systems within the floor plate, alternative drift expressions could be more appropriate. For example, in the case of floor diaphragms that are supported laterally only from one edge (e.g. central core wall systems) the diaphragm drift component might be estimated as 0.6 times the value obtained from Eq.(C6.4) with the $L_{dia,t}$ term set equal to twice the maximum distance from the floor edge to the vertical lateral load resisting system and with C_F =5.0.

CODE

7. EQUIVALENT VISCOUS DAMPING

The equivalent viscous damping (EVD) to be used to characterize the design displacement spectrum for the equivalent **SDOF** system, in accordance with Section 1.5, shall be determined from results of comprehensive inelastic dynamic analyses of structures with similar structural materials and forms as the structure under consideration. In lieu of such analyses the expressions provided in the following sections may be utilised.

A number of the EVD expressions refer to the displacement ductility, which is given by:

$$\mu = \Delta_d / \Delta_y \qquad (7.1)$$

7.1 EVD of Concrete Wall Buildings:

The equivalent viscous damping of RC wall structures well detailed to provide flexural plastic hinging shall be obtained from rational analyses or from Eq.(7.2).

$$\xi_{eq} = 0.05 + 0.444 \left(\frac{\mu - 1}{\mu \pi} \right) \qquad (7.2)$$

with the yield displacement obtained from rational structural analysis or, for wall structures with aspect ratio greater than 3.0, from Eq.(7.3).

$$\Delta_y = \frac{\phi_y}{2} H_e^2 \left(1 - \frac{H_e}{3H_n} \right) \qquad (7.3)$$

where ϕ_y is the yield curvature of the wall that can be estimated using the expressions provided in Annex 1, and the effective height, H_e, shall be determined in accordance with Section 5.7.

COMMENTARY

C7. Equivalent viscous damping is utilised within the Direct DBD approach to account for the effect that energy dissipation has on the dynamic response. Traditional area-based formulations for equivalent viscous damping (Jacobsen, 1960) are not able to successfully predict the response of certain hysteretic types. The equivalent viscous damping approach adopted here is based on adjusting area-based equivalent viscous damping expressions to match the results of non-linear time-history analyses.

The damping to be used is equivalent to the sum of the elastic and hysteretic damping of the structure, and is calibrated by inelastic time-history analyses using realistic estimates of elastic damping, and hysteretic response. It is important that simplistic rules, such as the elastic-perfectly-plastic rule, with elastic damping of $\xi_e = 0.05$ not be used unless the structure is actually characterised by such behaviour.

For background on the calibrated equivalent viscous damping expressions refer to Grant et al. (2005), Dwairi et al. (2007) and Pennucci et al. (2011).

C7.1 The equivalent viscous damping expression provided for RC wall structures assumes that the hysteretic response is characterised by the Takeda model (Otani, 1981) with the parameters β=0.0 and α=0.5 as per Fig. C7.1.
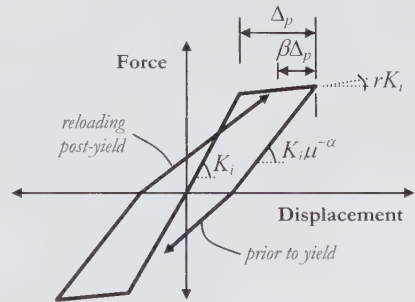

Fig. C7.1: Takeda hysteretic model typically used to characterise RC systems.

For RC wall structures with aspect ratio less than 3.0 shear deformations are likely to contribute significantly to the apparent yield displacement of the walls and should therefore be accounted for.

CODE

COMMENTARY

Note that in addition, Eq.(7.2) is only valid for walls with hysteretic properties that do not exhibit strength degradation. As such, if the yield mechanism is expected to be a mixed flexural-shear or pure shear type (to be avoided), then alternative expressions would be required.

As explained in the preface and the commentary to Section 1.5, the equivalent viscous damping expression of Eq.(7.2) should be used in combination with the spectral displacement reduction expressions provided in Section 1.5.1.

7.2 EVD of Concrete Frame Buildings: The equivalent viscous damping of well detailed RC frame structures shall be obtained from rational analyses or from Eq.(7.4).

$$\xi_{eq} = 0.05 + 0.565 \left(\frac{\mu - 1}{\mu \pi} \right) \qquad (7.4)$$

where μ is obtained from Eq.(7.1), with the yield displacement determined at the effective height of the structure (refer Section 5.7). The yield displacement shall be obtained from rational structural analysis.

C7.2 The equivalent viscous damping of RC frame structures is higher than RC walls because the beams are not typically subject to high axial loads, and as such, relatively "fat" hysteresis loops can be expected. Eq.(7.4) is a calibrated expression for systems with Takeda (Otani, 1981) hysteretic response with the parameters β=0.6 and α=0.3 (refer Fig.C7.1).

As explained in the preface and the commentary to section 1.5, the equivalent viscous damping expression of Eq.(7.4) should be used in combination with the spectral displacement reduction expressions provided in Section 1.5.1.

In order to obtain the yield displacement of RC frames for use in Eq.(7.4), one possibility is to use Eq.(C7.1):

$$\Delta_y = H_e \theta_y \qquad (C7.1)$$

For a given bay x, Eq.(C7.2) can be used to compute the bay yield drift.

$$\theta_{y,x} = 0.5 \varepsilon_y \frac{L_{b,x}}{h_{b,x}} \qquad (C7.2)$$

Expression Eq.(C7.2) was developed by Priestley (1998) and provides a simplified means of estimating the yield drift of an RC frame taking into consideration the beam and column flexural and shear deformations as well as beam-column joint deformations. The expression is supported by experimental results obtained from a large number of RC beam-column sub-assemblage tests.

CODE

COMMENTARY

For frames possessing bays of varying length, the yield drift for each bay should be computed at the level of interest. The proportion of overturning to be resisted by each bay is then used to establish a weighted-average value for the frame yield drift, in accordance with Eq.(C7.3).

$$\theta_{y,i} = \frac{\sum_{x=1}^{n_b} M_x \theta_{yx}}{M_{frame,i}} \tag{C7.3}$$

As an alternative to Eq.(C7.1), one can compute the frame equivalent viscous damping in a more refined manner using Eq.(C7.4):

$$\xi_{eq} = \frac{\sum_{i=1}^{n} \xi_i V_i \theta_i}{\sum_{i=1}^{n} V_i \theta_i} \tag{C7.4}$$

where the equivalent viscous damping of each storey, ξ_i, is first calculated by dividing the design storey drift, θ_i, by the storey yield drift, $\theta_{y,i}$, (from Eq.C7.3). The storey damping values are then combined to obtain the system damping through the weighted average expression of Eq.(C7.4). Note that while absolute values of storey shear, V_i, are not known at the start of the design procedure, only the storey shear proportions are required to use Eq.(C7.4) and these proportions can be obtained using the equivalent lateral force distribution indicated in Chapter 8.

7.3 EVD of Pre-Cast RC Structures: The equivalent viscous damping of pre-cast concrete frame and pre-cast concrete wall structures shall be evaluated with due consideration of the joint details adopted.

For connection details in pre-cast systems that ensure plastic hinges form within the concrete elements of the structure, the equivalent viscous damping may be approximated as per Eq.(7.5) for frames and Eq.(7.6) for walls and cantilever column structures.

$$\xi_{eq} = 0.05 + 0.565 \left(\frac{\mu - 1}{\mu \pi} \right) \tag{7.5}$$

C7.3 Special care should be taken in the yield curvature estimation of pre-cast concrete structures. Some types of foundation to column connections, like the case of grouted sleeves solutions where the spliced reinforcement coming from the foundation is placed in steel ducts inside the column end and then grouted with special low shrinkage grouts, lead to a yield curvature greater than one might estimate using expressions for traditional in-situ RC sections. Underestimation of the yield curvature leads to an over prediction of the system ductility and system damping which leads to a under prediction of the required design shear.

<table>
<tr><td>

CODE

$$\xi_{eq} = 0.05 + 0.444.\left(\frac{\mu - 1}{\mu\pi}\right) \qquad (7.6)$$

The ductility demand, μ, for pre-cast structures should be calculated from rational structural analysis that considers member deformations and the deformations of the joint details adopted.

Pre-cast connections formed with grouted bars
For the particular case of pre-cast connections formed with grouted bars, the equivalent viscous damping may be approximated as per Eq.(7.7) for frames and Eq.(7.8) for walls and cantilever column structures:

$$\xi_{eq} = 0.05 + 0.25.\left(1 - \frac{1}{\mu^{0.25}}\right) \qquad (7.7)$$

$$\xi_{eq} = 0.05 + 0.32.\left(1 - \frac{1}{\mu^{0.25}}\right) \qquad (7.8)$$

7.4 EVD of Hybrid Pre-stressed Frames and Walls: The equivalent viscous damping of well detailed prestressed structures combined with added energy dissipation devices that provide the structure with flag-shaped hysteretic response, shall be obtained from rational analyses or from Eq.(7.9):

$$\xi_{eq} = 0.05 + \frac{(0.063\lambda + 0.6)(1 - r)}{(\lambda + 1)(1 + r(\mu - 1))}\left(1 - \frac{1}{\mu}\right) \qquad (7.9)$$

where λ is the ratio of the prestressing resistance to the resistance of dissipation devices at peak response and μ is obtained from Eq.(7.1), with the yield displacement obtained from rational structural analysis.

</td><td>

COMMENTARY

Belleri and Riva (2008) calibrated an equivalent viscous damping expression for columns with pre-cast connections formed with grouted bars. The work considered an axial load ratio of 10% on the columns. The expression developed was of the form provided by Grant et al. (2005) in which the equivalent viscous damping is a function of the effective period. Eq.(7.7) is a simplified conservative form of the expression developed by Belleri and Riva (2008) that is independent of the effective period.
As explained in the preface and the commentary to section 1.5, the equivalent viscous damping expressions of Eq.s(7.5) to (7.8) should be used in combination with the spectral displacement reduction expressions provided in Section 1.5.1.

C.7.4 Hybrid pre-stressed frames and walls refers to systems such as those tested as part of the PRESSS program (Priestley et al. 1999) and elsewhere (eg. Christopoulos et al. 2002, Kurama and Shen 2004, Pampanin et al. 2006). The systems are characterised by flag-shaped hysteretic response similar to that illustrated in Fig. C7.2. Joints of hybrid systems resist seismic actions through a combination of pre-stressing (that provides self-centering capacity) and yielding non-prestressed reinforcement or other special devices that provide energy dissipation. The dynamic response of hybrid systems is considerably influenced by the factor λ, which is the ratio of the prestressing resistance, a, to the dampers bending resistance contribution, b (see Fig. C7.2). The equivalent viscous damping expression of Eq.(7.9) has been adapted from the work of Ceballos and Sullivan (2012) in which the results of non-linear time-history analyses were used to calibrate a general expression for the equivalent viscous damping of systems with flag-shaped hysteresis. It also agrees with the less general expression developed by Pennucci et al. (2009) for systems with λ=1.25. The expression should be used together with the spectral displacement reduction expressions provided in Section 1.5.1.
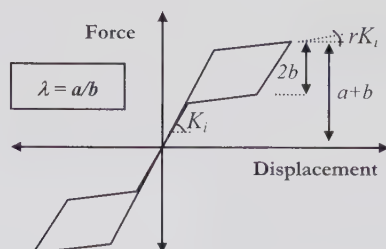
</td></tr>
</table>

CODE

COMMENTARY

Fig. C7.2: Flag shape hysteretic model typically used to characterise hybrid pre-stressed systems.

Yield drift expressions for hybrid systems should account for the proportions of strength provided by the pre-stressing in comparison to the mild reinforcement or other moment resisting components acting at the beam-column interface. See guidelines provided by the NZ Concrete Society (2010) for RC structures and Newcombe (2012) for timber pre-stressed structures.

7.5 EVD of Steel Frame Buildings: The equivalent viscous damping of well detailed steel moment-resisting frame structures shall be obtained from rational analyses or from Eq. (7.10).

$$\xi_{eq} = 0.05 + 0.577 \left(\frac{\mu - 1}{\mu \pi} \right) \tag{7.10}$$

where μ is obtained from Eq.(7.1), with the yield displacement obtained from rational structural analysis.

C7.5 The hysteretic behaviour on which Eq.(7.10) is based is the Ramberg-Osgood hysteretic model. The damping expression has been calibrated using the results of non-linear time-history analyses and should be used together with the spectral displacement reduction expressions of S1.5.1. If connection details or frame characteristics imply that a different hysteretic response should be anticipated then this should be accounted for in the equivalent viscous damping estimate.

In order to estimate the yield drift of steel frame structures, Priestley et al. (2007) propose the following expression:

$$\theta_y = 0.65 \varepsilon_y \frac{L_b}{h_b} \tag{C7.5}$$

As the expression is depth dependent, it requires that designers select a trial beam size (possibly from gravity design requirements) and iterate to find the appropriate seismic design solution. With knowledge of the storey yield drift, the yield displacement of a steel frame can then be obtained using the expressions provided in Section C7.2 for RC frames.

7.6 EVD of Dual Frame-Wall Buildings: The equivalent viscous damping of buildings possessing both structural frames and structural walls, shall be evaluated by firstly determining the damping of the individual frame and wall systems, using the relevant expressions from Sections 7.1 to 7.3. In evaluating the wall ductility

C7.6 For a given roof level displacement, the ductility demands on RC walls tend to be higher

CODE

for use within Eq.(7.2), the wall yield displacement shall be found substituting H_e for h_i in Eq.(6.10) if $H_e < H_{CF}$ and in Eq.(6.11) if $H_e > H_{CF}$. The frame-wall system damping value shall then be obtained by combining the damping components in accordance with Section 7.20.

7.7 EVD of Coupled RC Wall Buildings: The equivalent viscous damping of buildings possessing walls that are connected with coupling beams shall consider the degree of coupling. To quantify this, the factor β_C given by Eq.(6.14) can be used.
The system damping can be defined by:

$$\xi_{eq} = (1 - \beta_C)\xi_W + \beta_C \frac{\sum \xi_{CBi} V_{CBi}}{\sum V_{CBi}} \qquad (7.11)$$

where the wall damping, ξ_W, is obtained using Eq.(7.2) with the wall ductility defined according to Eq.(7.1) and with the wall yield displacement obtained by substituting $h_i = H_e$ in Eq.(6.10) if $H_e < H_{CF}$ and in Eq.(6.11) if $H_e > H_{CF}$.

The damping component for the coupling beam at level i, ξ_{CBi}, shall be obtained in accordance with:

$$\xi_{CBi} = 0.05 + 0.565\left(\frac{\mu_{CBi} - 1}{\mu_{CBi}\pi}\right) \qquad (7.12)$$

where μ_{CBi} is obtained from:

$$\mu_{CBi} = \theta_i / \theta_{yCBi} \qquad (7.13)$$

where θ_i is the storey drift associated with the design displacement profile (Section 6.5) and θ_{yCBi} is the coupling beam yield drift at level i, obtained in accordance with the following subsections.

7.7.1 Yield Drift of Traditionally Reinforced Coupling Beams: The yield drift of traditionally reinforced coupling beams shall be obtained from rational structural analysis or from:

$$\theta_{yCBi} = 0.5\phi_{yCB}\left(0.5L_{CB} + L_{sp}\right)\left(1 + F_V\right) \qquad (7.14)$$

where ϕ_{yCB} is the coupling beam yield curvature (see Annex 1), L_{CB} is the coupling beam clear length, L_{sp} is the strain penetration length which can be taken as $L_{sp} = 0.022 f_{ye} d_{bl}$ (f_{ye} in MPa) and

COMMENTARY

in dual frame-wall buildings because the frames restrain the upper levels of the wall, causing the wall curvatures to concentrate over the lower levels below a contraflexure height H_{CF}. In line with the Equivalent SDOF concept, the ductility demand for evaluation of the equivalent viscous damping offered by the RC walls should be evaluated at the effective height of the system. See Sullivan et al. (2006) for additional guidance.

C7.7 The equivalent viscous damping expression proposed for coupled wall buildings assumes that the hysteretic response of coupling beams is well characterised by the Takeda model (Otani, 1981) with the parameters $\beta=0.6$ and $\alpha=0.3$ (see Fig. C7.1) and should be used together with the spectral displacement reduction expressions of S1.5.1.

C7.7.1 The F_V coefficient has been proposed by Priestley et al. (2007) as a simplified means of accounting for shear deformations in the response of coupling beams. Analytical models for shear deformations in the inelastic range require further development and future research should aim to refine the manner with which shear deformations are accounted for in the DBD procedure.

CODE	COMMENTARY

CODE

F_V is a shear flexibility coefficient given by $F_I = 3(h_{CB}/L_{CB})^2$.

7.7.2 Yield Drift of Diagonally Reinforced Coupling Beams: The yield drift of diagonally reinforced coupling beams shall be obtained from rational structural analysis or from:

$$\theta_{yCBi} = 0.75\phi_{yCB}\left(0.5L_{CB} + L_{SP}\right) \qquad (7.15)$$

where the symbols are as per Eq.(7.14).

7.8 EVD of Steel Concentrically-Braced Frame Buildings: The equivalent viscous damping of steel concentrically braced frames buildings possessing tension-yielding braces that provide equal tension resistance in either direction of shaking can be obtained from:

For $\mu \leq 2$:
$$\xi_{eq} = 0.03 + \left(0.23 - \bar{\lambda}/15\right)\left(\mu - 1\right) \qquad (7.16a)$$

and for $\mu > 2$:
$$\xi_{eq} = 0.03 + \left(0.23 - \bar{\lambda}/15\right) \qquad (7.16b)$$

where μ shall be obtained from Eq.(7.1), and the yield displacement shall be obtained from rational structural analysis.

7.9 EVD of Steel Eccentrically-Braced Frame Buildings: The equivalent viscous damping of eccentrically braced steel frame buildings shall be obtained from rational analyses or from:

$$\xi_{eq} = 0.05 + 0.519\left(\frac{\mu - 1}{\mu\pi}\right) \qquad (7.17)$$

where μ shall be obtained from Eq.(7.1), and the yield displacement shall be obtained from rational structural analysis.

7.10 EVD of Steel Buildings with Buckling Restrained Braces: The equivalent viscous damping of buildings stabilised by steel buckling-restrained braces can be obtained from:

COMMENTARY

7.8 Work by Wijesundara et al. (2011) has shown that calibrated equivalent viscous damping values for CBF systems increase rapidly with non-linear response at low ductility levels and then remain fairly constant at high values of ductility, depending principally on the brace normalised slenderness. Eq.s (7.16a) and (7.16b) are taken from the work of Wijesundara et al. (2011) and should be used with the spectral displacement reduction expressions provided in S.1.5.1. Note that the studies undertaken by Wijesundara et al. (2011) assume the steel structures can rely on only 3% elastic damping.
For calculation of the ductility demand for use in Eq.(7.16), note that the ductility demand should be based on the tension brace ductility demand and not the buckling ductility demand, which is already accounted for within Eq.(7.16) through the dependency on the slenderness coefficient.

C7.9 The equivalent viscous damping expression shown for eccentrically-braced frame buildings corresponds to a bi-linear hysteretic shape (with $r = 0.2$). The expression was calibrated through non-linear time-history analyses by Grant et al. (2005) and Dwairi et al. (2007) and should be used together with the spectral displacement reduction expressions of S.1.5.1. Improved expressions that more accurately consider the hysteretic response of EBF systems should be developed as part of future work.

C7.10 The equivalent viscous damping expression shown for buckling restrained brace (BRB) systems corresponds to a bi-linear hysteretic shape (with $r = 0.2$). The expression

<div style="display:flex">
<div>

CODE

$$\xi_{eq} = 0.05 + 0.519\left(\frac{\mu - 1}{\mu\pi}\right) \qquad (7.18)$$

where μ is obtained from Eq.(7.1), with the yield displacement obtained from rational structural analysis or using the yield drift profile obtained from:

$$\theta_{iy} = \frac{2\varepsilon_y / \gamma_i}{\sin 2\alpha_i} + \rho\varepsilon_y \tan\alpha_i + 2\rho\varepsilon_y \frac{\sum_{i=1}^{n-1} h_i}{L} \qquad (7.19)$$

In which the axial strain in the columns can be assumed to be a fraction of the yielding strain of the column steel grade using the ρ factor.

$$\varepsilon_{c,y} = \rho\varepsilon_y \text{ with } \rho < 1 \qquad (7.20)$$

and the brace deformation components are a function of the brace characteristics, quantified through:

$$\gamma_i = 1 \Big/ \left(\frac{L_{core}}{L_{br}} + \sum_1^t \frac{A_{core}}{A_i}\frac{L_i}{L_{br}}\right) \qquad (7.21)$$

7.11 EVD of Composite Frame Structures:
The equivalent viscous damping of steel frames detailed to work compositely with concrete floors, and of steel columns detailed to work with concrete beams, shall be evaluated through rational analyses, with consideration of the likely hysteretic shape that the system will exhibit.

</div>
<div>

COMMENTARY

was calibrated through non-linear time-history analyses by Grant et al. (2005) and Dwairi et al. (2007). The expression should be used together with the spectral displacement reduction factors of S.1.5.1. Improved expressions that more accurately consider the hysteretic response of BRB systems should be developed as part of future work.

C7.11 At this stage no studies appear to have been done on the equivalent viscous damping of composite frame structures, and hence special studies are recommended. However, for a weak beam/strong column design of systems with concrete beams, the equivalent viscous damping may be assumed similar to that of concrete frames, since most of the hysteretic energy absorption will occur in the beams. It is also hypothesised that Eq.(7.4) will give reasonable results for steel beam concrete slab systems, since, comparing Eq.(7.4) with Eq.(7.10), it is apparent that there is little differences between the equivalent viscous damping expressions of steel frame and concrete frame systems.

In order to obtain a design value for the yield drift of composite frame systems, one can use Eq.(C7.6) which was verified analytically for composite frames by Norlund (2010).

$$\theta_{y,x} = 0.5\varepsilon_y \frac{L_{b,x}}{h_{b,x}} \qquad (C7.6)$$

</div>
</div>

CODE

7.12 EVD of RC Bridge Structures:

The equivalent viscous damping of RC bridge structures shall take into consideration the hysteretic properties of the various structural elements in the bridge. Expressions for typical RC bridge components are given in the following equations. A combined system value shall be obtained in accordance with the requirements of Section 7.20.

7.12.1 RC Bridge Piers:

Unless subject to special studies, the equivalent viscous damping of well detailed RC bridge piers shall be computed through:

$$\xi_{pier} = 0.05 + 0.444 \left(\frac{\mu - 1}{\mu \pi} \right) \qquad (7.22)$$

where μ is obtained from Eq.(7.1), with the yield displacement obtained from rational structural analysis or from:

$$\Delta_y = C_1 \phi_y \left(H_{pier} + C_3 L_{sp} \right)^2 \qquad (7.23)$$

where the strain penetration length is given by $L_{sp} = 0.022 f_y d_{bl}$, the section yield curvature can be obtained through sectional analysis or from Annex 1, and the coefficients C_1 and C_3 are dependent on the end fixity of the pier (Table 7.1).

Table 7.1: Fixity Coefficients of Bridge Piers

Pier End Conditions	C_1	C_3
Fixed-Pinned	1/3	1
Fixed-Fixed	1/6	2
Fixed-Flexible	$1/6*(1-C_2)^{-1}$	2

Where C_2 is given by:

$$C_2 = \frac{4EI_p \left(L_{S1}.L_{S2} \right)}{6I_{ss} \left(H_{pier} + L_{sp} \right) \left(L_{S1} + L_{S2} \right)} \qquad (7.24)$$

7.12.2 RC Bridge Decks and Abutments

Where bridge decks are restrained by abutments that are designed to respond elastically, the portion of load transferred through the deck to the abutments shall be assigned 5% (elastic) damping. Where the abutments are designed to yield, the hysteretic properties shall be considered in setting the equivalent viscous damping of the deck-abutment system.

COMMENTARY

C7.12 The equivalent viscous damping expression proposed by Eq.(7.22) for RC bridge piers assumes that the hysteretic response is characterised by the Takeda model (Otani, 1981) with the parameters β=0.0 and α=0.5. The expressions should be used together with the spectral displacement reduction expressions of S.1.5.1. In some cases this can be conservative, particularly when flexibility and damping of foundations are considered.

C7.12.1 To define the EVD of a pier care is required to properly account for the degree of end fixity when calculating the ductility demand. Piers that have a higher degree of end fixity have lower yield displacements and this should be accounted for in estimating the displacement ductility and equivalent viscous damping. The expressions provided by Eq.(7.23) and Eq.(7.24) are taken from Priestley et al. (2007).

The third row of Table 7.1 provides indications for fixed-flexible pier restraint conditions in the longitudinal direction. For more general restraint conditions the designer can gauge the effective restraint conditions by developing a structural model of the bridge in which each expected plastic hinge is modelled as a pin release together with an applied moment equal to the flexural capacity of the hinge, and other elements are modelled with their elastic (cracked) stiffness, as illustrated in Fig. C7.3.
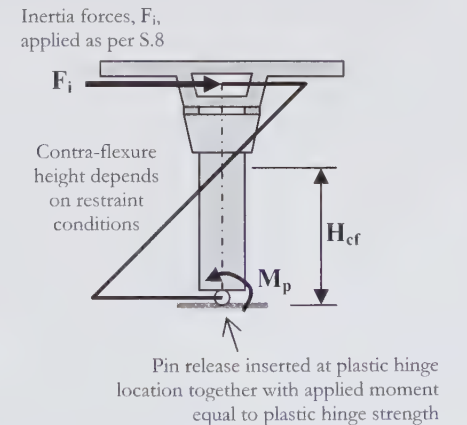
Inertia forces, F_i, applied as per S.8

F_i

Contra-flexure height depends on restraint conditions

H_{cf}

M_p

Pin release inserted at plastic hinge location together with applied moment equal to plastic hinge strength

Fig. C7.3: Bridge modelling and analysis approach in case of uncertain restraint conditions.

CODE

7.12.3 RC Pier Foundations: For the equivalent viscous damping of various foundation systems refer to the expressions provided in Section 7.12.5 for pile-pier systems and Section 7.18.
If no specific assessment of the foundation damping is undertaken, a value of 5% can be conservatively adopted provided that foundation flexibility is properly accounted for.

7.12.4 Bridge Bearings: Bridge bearings shall be assumed to respond elastically (5% damping) unless special seismic bearings have been selected, in which case, the relevant considerations made in the isolation section (7.16) should be utilised.

7.12.5 RC Bridge Pile-Piers: In the event that the bridge pier is continued into the ground as a pile, the equivalent viscous damping of the combined pile-pier system shall be obtained as a function of the ground conditions. In lieu of special studies, the following expressions shall be used:

Sand, pinned pier head, $\phi=30°$;

$$\xi_{pier} = 0.094 + \frac{0.02}{\mu^{0.313}} + 0.078\left(\frac{\mu-1}{\mu\pi}\right) \quad (7.25a)$$

Sand, pinned pier head, $\phi=37°$;

$$\xi_{pier} = 0.085 + \frac{0.02}{\mu^{0.313}} + 0.073\left(\frac{\mu-1}{\mu\pi}\right) \quad (7.25b)$$

Sand, fixed pier head, $\phi=30°$;

$$\xi_{pier} = 0.024 + \frac{0.02}{\mu^{0.313}} + 0.071\left(\frac{\mu-1}{\mu\pi}\right) \quad (7.25c)$$

Sand, fixed pier head, $\phi=37°$;

$$\xi_{pier} = 0.020 + \frac{0.02}{\mu^{0.313}} + 0.067\left(\frac{\mu-1}{\mu\pi}\right) \quad (7.25d)$$

Clay, pinned pier head, $p_u=20kPa$;

$$\xi_{pier} = 0.158 + \frac{0.02}{\mu^{0.313}} + 0.066\left(\frac{\mu-1}{\mu\pi}\right) \quad (7.25e)$$

COMMENTARY

An initial estimate of the system damping should be made so that a trial design base shear can be found and a set of equivalent lateral forces distributed to the model in line with the guidelines of Section 8. Static analyses should then be undertaken to identify the inelastic 1st mode moment distribution and from this, the effective point of contra-flexure in the piers. The yield displacement and EVD can then be calculated and the design base shear updated, with iterations carried until a convergent solution is obtained. Note that this iterative analysis approach is also a useful means of considering likely abutment deformations and damping contributions.

C7.12.3 For bridge systems in which significant energy dissipation is expected from both foundation deformations and inelastic structural response, Section 7.20 indicates how the system equivalent viscous damping can be set.

C7.12.5 Suarez and Kowalsky (2007) obtained expressions for the equivalent viscous damping of pile-piers (also known as drilled shaft bents) for various soil conditions through a number of non-linear time-history analyses. The equivalent viscous damping expressions provided in Eq.s (7.25a) to (7.25h) stem from the work of Suarez and Kowalsky (2007) with the ductility-dependent coefficient modified here by a factor of 0.7 so that the damping values can be used with the spectral reduction expressions of S.1.5.1.
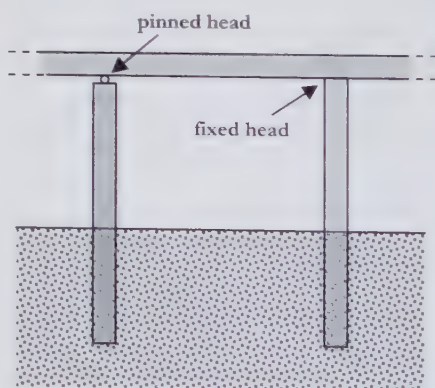

Fig. C7.4: RC bridge pile-piers.

CODE

Clay, pinned pier head, p_u=40kPa;

$$\xi_{pier} = 0.137 + \frac{0.02}{\mu^{0.313}} + 0.076\left(\frac{\mu-1}{\mu\pi}\right) \quad (7.25f)$$

Clay, fixed pier head, p_u=20kPa;

$$\xi_{pier} = 0.067 + \frac{0.02}{\mu^{0.313}} + 0.057\left(\frac{\mu-1}{\mu\pi}\right) \quad (7.25g)$$

Clay, fixed pier head, p_u=40kPa;

$$\xi_{pier} = 0.056 + \frac{0.02}{\mu^{0.313}} + 0.061\left(\frac{\mu-1}{\mu\pi}\right) \quad (7.25h)$$

7.13 EVD of Timber Framed Wall Structures: In lieu of accurate studies, the equivalent viscous damping of walls formed of timber framing with plywood sheathing shall be obtained from:

$$10\% \leq \xi_{eq} = 6\theta_c \leq 18\% \quad (7.26)$$

where θ_c is the design drift (minimum of values from Table 2.1 or Table 2.5).

7.14 EVD of Timber Portal Structures with Annular Bolted Joints: In lieu of accurate studies, the equivalent viscous damping of timber portal structures with annular bolted joints shall be obtained from:

$$\xi_{eq} = \xi_0 + \frac{a_t}{\pi}\left(1 - \frac{1}{\mu^{0.5}}\right) \quad (7.27)$$

where a_t and ξ_0 are constants that depend on the dowel diameter $\phi_{d.}$. Suggested values of these parameters are $a = 60$ and $\xi_0 = 10\%$, for dowel diameter $\phi_{d.} = 12$ mm; $a = 54$ and $\xi_0 = 8\%$ for dowel diameter $\phi_{d.} = 16$ mm. The ductility, μ, is obtained from Eq.(7.1), with the yield displacement obtained from:

COMMENTARY

C7.13: Various experimental and analytical studies (Folz and Filiatrault 2001, Filiatrault and Folz 2002) of timber-framed wall structures indicate that the equivalent viscous damping values of timber-framed systems are relatively high, and are essentially independent of the number of nails connecting the panel to the frame. Other less conservative expressions for the equivalent viscous damping of timber-framed wall structures are available in the literature (e.g. Pang et al. 2010), but Eq.(7.26) has been proposed here due to its simplicity and general applicability to various timber-framed wall systems. It should be used together with the spectral displacement reduction expressions of S.1.5.1. Future revisions of this document may aim to include more accurate expressions.

C7.14: Eq. (7.27) is a general formulation of the form suggested by Priestley (2003). Eq. (7.27) is based on the general assumption that the energy dissipation of a glulam frame is mostly due to plastic deformation of its connections. For fastened connections, the hysteretic dissipation is mostly due to the steel dowels that embed in the wood during the load action. Sartori (2008) proposes values for the parameters a and ξ_0 calibrated on the experimental outcomes of cyclic tests on full-scale fastened glulam joints, carried out according to UNI EN 12512 (2006). As such, values have been affected by the load protocol and future research should aim to calibrate the damping expressions to account for dynamic seismic response using NLTH analyses.

CODE

$$\Delta_y = \delta_y \frac{\gamma_t \beta_t h_{col}/L}{1+\gamma_t \beta_t L/h_{col}} + \frac{h_{col}}{2000}(h_{col}/L+1)\gamma_t \quad (7.28)$$

where δ_y is the dowel slip at the conventional yield point.

7.15 EVD of Masonry Structures: The equivalent viscous damping of unreinforced Masonry structures shall be set considering the likely failure mechanism of the structure and expected deformation demand.

7.16 EVD of Structures with Seismic Isolation: The equivalent viscous damping of structures with isolation systems shall be based on rational analyses and shall consider the actual cyclic behaviour and mechanical parameters of each type of isolation system, including the isolated structure. In lieu of detailed studies, the following expression for the system damping of base isolated structures may be used:

$$\xi_{eq} = \frac{\xi_{IS} D_d V_b + \xi_{el}(\Delta_d - D_d)V_s}{\Delta_d V_b} \quad (7.29)$$

COMMENTARY

C7.15 Various failure modes can develop in Masonry Structures (see, for example, Priestley et al. 2007) and these should be considered in setting the equivalent viscous damping. Equivalent viscous damping expressions that exist in the literature (e.g. Gambarotta and Brencich 2009) are preliminary and experimental research in this area is on-going. In the interim, for simplified design purposes the following expressions are proposed:

For masonry systems that exhibit shear-type mechanisms, the EVD may be approximated as:

$$\xi_{eq} = 0.05 + 25(\theta_{avg} - 0.001)$$
$$\text{but} \quad 0.05 \le \xi_{eq} < 0.20 \quad (C7.7)$$

For masonry systems that exhibit rocking-type mechanisms, the EVD may be approximated as:

$$\xi_{eq} = 0.05 + 10(\theta_{avg} - 0.002)$$
$$\text{but} \quad 0.05 \le \xi_{eq} < 0.14 \quad (C7.8)$$

For mixed shear-rocking mechanisms it is suggested that equivalent viscous damping values are interpolated between the values given by Eq.(C7.7) and Eq.(C7.8).

C7.16 The equivalent viscous damping of structures with isolation should consider the proportions of work-done by the different sources of energy dissipation. For base isolated structures, Eq.(7.29) factors the damping offered by the isolation devices by the shear and displacement imposed on the devices and then combines this with the damping offered by the overlying structure, factored by the shear and relative deformation imposed on the overlying structure. As the overlying structure is expected to respond in the elastic range, the elastic damping symbol is used in Eq.(7.29) and can typically be assumed equal to 5%. For building structures, the shear in the overlying structure is likely to be marginally less than the total base

CODE

Expressions for the evaluation of the equivalent viscous damping for different isolation devices are provided in sections 7.16.1 to 7.16.4.

7.16.1 Isolation Devices with Bi-Linear Hysteretic Response

(i) Lead Rubber Bearings:
For lead-rubber bearings subject to displacement ductility demands of between 5 and 50, the equivalent viscous damping shall be calculated as:

$$\xi_{IS} = \beta_1 - \beta_2 \cdot \ln(\mu) \qquad (7.30)$$

where μ is the ductility demand on the isolation device at the design displacement D_d and β_1 and β_2 are two parameters that depend on the post yielding stiffness ratio (r_Δ) of the isolation system. The values of β_1 and β_2 for three typical values of post yielding stiffness ratio, r_Δ, are listed in Table 7.2. Linear interpolation is permitted for post-yield stiffness ratios between 5% and 15%.

Table 7.2: Damping parameters (see Eq. (7.30)) for bi-linear systems with 5<μ<50 with different post-yield stiffness ratios.

r_Δ	β_1	β_2
5%	0.4830	0.0735
10%	0.4130	0.0705
15%	0.3015	0.0545

For lead-rubber bearings subject to ductility demands of 1.0 or less, the equivalent viscous damping shall be taken as the damping offered by the rubber only, and shall be interpolated for ductility demands between 1.0 and 5.0.

(ii) Friction Pendulum Bearings:
For friction pendulum bearings the equivalent viscous damping shall be calculated as:

$$\xi_{IS} = \frac{0.4635}{(\Lambda + 0.65)^{0.8}} \le 0.35 \qquad (7.31)$$

where Λ (=F_{el}/F_{FR}) is a design parameter given by the ratio between the elastic force (F_{el}) of the isolation device at the design displacement (D_d) to the friction resistance of sliding bearings (F_{FR}).

COMMENTARY

shear because it does not include the shear contribution of the ground level slab. However, it should be conservative to ignore the difference between V_s and V_b for base isolated building structures, and in doing so, Eq.(7.29) simplifies to:

$$\xi_{eq} = \frac{\xi_{IS} D_d + \xi_{el}(\Delta_d - D_d)}{\Delta_d} \qquad (C7.9)$$

There are a large range of isolation systems available in practice. Equivalent viscous damping expressions are provided here for the most commonly used isolation devices, which include: (i) Lead-Rubber Bearings (LRB), (ii) High-Damping Rubber Bearings (HDRB), (iii) Friction Pendulum Bearings (FPB), (iv) Combinations of Flat Sliding Bearings (FSB) and Low-Damping Rubber Bearings (LDRB) (FSB+LDRB), (v) Combinations of FSB and nonlinear (SMA-based) re-centring Devices (SMA) (FSB +SMA). Auxiliary linear or nonlinear viscous dampers may be used to increase the energy dissipation capacity of the isolation system.
The EVD values obtained using the expressions presented for base isolation devices in Section 7.16 should be used together with the spectral displacement reduction expressions of S.1.5.2.

Bilinear isolation systems
The post-yielding stiffness ratio of LRB isolation devices typically range between 5% and 15%. Ductility demands of the order of 30-40 can be reached by LRBs. The equivalent viscous damping ratio of a LRB typically ranges between 15% and 25%.
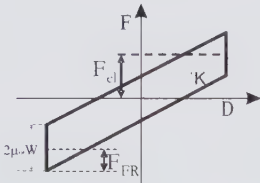

Fig. C7.4: Bi-linear hysteretic model used to represent behaviour of LRB and FPB devices.

For FPB (see Fig. C7.4), the parameter Λ can also expressed as follows:

$$\Lambda = \frac{D_d}{R} \cdot \frac{1}{\mu_{IR}} \qquad (C7.10)$$

CODE

COMMENTARY

where R and μ_{FR} are the radius of curvature and the friction coefficient of the sliding bearings, respectively. For FPB, the ratio D_d/R typically ranges from $1.5\mu_{FR}$ to 15% (Priestley et al. 2007).

7.16.2 Visco-Elastic Isolation Devices

(i) Low and High damping rubber bearings:
The equivalent viscous damping offered by low and high damping rubber bearings shall be based on qualification tests of the bearing device and shall account for the shear strain expected at the design limit state.

C7.16.2 The cyclic behaviour of rubber bearings is typically best described assuming visco-elastic response. The viscous constant and elastic stiffness of bearings will vary from manufacturer to manufacturer and therefore expected values should be obtained from qualification test results (i.e. see manufacturer brochure). Note that the equivalent viscous damping ratio of HDRBs typically ranges between 10% and 20%. Also note that the response of HDRBs is sometimes alternatively represented using a bi-linear hysteretic response. However, the visco-elastic model is preferred because it more realistically represents the actual cyclic behaviour of the bearings. As stated earlier, the EVD obtained for visco-elastic devices should be used together with the spectral displacement reduction expressions of S.1.5.2.

7.16.3 Combinations of Isolation Devices:
The equivalent viscous damping of combinations of different types of isolation devices shall be determined in line with Section 7.20.

C7.16.3 When an isolation system is formed through the combination of different devices it is recommended that the equivalent viscous damping offered by the individual devices be calculated and then combined in line with Section 7.20.

If a combined isolation system involves the use of sliding bearings, it should be noted that sliding bearings used in seismic isolation typically exploit low values of friction (2-3%) between PTFE (Polytetrafluoroethylene or Teflon) pads in contact with lubricated polished stainless steel surfaces.

7.16.4 Auxiliary Viscous Dampers: The contribution of auxiliary Viscous Dampers (VD's) to the equivalent viscous damping of the IS shall be evaluated by rational analyses or using the recommendations in Section 7.17.

CODE

7.17 EVD of Structures with Added Dampers:

The equivalent viscous damping of structures with added dampers shall consider the actual mechanical characteristics of the devices utilised and the elastic flexibility of the structures containing the devices. In lieu of more advanced analyses, the equivalent viscous damping shall be defined as:

$$\xi_{eq} = \xi_{eq,st} + \frac{\beta}{1+\alpha} \qquad (7.32)$$

Where $\xi_{eq,st}$ is the equivalent viscous damping offered by the structure (without dampers) for the system design displacement, β is the ratio of the shear resistance offered by the dampers to the design base shear of the structure and α is the viscous damper power constant.

7.18 EVD of Shallow and Piled Foundation

Systems: The equivalent viscous damping of foundation systems shall be defined through rational analysis or experimental data. In lieu of such analysis or data, the equivalent viscous damping of a shallow foundation system on sand can be obtained following the procedure provided in Annex 4, and the equivalent viscous damping of deep/piled foundations can be taken equal to 5%.

7.19 EVD of Retaining Structures: The

equivalent viscous damping of retaining structures shall be defined through rational analysis.

7.20 EVD of Combined Systems:

For systems in which different independent sources of energy dissipation exist, the equivalent SDOF system damping shall be defined through rational analysis or using:

$$\xi_{sys} = \frac{\xi_1 V_1 \Delta_1 + \xi_2 V_2 \Delta_2 + ... + \xi_n V_n \Delta_n}{V_{Base} \Delta_d} \qquad (7.33)$$

COMMENTARY

C17.7 Eq.(7.32) stems from the work of Peckan et al. (1999), Sullivan (2009) and Lago (2011). Lago (2011) and Sullivan and Lago (2012) present a simplified DDBD approach for structures fitted with viscous dampers, in which the proportion of equivalent SDOF lateral force resisted by the dampers (i.e. the equivalent lateral force associated with F_d from Fig. C6.8 divided by V_{Base}) is selected in order to control the system damping, as per Eq.(7.32). The power coefficient, α (illustrated earlier in Fig.C6.8) should be set equal to 1.0 for linear viscous dampers and to a value of between 0.10 and 0.40 for non-linear viscous dampers (check with damper manufacturers to see what value of α they can provide). The damper constants, $C_{d,i}$, required to provide the selected system damping should be identified following the recommendations of Section 8.

The equivalent viscous damping given by Eq.(7.32) should be used in conjunction with the spectral displacement reduction expressions given in S.1.5.2.

C7.18. The equivalent viscous damping of shallow foundations was found by Paolucci et al. (2009) to typically vary from 5% to 20%. Expressions for the stiffness degradation and equivalent viscous damping of shallow foundations are given in Annex 4.

There currently appears to be limited data on the equivalent viscous damping for deep foundations. In the interim, a value of 5% is recommended for design purposes.

C7.19 Preliminary guidelines for the equivalent viscous damping of retaining structures are provided in Annex 3.

C.7.20 The equivalent SDOF system damping of combined systems should be set considering the proportion of work-done by the individual systems. This is reflected in Eq.(7.33). The research findings of Maley (2011) indicate that using work-based approaches for mixed systems leads to reasonably conservative results.

CODE

where the shear components relate to the resistance offered to the equivalent SDOF system, the displacements are measured at the effective height, and ξ are the damping values of the contributing sources.

For certain systems, such as frame-wall systems linked with effectively rigid diaphragms, Eq.(7.33) can be approximated using overturning resistances:

$$\xi_{sys} = \frac{\xi_1 M_1 + \xi_2 M_2 + ... + \xi_n M_n}{M_{total}} \qquad (7.34)$$

The equivalent viscous damping of a soil-structure interacting system can be assumed as:

$$\xi_{eq} = \frac{\xi_{st}\Delta_{st} + \xi_f \Delta_f}{\Delta_{st} + \Delta_f} \qquad (7.35)$$

where Δ_{st} and Δ_f are the contributions to total structural displacement at the effective height of structural distortion and foundation rotation, respectively, while ξ_{st} and ξ_f are the corresponding damping ratios for structure and foundation.

COMMENTARY

If a refined estimate of the equivalent viscous damping of frame systems is required (see commentary of Section 7.2) with different storey ductility demands expected up the height of the structure, Eq.(7.33) could be modified such the storey drifts, θ_i, are used in place of the Δ_i terms in order to give the frame system damping.

The research findings of Sullivan et al. (2006) indicate that the simplified expression of Eq.(7.41) is suitable for frame-wall structures.

Eq.(7.35) comes both from considerations regarding the sum of energy dissipation at the structural and foundation levels (Priestley et al. 2007) and from the equivalent SDOF oscillator concept for SSI analyses, introduced by Wolf (1985). ξ_f was found to vary typically from 5% to 20% for shallow foundations. Note from Eq. (7.35) that for a rigid foundation $\xi_{eq} \rightarrow \xi_s$, and for a rigid structure $\xi_{eq} \rightarrow \xi_f$.

CODE

8. STRUCTURAL ANALYSES FOR DESIGN FORCES

8.1 Distribution of Base Shear Force: The base shear force shall be distributed as equivalent lateral forces at the seismic mass locations, in line with the following subsections.

8.1.1 Lateral Force Vector for Buildings: The base shear force shall be distributed to the locations of floor mass of the building in accordance with the relationship:

Floors 1 to n-1:

$$F_i = kV_{Base}\left(m_i\Delta_i\right)/\sum_{i=1}^{n}\left(m_i\Delta_i\right) \qquad (8.1a)$$

Roof (Floor n):

$$F_n = (1-k)V_{Base} + kV_{Base}\left(m_n\Delta_n\right)/\sum_{i=1}^{n}\left(m_i\Delta_i\right) \quad (8.1b)$$

For building structures in which the main lateral resisting system forms plastic hinges over the full height of the structure (e.g. frame structures), the value of k to be used in Eq.(8.1) is $k = 0.9$. For building structures in which the plastic hinges offering the main lateral resistance form at the base of the building (e.g. RC wall structures), $k = 1.0$.

COMMENTARY

C8. The design procedure of Chapter 5 provides a design base shear for an equivalent SDOF representation of the structure. The designer must then detail the structure to form a suitable plastic mechanism that ensures the structure possesses the design base shear resistance at the design displacement. This chapter sets out how the design base shear is utilised to identify the strength of plastic hinge regions of the plastic mechanism. Chapter 9 will present capacity design requirements aimed at ensuring the design plastic mechanism is developed and can be maintained during intense seismic shaking.

C8.1 The base shear force is distributed to the seismic masses in proportion to the product of their mass and displacement.

(a) Base shear of equivalent SDOF System

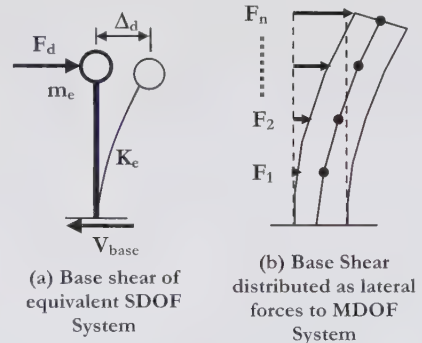(b) Base Shear distributed as lateral forces to MDOF System

Fig. C8.1: Distribution of Equivalent SDOF Design Base Shear to MDOF structure.

For frame buildings, particularly those of about 10 storeys or higher, the design displacement profile of Eq.(8.1) assumes that 10% of the base shear will be additionally applied at roof level to mitigate unfavourable higher-mode effects on the displaced shape. The displaced shape of wall structures is less affected by higher modes owing to the high elastic stiffness of the wall sections above the base plastic hinge. As such, for wall or similar structural systems the value of k can be taken equal to 1.0.

CODE	COMMENTARY

8.1.2 Lateral Force Vector for Bridges: The base shear force shall be distributed to the seismic mass locations of the bridge in accordance with the relationship:

$$F_i = V_{Base}(m_i \Delta_i) / \sum_{i=1}^{n}(m_i \Delta_i) \qquad (8.2)$$

8.2 Structural Analysis to Determine Required Moment Capacity at Plastic Hinges:

8.2.1 The structure shall be analysed under the design lateral force vector to determine the required moment capacity of potential plastic hinge locations.

8.2.2 The structural analysis shall be based on effective stiffness of structural members at expected displacement response, or alternatively may be determined from a rational equilibrium analysis. Lateral forces should not be distributed to members based on elastic section properties unless the response is expected to be elastic.

C8.2 DDBD is intended to provide direct information on the required flexural strength of plastic hinges. Two methods of structural analysis are suggested. The first involves a conventional structural analysis, though the member stiffness adopted in the analysis should be reduced from the elastic values by dividing by the expected member displacement- or rotational-ductility. As the plastic hinges are typically expected at column bases in moment-resisting frames, care is needed in modelling the stiffness of first-storey columns (see Priestley et al. 2007). Note that iteration may be required since stiffness depends on strength, which will not initially be known.

The second method is based on equilibrium requirements, rather than stiffness properties. This procedure is outlined in Section 5.5.2 of Priestley et al. (2007). In the case of frame buildings, the equilibrium method requires rational decisions to be made about the vertical distribution of beam seismic shear up the buildings. .

8.3 Structural Analysis to Determine Required Properties of Viscous Dampers: The design damper forces shall be set to be compatible with the assumed system equivalent viscous damping from Section 7.17. The viscous damper constant, $C_{d,i}$, of dampers located at level i, shall be found from rational analysis or, in the case that dampers are designed to provide the same storey shear proportion β at all storeys, through the following equation:

$$C_{d,i} = \beta V_i \left(\frac{T_e}{2\pi \delta_{di}} \right)^{\alpha} \qquad (8.3)$$

where V_i is the design storey shear at level i, δ_{di} is the damper displacement demand at level i and α is the damper power constant.

C8.3 In Section 7.17 the system damping for structures with added dampers is set be selecting β, the proportion of shear that will be resisted by the damping system. As such, Cl.8.3 requires that this design shear proportion be respected when setting the damper design forces. In the case that damper design forces are set to be proportional to the design storey shear up the whole building height, then the damper force, $F_{i,d}$, is given by:

$$F_{i,d} = \beta V_i = \beta \sum_{i=i}^{j=n} F_j \qquad (C8.1)$$

where the equivalent lateral force, F_i, is found from Section 8.1, such that the sum indicated on the right side of Eq.(C8.1) is simply providing the design storey shear at level i.

CODE

COMMENTARY

If designers wish to utilise a distribution of dampers that does not provide a uniform β value up the building height, then they should refer to Lago (2011) where relevant guidelines are provided.

Within Eq.(8.3) note that it is the damper local displacement demand, δ_{di}, (such that the stroke on the damper is equal to $+/- \delta_{di}$) that should be used and not the storey displacement demand. The local displacement demand should be found with account for structural deformations expected under application of the design damper forces.

Finally, note that the design damper forces defined in Eq.(C8.1) are those associated with the first mode of vibration. Peak damper design forces should be established in accordance with the capacity design recommendations of Section 9.

CODE	COMMENTARY

9. CAPACITY DESIGN REQUIREMENTS

The intended distribution and location of plastic hinges must be ensured by application of an appropriate capacity design hierarchy of strength with design moments and shears in regions required to remain elastic being amplified to account for possible increased material strength in plastic hinge locations, and higher mode dynamic amplification. Amplified moments and shears may be determined through Non-Linear Time-History analyses as per Section 9.1, or by the Effective Modal Superposition method of Section 9.2, or the Approximate method of Section 9.3. However, in the case of very irregular bridges or structures that are isolated with non-linear devices, non-linear time-history analyses shall be undertaken in order to verify the performance of the structure and obtain final capacity design forces.

C9. Capacity design aims to protect the structure from the development of unwanted inelastic mechanisms. As capacity design forces can be intensity dependent, capacity design forces should be established for the Performance Level 3 earthquake as defined in Table 1.1.

The distribution of forces that should be used for the design of the superstructure and substructure in base isolated structures should consider the type of isolation system and the effects of higher modes on the system behaviour. The guidelines provided in Annex 6 can be followed for preliminary capacity design of base isolated structures. However, given the complexity of the response, detailed design shall validate the performance of irregular bridges and base isolated structures through non-linear time-history analyses. Note that a higher than expected seismic intensity should cause significant increases in displacement demands only at the isolation level, with the overlying structure being effectively "isolated", remaining in the elastic range. As a result, a capacity design philosophy is assured by designing the isolation system as the "weak link" and traditional capacity design requirements for the superstructure need not be enforced. However, some capacity design considerations should be followed to account for uncertainties in the distribution of equivalent lateral forces, as discussed in Annex 6.

9.1 Non-Linear Time-History Analyses to Determine Capacity Design Force Levels:

Capacity design moments and shears may be determined through non-linear time-history (NLTH) analyses. In modelling the structure for the NLTH analyses, the resistance of plastic hinge actions shall be modelled with overstrength resistance values, set in accordance with Section 3.1, whereas all other elements and actions shall be modelled with elastic properties. The analyses shall be undertaken using a set of spectrum compatible accelerograms and the average of the maximum recorded forces shall be adopted as capacity design forces. The number of accelerograms selected shall ensure that the mean response is not significantly affected by the inclusion of additional records.

C9.1 NLTH analyses are considered the most accurate means of predicting the seismic response of a structure. However, the analyses require an advanced level of knowledge in order to ensure that the non-linear dynamic response is adequately predicted. Usually, NLTH analyses are undertaken using expected material strength and stiffness properties. However, for capacity design it is important that the possibility of plastic hinge overstrength be properly accounted for. As such, when using NLTH analyses to establish capacity design forces, Section 9.1 requires that overstrength properties be assigned to plastic hinge actions. This aims to ensure that the maximum feasible inelastic forces develop, and therefore a reasonable estimate of the maximum capacity design forces is obtained.

CODE

COMMENTARY

The number of accelerograms typically required by codes for NLTH analyses is seven. However, there appears to be little statistical basis to support the use of seven accelerograms, hence the more general requirement stated in Section 9.1.

Also note that it has not been specified whether accelerograms should be from real earthquake records, artificial records or real records modified by the introduction of wavelets (see Hancock et al. 2006). For guidance on the selection of accelerograms see Iervolino and Cornell (2005) and Watson-Lamprey and Abrahamson (2006). Beyer and Bommer (2007) and Grant (2011) make considerations for the selection of accelerograms for bi-directional excitation. To that extent, note that while the DDBD procedure can typically be undertaken considering each earthquake excitation direction separately (particularly when torsion response is small) capacity design forces should be set with account for bi-directional and vertical excitation effects.

9.2 Effective Modal Superposition to Determine Capacity Design Force Levels: Capacity design moments and shears may be determined by combining modal moments or shears by SSRS or CQC combination rules, from a modal analysis based on effective member stiffness at maximum displacement response. The first mode response $S_{I,Di}$ may be taken as the design moments or shears resulting from the structural analysis defined in Section 8.2, amplified for possible enhancement of material strengths. For the SSRS combination rule, the enhanced action, $S_{CD,i}$ is found from Eq.(9.1):

$$S_{CD,i} = \sqrt{(\phi^o S_{1D,i})^2 + S_{2,i}^2 + S_{3,i}^2 + .. + S_{n,i}^2} \qquad (9.1)$$

The value of the overstrength factor ϕ^o may be determined from moment-curvature analysis of the plastic hinges. Alternatively a value of $\phi^o = 1.25$ may be assumed.

C9.2 There are a number of modal analysis procedures outlined in Priestley et al. (2007) that have been developed to determine capacity design forces. All are based on the assumption of a modal superposition combining the inelastic first mode forces with the elastic higher mode forces, and all give similar results. Although not fully checked on all structural types, Priestley et al. (2007) argue that the **Effective Modal Superposition** approach, which is based on a structural model similar to the first option described in Clause C8.2 provides the most consistent results.

CODE

COMMENTARY

9.3 Approximate Methods for Determining Capacity Design Force Levels: As an alternative to the refined approaches of Section 9.1 and 9.2, the equations provided in the following subsections may be used for certain structural types and actions.

9.3.1 General Provisions: The required dependable strength of capacity-protected elements shall be determined from:

$$S_{CP} = \phi^0 \omega S_E \qquad (9.2)$$

9.3.2 Frame Buildings:

(a) Column Moments

(i)One way frames: The dynamic amplification factor, ω_f for flexure, is height and ductility dependent as shown in Fig.9.1, where from level 1 to the ¾ point of structure height:

$$\omega_{f.c} = 1.15 + 0.13\left(\mu/\phi^0 - 1\right) \qquad (9.3)$$

and at the top and bottom of the frame

$$\omega_f = 1.00 \qquad (9.4)$$

C9.3 The equations in this section are based on analyses on extensive inelastic time-history analyses, and are intended to be adequately conservative for design purposes.

C9.3.1 The basic capacity design Eq.(9.2) relates the required dependable strength of the capacity-protected action (generally flexural strength or shear strength) to the value calculated from the design lateral force distribution, including an overstrength factor ϕ^0 and a dynamic amplification factor ω. The overstrength factor will normally be found from moment-curvature analysis based on maximum feasible strengths in line with Section 3.1, or may conservatively be taken as 1.25.

The dynamic amplification factor represents the ratio of the expected maximum force to the overstrength force associated with the 1st mode formation of a mechanism. The expressions presented in Eq.(9.3) and Eq.(9.4) are empirical expressions obtained from a suite of non-linear time-history analyses as reported by Priestley et al. (2007).

Where flexural reinforcement for the wall is from the same steel batch up the wall height, the dependable moment capacity at heights above the base may be based on the same reinforcement yield strength as used to determine the overstrength base moment capacity.

Figure 9.1 Dynamic Amplification of Column Moments.

CODE

(ii) Two-way frames: For two-way frames the design moment corresponding to lateral forces shall be based on biaxial response, with the displacement ductility factor μ in Eq.s (9.3) and (9.4) being replaced by $\mu/\sqrt{2}$.

(b) Column shears: Overstrength and dynamic amplification factors for shear in columns shall be combined as in Eq.(9.5) which relates the required dependable shear strength to the shear determined from the lateral force distribution:

$$\phi_S V_N \geq \min\left[\phi^o V_E + 0.1\mu V_{E,base}, \frac{M_t^o + M_b^o}{h_{col}}\right] (9.5)$$

9.3.3 Structural Walls:

(a) Wall Moments: The design moments for cantilever walls shall conform to the bilinear envelope of Fig.9.2, where the wall-base moment is amplified for overstrength effects, and the moment capacity at mid-height is defined by

$$M_{0.5H}^o = C_{1,T}.\phi^o M_B \qquad (9.6)$$

where:

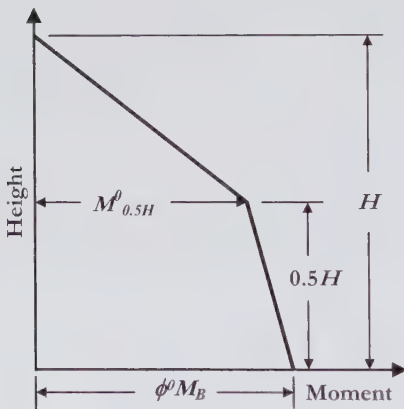$$C_{1,T} = 0.4 + 0.075T_i\left(\frac{\mu}{\phi^o} - 1\right) \geq 0.4 \qquad (9.7)$$

COMMENTARY

C9.3.3 The period T_i in Eq.(9.7) is the initial elastic period, including effects of cracking. Note that this period can be related with adequate accuracy to the effective period used in the DDBD process by $T_i = T_e/\sqrt{\mu}$. For comparatively short walls, it will normally be appropriate to carry the flexural reinforcement up the full height of the wall without terminating any bars.

Figure 9.2 Capacity Moments for Walls.

CODE

In determining the required level of wall flexural reinforcement, allowance shall be made for variation of axial force with height, and for tension-shift effects.

(b) Wall Shear Forces: The provided shear strength of a cantilever wall shall conform to the linear envelope of Fig.9.3. The wall-base dynamic amplification factor for shear shall be taken as:

$$\omega_v = 1 + \frac{\mu}{\phi^0} C_{2,T} \qquad (9.8)$$

where

$$C_{2,T} = 0.067 + 0.4(T_i - 0.5) \leq 1.15 \qquad (9.9)$$

The design shear capacity at the wall top shall be not less than

$$V_n^0 = (0.9 - 0.3T_i)V_B^0 \geq 0.3V_B^0 \qquad (9.10)$$
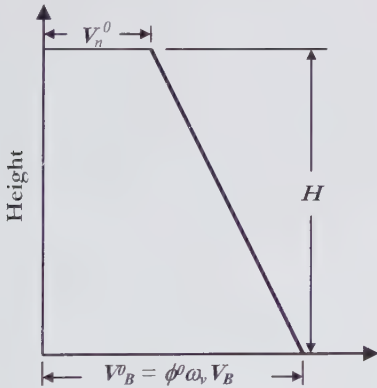
Figure 9.3 Wall Design Shear Forces.

9.3.4 Dual Wall-Frame Buildings: When the proportion of overturning resistance allocated to the frames of dual structural systems falls in the range $0.2 \leq \beta_F \leq 0.6$ the following provisions apply. When $\beta_F \leq 0.2$, the walls should be designed as cantilever walls to Cl.9.3.3, and when $\beta_F \geq 0.6$ the frames should be designed in accordance with Cl.9.3.2.

COMMENTARY

Unlike wall moments, shears at the base of RC walls are not effectively limited by the formation of a plastic hinge. As such, the magnification illustrated in Fig. 9.3 shows that the 1st mode design forces are magnified over the full height of the walls.

C.9.3.4 When $\beta_F < 0.2$, the frames may still be designed to the provisions of this section, and when $\beta_F > 0.6$ the walls may be designed to these provisions.

CODE

(a) Column Moments: Columns shall have dependable flexural strength not less than:

$$M_{C,D} = 1.3\phi^o M_{CE} \qquad (9.11)$$

(b) Column Shear Force: Columns shall have dependable shear strength not less than:

$$V_{C,D} = 1.3\phi^o V_{CE} \qquad (9.12)$$

(c) Wall Moments: Wall moments shall be designed to the bilinear envelope defined in Cl.9.3.3(a) but the mid-height moment, $M^o_{0.5H}$, shall not be set less than 1.2 times the mid-height moment due to first mode response.

(d) Wall Shear Forces: The provided shear strength of a wall of a dual structural system shall conform to the envelope of Fig.9.3, where:

$$\omega_v = 1 + \frac{\mu_{sys}}{\phi^o} C_{3,T} \qquad (9.13)$$

where:

$$C_{3,T} = 0.4 + 0.2(T_i - 0.5) \leq 1.15 \qquad (9.14)$$

The shear force at the wall top may be taken as:

$$V_n^0 = 0.4 V_B^0 \qquad (9.15)$$

9.3.5 Bridge Piers: The capacity design shear in bridge piers shall account for overstrength of the plastic hinge and higher mode effects. In lieu of accurate studies, the following expression shall be satisfied:

$$\phi_S V_N \geq \omega \phi^o V_E \qquad (9.16)$$

where the overstrength factor, ϕ^o, should be set in line with the requirements of Section 3.1, and the dynamic magnification factor shall be set using rational analyses.

COMMENTARY

C.9.3.4(a) Influence of higher modes on column moments is less apparent in frames of dual systems. Also it should be noted that the consequences of column plastic hinging are minimal, since the wall stiffness and strength will control the deformation, avoiding the potential for a soft-story mechanism to form.

C.9.3.4(c) An alternative approach for flexural reinforcement requirements in RC frame-wall structures proposed by Sullivan et al. (2006) is to simply utilise constant reinforcement corresponding to the required base strength up the full height of the wall. This may be expected to be conservative, but depending on the expected seismic intensity, some minor flexural yielding may still occur. While minor yielding may occur, curvature ductility demands are not expected to be excessive in the upper levels.

C.9.3.4(d) The form of the wall shear force envelope is the same as for simple cantilever walls, but the system ductility, rather than the wall ductility is used, and the period-dependent coefficient, $C_{3,T}$ results in lower amplification than in simple cantilever walls.
Note that while Section 9.3.4(d) is intended to be conservative, this may not always be the case as there are several outstanding issues for the simplified capacity design of frame-wall structures, as discussed by Sullivan (2010).

C.9.3.5 For bridge piers the primary concern is determining the maximum feasible shear force that can be developed. The overstrength factor, ϕ^o, should be expected to be the main cause for amplification in Eq.(9.16). However, dynamic amplification related to higher mode effects can be significant when (i) pier mass is a significant proportion of the total mass; (ii) the superstructure supported by a cantilever pier has a wide torsional mass inertia; and (iii) superstructures are flexible. One can use a value of $\omega = 1.0$ when the pier mass is less than 10% of the superstructure mass and torsional mass inertia of the deck is low. When the deck torsional inertia is large, significant bending moments can be developed at the top of a pier, shifting the point of contraflexure down the pier

CODE

COMMENTARY

height and increasing the shears in the pier. For this reason, Priestley et al. (2007) suggest that a point of contraflexure located at 85% of the pier height measured to the centre of superstructure mass. If higher mode effects are likely to be very significant, NLTH analyses (as per Section 9.1) or effective modal superposition (Section 9.2) should be used to gauge peak shear demands.

9.3.6 Bridge Decks and Abutments: Capacity design forces for bridge decks and abutments shall consider both the potential for overstrength at plastic hinges and higher mode effects.

C.9.3.6 Overstrength at plastic hinges and higher mode effects may have a significant influence on the maximum transverse moments and shears developed in the superstructure, and on the maximum abutment reactions. However, the ϕ^o value corresponding to flexural overstrength at plastic hinges should not always be applied to superstructure forces. It may in fact be appropriate to use an estimate of plastic hinge capacity lower than the design level in determining the superstructure demands (refer to recommendations of Priestley et al. (2007) Section 10.5.2). In the longitudinal direction, the effects of higher modes on the deck forces should not be significant for typical bridge types.

9.3.7 Structures with Added Dampers: Capacity design forces for dampers and their supporting structural elements shall be established using rational analysis with account for uncertainties in peak velocity demands and damper properties.

C9.3.7 In the case of linear viscous dampers, capacity design forces can be greatly affected by higher mode effects on velocity demands. In addition, the design forces identified in Section 8 to identify damper constants utilise the pseudo velocity but the peak capacity design forces should actually be based on the real velocity demands, which tend to be considerably greater than pseudo velocity demands for high damping values and effective periods greater than 1.0s (see Lago 2011). Work by Lago (2011) has shown that an effective modal analysis approach (section 9.2) can be used with a CQC combination to provide acceptable estimates of peak forces in frame and wall structures fitted with viscous dampers, provided that the higher mode damping contribution is properly evaluated and differences between pseudo and real spectral velocity demands are accounted for.

Capacity design forces for structures fitted with non-linear viscous dampers are likely to be relatively unaffected by the assumed peak velocity, and the main uncertainty will be related to the damper constant provided by the

CODE

COMMENTARY

manufacturer. In addition, designers should account for the fact that forces in non-linear viscous dampers remain high until close to peak structural displacement demands (see Fig. C6.8). A simplified means of doing this is to sum the peak capacity design damper forces with the capacity design structural forces expected at peak displacement response.

9.3.8 Floor Diaphragms: In building structures floor diaphragms and their connections shall be designed to behave elastically. The capacity design accelerations for the design of floor systems should be defined through rational analysis or can be approximated as Eq.(9.17).

For wall structures:

$$PFA = 2.5PGA \qquad (9.17a)$$

For frame structures:

$$PFA = 2.0PGA \qquad (9.17b)$$

Where the *PGA* should be taken for the site under consideration at the return period corresponding to the Performance Level 3 limit state (Table 1.1).

C9.3.8 In reviewing the results of a large number of non-linear dynamic analyses of floor diaphragms forming part of RC wall structures, it was observed by Rivera (2009) that the peak floor acceleration (PFA) at the first floor is correlated with the frequency of the floor itself and that this acceleration appears to be unaffected by the ductility developed within the main lateral load resisting system. Furthermore, the first floor accelerations were typically the maximum accelerations up the building height with the roof level accelerations occasionally registering higher accelerations. Rather than undertake a specific spectral analysis, Eq.(9.17a) assumes that the PFA can be conservatively set equal to the spectral acceleration plateau which is typically 2.5 times the PGA. While it is anticipated that the level of conservatism given by Eq.(9.17a) should be reasonable for structural wall buildings, the work of Fleischmann et al. (2002) indicates that it could greatly overestimate the floor accelerations in frame buildings. This research was further supported by the work of Lavelle (2009) who found PFA values of up to 2.0PGA for RC frame structures, with lower values for taller (long period) buildings. As such, Eq.(9.17b) indicates a lower peak floor acceleration value for floors of frame systems. Future research should aim to refine and better verify Eq.(9.17) and designers are encouraged to consider the use of NLTH analyses to quantify floor accelerations more accurately.

To check the capacity of the floor diaphragm and its connections, the peak floor acceleration obtained from Eq.(9.17) should be multiplied by the expected seismic weight of the storey under consideration and the force obtained should then be applied as a horizontal uniformly distributed load along the centre of the diaphragm.

BIBLIOGRAPHY

Akcelyan, S. (2011) "Direct displacement based design of concentrically braced steel frames" *MSc dissertation*, European School for Advanced Studies in Reduction of Seismic Risk (ROSE School), IUSS Pavia, Italy.

Antoniou, S. and Pinho R. (2004) "Advantages and limitations of adaptive and non adaptive force-based pushover procedures," *Journal of Earthquake Engineering*, Vol. 8, No. 4, pp. 497-522.

Adhikari, G. (2007) "Direct displacement based design: long span bridges with/without in-plane movement joint" *MSc dissertation*, European School for Advanced Studies in Reduction of Seismic Risk (ROSE School), IUSS Pavia, Italy.

Belleri A. and Riva P. (2008). "Direct Displacement Based Design and Force Based Design of Precast Concrete Structures", *Proceedings IALCCE'08*, Varenna, Italy.

Belleri A. and Riva P. (2008). "Seismic Behaviour Of Grouted Sleeve Precast Column To Foundation Connections: Results Applied To The Direct Displacement Based Design", *14th World Conference on Earthquake Engineering*, October 12-17, Beijing, China.

Beyer, K., Abo-El-Ezz, A., Dazio, A. (2010) "Quasi-static tests on different types of masonry spandrels", *Report*, Institute of Structural Engineering Swiss Federal Institute of Technology, Zurich.

Beyer, K. and Bommer, J.B., (2007) "Selection and Scaling of Real Accelerograms for Bi-Directional Loading: A Review of Current Practice and Code Provisions" *Journal of Earthquake Engineering*, Vol. 11, Supp. 1, pp. 13-45.

Beyer, K., Dazio, A., Priestley, M.J.N., (2008) "Seismic Design of Torsionally Eccentric Structures with U-Shaped RC Walls" *Research Report ROSE-2008/03*, IUSS press (www.iusspress.it).

Bommer, J.J. and Mendis, R. (2005) "Scaling of Spectral Displacement Ordinates with Damping Ratios" *Earthquake Engineering and Structural Dynamics*, Vol. 34, pp. 145-165.

Calvi, G.M., Sullivan, T.J., Villani, A., (2010) "Conceptual seismic design of cable stayed bridges" *Journal of Earthquake Engineering*, Vol. 14, No. 8, pp. 1139-1171.

Cardone, D., Dolce, M., Palermo, G., (2008) "Force-Based vs. Direct Displacement-Based Design of buildings with seismic isolation" *14th World Conference on Earthquake Engineering*, October, Beijing, China.

Cardone, D., Dolce, M., Palermo, G., (2009a) "Direct displacement-based design of seismically isolated bridges" *Bulletin of Earthquake Engineering*, Vol. 7, No. 2, pp. 391-410.

Cardone, D., Dolce, M., Gesualdi, G., (2009b) "Lateral force distributions for the linear static analysis of base-isolated buildings" *Bulletin of Earthquake Engineering*, DOI 10.1007/s10518-009-9104-y.

Cardone, D., Palermo, G., Dolce, M. (2010) "Direct Displacement-Based Design of Buildings with Different Seismic Isolation Systems", *Journal of Earthquake Engineering*, Vol. 14, No. 2, pp. 163-191.

Cebellos, J.L., and Sullivan, T.J. (2012) "Development of Improved Inelastic Displacement Prediction Equations for the Seismic Design of Hybrid Systems" *Bulletin of the New Zealand Society for Earthquake Engineering*, Vol. 45, No. 1.

CEN (1998) *Eurocode 8 – Design Provisions for Earthquake Resistant Structures*, prEN-1998-1:200X, European Committee for Standardization, Brussels, Belgium.

CEN (2004a) *Eurocode 8 – Design Provisions for Earthquake Resistant Structures*, EN-1998-1:2004, European Committee for Standardization, Brussels, Belgium.

CEN (2004b) *Eurocode 5: Design of timber structures - Part 1-1: General - Common rules and rules for buildings*, EN 1995-1-1:2004, European Committee for Standardization, Brussels, Belgium.

CEN (2004c) *Hot Rolled Products of structural steels Part 2: Technical delivery conditions for non-alloy structural steels*, EN 10025-2:2004, European Committee for Standardization, Brussels, Belgium.

CEN (2005) *Eurocode 3: Design of steel structures - Part 1-1: General rules and rules for buildings*, EN 1993-1-1:2005, European Committee for Standardization, Brussels, Belgium.

Cecconi M., Vecchietti S., Pane V., (2007) "The DDBD Method in the design of cantilever diaphragm walls", *60th Canadian Geotechnical Conference & 8th Joint CGS/IAH-CNC Groundwater Conference-The Diamond Jubilee*, Ottawa, Canada, October 2007, pp. 912-919.

Christopoulos, C., Filiatrault, A., Uang, C.M., Folz, B. (2002) "Post-tensioned Energy Dissipating Connections for Moment Resisting Steel Frames" *ASCE Journal of Structural Engineering*, Vol.128, No.9, pp.1111-1120.

Christovasilis, I.P., Filiatrault, A., Wanitkorkul, A., (2007) "Seismic Testing of a Full-scale Two-story Wood Light-Frame Building: NEESWood Benchmark Test", *NEESWood Report NW-01*, University at Buffalo, Buffalo, NY.

Constantinou M., Caccese J., Harris H.G., (1987) "Frictional characteristics of Teflon-steel interfaces under dynamic conditions" *Earthquake Engineering and Structural Dynamics*, Vol. 15, No. 6, pp. 751-759.

Constantinou M.C., Mokha A., Reinhorn A.M., (1988) "Teflon Bearings in Aseismic Base Isolation: Experimental Studies and Mathematical Modeling" *Report N. NCEER-88/0038*, NCEER, Buffalo, NY.

Dazio, A. and Beyer, K., (2010) "Seismic behaviour of different types of masonry spandrels", *14th European Conference on Earthquake Engineering*, Ohrid, Macedonia, 30 August - 3 September 2010.

Della Corte G. (2006). "Vibration mode vs. collapse mechanism control for steel frames" *Proceedings of the Fourth International Specialty Conference on Behaviour of Steel Structures in Seismic Areas (STESSA 2006)*, Yokohama, Japan, 14-17 August 2006, pp. 423-428.

Della Corte, G. and Mazzolani, F.M. (2008) "Theoretical developments and numerical verification of a displacement-based design procedure for steel braced structures" *Proceedings of the 14th World Conference on Earthquake Engineering*, Beijing, China, 12-17 October.

Della Corte, G. and Mazzolani, F.M. (2009). "Direct displacement based design of steel chevron bracing" *Proceedings of the XIII Italian Congress on Seismic Engineering* (ANIDIS), Bologna, Italy.

Dolc,e M., Cardone, D., Croatto, F. (2005) "Frictional Behaviour of Steel-PTFE Interfaces for Seismic Isolation" *Bulletin of Earthquake Engineering*, Vol. 3, No. 1, pp. 75-99.

Dolce, M., Cardone, D., Marnetto, R. (2000) "Implementation and Testing of Passive Control Devices Based on Shape Memory Alloys" *Earth Eng Struct Dyn*, Vol. 29, pp. 945–968.

Dwairi, H.M., Kowalsky, M.J., Nau, J.N. (2007) "Equivalent Damping in Support of Direct Displacement-Based Design" *Journal of Earthquake Engineering*, Vol. 11, No. 4, July 2007, pp. 512 – 530.

Englehart, M.D. and Popov, E.P. (1989) "Behaviour of Long Links in Eccentrically Braced Frames" *Report No. UCB/EERC-89/01*, Earthquake Engineering Research Centre, UC Berkeley, California.

Faccioli, E., Paolucci, R., Rey, J. (2004) "Displacement Spectra for Long Periods". *Earthquake Spectra*, Vol. 20, pp. 347-376.

Faccioli, E. and Villani, M., (2009) "Seismic Hazard Mapping for Italy in Terms of Broadband Displacement Response Spectra". *Earthquake Spectra*, Vol. 25, No. 3, pp. 515-539.

Filiatrault, A. and Folz, B., (2002) "Performance-Based Seismic Design of Wood Framed Buildings", *ASCE Journal of Structural Engineering*, Vol. 128, No. 1, pp. 39-47.

Fleischman, R.B., Farrow, K.T., Kristin, E., (2002) "Seismic Performance of Perimeter Lateral-System Structures with Highly Flexible Diaphragms" *Earthquake Spectra*, Vol. 18, No.2, pp. 251-286.

Folz, B. and Filiatrault, A. (2001) "Cyclic Analysis of Wood Shear Walls", *ASCE Journal of Structural Engineering*, Vol. 127, No.4, pp. 433-441.

Gambarotta, L. and Brencich, A. (2009) "Direct Displacement Based Approaches to the Seismic Analysis of Masonry Structures" *Final Report* of Research Unit 5, Research line IV, RELUIS PE2005-2008, 68 pages.

Gattesco, N., Clemente, I., Macorini, L., Noè, S., (2008) "Experimental Investigation of the Behaviour of Spandrels in Ancient Masonry Buildings", *Proceedings of the 14th World Conference on Earthquake Engineering*, October 12-17, Beijing, China.

Gazetas, G. (1991) "Foundation Vibrations" In *Foundation Engineering Handbook*, 2nd Edition, edited by H. – Y. Fang, , Van Nostrand Reinhold, New York, Chapter 15, pp. 553-593.

Goggins, J.G. and Sullivan, T.J. (2009) "Displacement-based seismic design of SDOF concentrically braced frames" in *STESSA 2009*, Mazzolani, Ricles & Sause (eds), Taylor & Francis Group, pp. 685-692.

Grant, D.N. (2011) "Response Spectral Matching of Two Horizontal Ground Motion Components" *ASCE Journal of Structural Engineering*, Vol.137, No. 3, pp. 289-297.

Grant, D.N., Blandon, C.A., Priestley, M.J.N. (2005) "Modelling Inelastic Response in Direct Displacement Based Design" *Research Report ROSE-2005/03*, IUSS press, Pavia, Italy.

Graziotti, F., Magenes, G., Penna, A., Galasco, A. (2011). "Comportamento Ciclico Sperimentale nel Piano di Fasce in Muratura di Pietra", *Proc. 14th Convegno ANIDIS*, October 18-22, Bari, Italy, paper 152 (*in Italian*).

Gulkan, P., and Sozen, M. (1974). "Inelastic Response of Reinforced Concrete Structures to Earthquake Motions" *ACI Journal*, Vol. 71, No.12, pp. 604-610.

Hancock, J., Watson-Lamprey, J. A., Abrahamson, N. A., Bommer, J. J., Markatis, A., McCoy, E., Mendis, R. (2006) "An Improved Method of Matching Response Spectra of Recorded Earthquake Ground Motion using Wavelets." *Journal of Earthquake Engineering*, Vol.10, Sp. Issue 1, pp. 67–89.

Higashino, M. and Okamoto, S. (2006) Response Control and Seismic Isolation of Buildings. *Taylor & Francis, Ltd.*, UK.

Hilje, T., Sullivan, T.J., Pennucci, D. (2010) "Accounting for torsion in the DBD of multi-storey wall structures" *Proceedings of SECED young engineers conference*, The Institution of Civil Engineers, London, UK.

Iervolino, I. and Cornell, C.A. (2005) "Record Selection for Non-linear Seismic Analysis of Structures", *Earthquake Spectra*, Vol.21, No. 3, pp.685-713.

Iqbal, A., Pampanin, S., Buchanan, A. (2008) "Seismic Behaviour of Prestressed Timber Columns under Bi-directional Loading" *10th World Conference on Timber Engineering* (WCTE 2008), 2-5 June 2008. Miyazaki, Japan.

Jacobsen, L.S. (1960) "Damping in Composite Structures", *Proceedings of the 2nd World Conference of Earthquake Engineering*, Vol.2 Tokyo and Kyoto, Japan, pp.1029-1044.

Khan, E. and Sullivan, T.J. (2011) "Direct Displacement-Based Design of a Reinforced Concrete Deck Arch Bridge" *Proceedings of International Conference on Earthquake Engineering and Seismology* (ICEES 2011), NUST, Islamabad, Pakistan, paper No. 37.

Kramer, S. (1996) *Geotechnical Earthquake Engineering*, Prentice-Hall International Series in Civil Engineering and Engineering Mechanics, 653 pages.

Kurama, Y. and Shen, Q., (2004) "Posttensioned hybrid coupled walls under lateral loads" *Journal of Structural Engineering*, 130(2), pp.297-309.

Lago, A. (2011) "Seismic Design of Structures with Passive Energy Dissipation Systems" *PhD thesis*, European School for Advanced Studies in Reduction of Seismic Risk (ROSE School), IUSS Pavia, Italy.

Lavelle, G. (2009) "Considering Diaphragm Flexibility in the Displacement-Based Design of RC Frame Structures" *MSc dissertation*, European School for Advanced Studies in Reduction of Seismic Risk (ROSE School), IUSS Pavia, Italy.

Loss, C. (2007) "Il Direct Displacement Based Design Applicato a Strutture di Legno Intelaiate:Analisi Numerico-Probabilistica per la Calibrazione di una Metodologia di Calcolo," *Department of Civil and Mechanical Structural Systems,* University of Trento, Trento, Italy.

Magenes, G., Morandi, P., Penna, A. (2008a). "Test Results on the Behaviour of Masonry Under Static Cyclic In Plane Lateral Loads", *ESECMaSE project report RS-01/08*, Department of Structural Mechanics, University of Pavia.

Magenes, G., Morandi, P., Penna, A. (2008b). "In-Plane Cyclic Tests on Calcium Silicate Masonry Walls", *Proceedings of the 14th International Brick/Block Masonry Conference*, Sydney, Australia, 17-20 February 2008, paper 193, CD-ROM.

Magenes, G., Morandi, P., Penna, A. (2008c). "Experimental In-Plane Cyclic Response of Masonry Walls with Clay Units", *Proceedings of the 14th World Conference on Earthquake Engineering*, October 12-17 2008, Beijing, China, Paper ID: 12-03-0095.

Magenes, G., Penna, A., Galasco, A., Rota, M. (2011a). "Double-Leaf Stone Masonry.Characterisation of Mechanical Properties and Cyclic Testing of Masonry Walls", *Report*, IUSS Press, Pavia (*in press*).

Magenes, G., Penna, A., Graziotti, F. (2011b). "Quasi-Static Cyclic Testing of Full-Scale Stone Masonry Spandrels", *Research Report*, IUSS Press, Pavia (*in press*).

Maley, T.J. (2011) "Seismic Design of Mixed MRF Systems" *PhD thesis*, European School for Advanced Studies in Reduction of Seismic Risk (ROSE School), IUSS Pavia, Italy.

Mander, J.P., Priestley, M.J.N., Park, R. (1988) "Theoretical Stress-strain Model for Confined Concrete." *Journal Structural Engineering* ASCE, Vol. 114, No. 8, pp. 1804-1826.

Marriot, D. (2009) "The development of high-performance post-tensioned rocking systems for seismic design of structures" *PhD thesis*, University of Canterbury, Christchurch, New Zealand.

McCormick, J., Aburano, H., Ikenaga, M., Nakashima, M. (2008) "Permissible Residual Deformation Levels for Building Structures Considering both Safety and Human Elements", *Proceedings of 14th World Conference in Earthquake Engineering*, Beijing, China, Paper No. 05-06-0071.

Moayed Alaee, S.A. (2011) "Direct Displacement Based Seismic Design of Cold-Formed Steel Frame-Wood Panel Structures" *PhD thesis*, European School for Advanced Studies in Reduction of Seismic Risk (ROSE School), IUSS Pavia, Italy, 358pages.

Naeim, F. and Kelly, J.M. (1999) *Design of seismic isolated structures*, John Wiley & Sons, Inc., New York.

Nakaki, S.D. (2000) "Design Guidelines for Precast and Cast-in-Place Concrete Diaphragms," *Technical Report*, EERI Professional Fellowship, Earthquake Engineering Research Institute, Berkeley, California.

Newcombe, M. (2012) "Seismic Design of Post-Tensioned Timber Frame and Wall Buildings" *PhD thesis*, Supervised by S. Pampanin & A. Buchanan, University of Canterbury, Christchurch, New Zealand.

Norlund, M. (2010) "Displacement Based Design Developments of Composite Moment Resisting Frame Structures" *MSc dissertation*, European School for Advanced Studies in Reduction of Seismic Risk (ROSE School), IUSS Pavia, Italy.

NZ Concrete Society (2010) *PRESSS design handbook*, Edited by Stefano Pampanin, NZ Concrete Society, Auckland, New Zealand.

Otani, S. (1981) "Hysteresis models of reinforced concrete for earthquake response analysis" *Journal of the Faculty of Engineering*, University of Tokyo, Vol. XXXVI, No.2, pp. 125-159.

Ötes, A. and Löring, S. (2003). "Tastversuche zur Identifizierung des Verhaltensfaktors von Mauerwerksbauten fur den Erdbebennachweis", *Report*, University of Dortmund, Germany (*in German*).

Palermo, A., Pampanin, S., Fragiacomo, M., Buchanan, A.H., Deam, B.L. (2006) "Innovative seismic solutions for multi-storey LVL timber buildings" *9th World Conference on Timber Engineering WCTE 2006*, Portland, USA, August 6-10.

Pampanin, S., Amaris, A., Akguzel, U., Palermo, A. (2006) "Experimental investigation on high-performance jointed ductile connections for precast frames" *Proceedings of First European Conference on Earthquake Engineering and Seismology*, Geneva, Switzerland.

Pang, W., Rosowsky, D.V., van de Lindt, J.W., Pei, S., (2010). "Simplified Performance-Based Design of NEESWOOD Capstone Building and Pre-Test Performance Evaluation", *Proceedings of the 9th U.S. National and 10th Canadian Conference on Earthquake Engineering*, July 25-29, Toronto, Canada.

Pane, V., Cecconi, M. and Vecchietti, S., (2007). "Il Metodo DDBD per il Progetto agli Spostamenti di Strutture di Sostegno", *XII Convegno Nazionale di Ingegneria Sismica*, Pisa, 10-14 giugno 2007, su CD rom.

Paolucci R., Prisco, d.C., Figini, R., Petrini, L., Vecchiotti, M. (2009) "Interazione Dinamica Non-Lineare Terreno-Struttura nell'ambito della Progettazione Sismica agli Spostamenti" *Progettazione Sismica*, Vol. 1, No, 2, Italy.

Pekcan, G., Mander, J.B., Stuart, S.C. (1999) "Fundamental considerations for the design of non-linear viscous dampers" *Earthquake Engineering and Structural Dynamics*, Vol. 28, pp. 1405-1425.

Penna, A., Magenes, G., Calvi, G.M., Costa, A.A. (2008). "Seismic Performance of AAC Infill and Bearing Walls with Different Reinforcement Solutions", *Proceedings of the International Brick/Block Masonry Conference*, Sydney, CD-ROM, paper No. 194.

Pennucci, D., Calvi, G.M., Sullivan, T.J. (2009) "Displacement-Based Design of Pre-Cast Walls with Additional Dampers" *Journal of Earthquake Engineering*, Vol 13, No. S1.

Pennucci, D., Sullivan, T.J., Calvi, G.M., (2011) "Performance-Based Seismic Design of Tall RC Wall Buildings" *Research Report ROSE-2011/02*, IUSS press (www.iusspress.it).

Pennucci, D., Sullivan, T.J., Calvi, G.M., (2011a) "Displacement Reduction Factors for the Design of Medium and Long Period Structures" *Journal of Earthquake Engineering*, Vol. 15, Supplement 1, 1-29.

Pettinga, J.D. and Priestley, M.J.N., (2005) "Dynamic Behaviour of Reinforced Concrete Frames Designed with Direct Displacement-Based Design" *Research Report ROSE - 2005/02*, IUSS press.

Priestley, M.J.N. (1998) "Brief Comments on Elastic Flexibility of Reinforced Concrete Frames and Significance to Seismic Design", *Bulletin of NZSEE*, Vol. 31, No.4, page 246.

Priestley, M.J.N (2003) "Myths and Fallacies in Earthquake Engineering Revisited," *The Mallet Milne Lecture*, IUSS Press, Pavia, Italy. (www.iusspress.it).

Priestley, M. J. N., Calvi, G.M., Kowalsky, M. J. (2007) "Direct Displacement-Based Seismic Design" *IUSS Press*, Pavia, Italy. 720 pages (www.iusspress.it).

Priestley, M.J.N. and Grant, D.N. (2006) "Viscous Damping for Analysis and Design" *Journal of Earthquake Engineering*, Vol. 9, No. SP2, pp. 229-255.

Priestley M.J.N., Sritharan, S., Conley, J.R., Pampanin, S. (1999) "Preliminary Results and Conclusions from the PRESSS Five-story Precast Concrete Test Building", *PCI Journal*, Vol.44, No. 6, pp. 42-67.

Rivera, J. (2008) "On the Development of Seismic Design Forces for Flexible Floor Diaphragms in Reinforced Concrete Wall Buildings" *PhD thesis*, European School for Advanced Studies in Reduction of Seismic Risk (ROSE School), IUSS Pavia, Italy, 225pages.

Robinson, W.H. (1982) "Lead-Rubber Hysteretic Bearings suitable for Protecting Structures during Earthquakes" *Earthquake Engineering and Structural Dynamics*, Vol. 10, No. 4, pp. 593-604.

Salawdeh, S. (2012) "Seismic design of concentrically braced steel frames" *PhD thesis*, National University of Ireland, Galway, Ireland, 280pages.

Sartori, T. (2008) "Comportamento Dissipativo di Giunti a Completo Ripristino nelle Strutture di Legno, Analisi Numerico-Sperimentale per l'Applicazione alla Progettazione Sismica DDBD," *Department of Civil and Mechanical Structural Systems*, University of Trento, Trento, Italy.

Shibata, A. and Sozen, M., (1976). "Substitute Structure Method for Seismic Design in R/C." *Journal of the Structural Division, ASCE*, 102(1), pp. 1-18.

Skinner R.I., Robinson W.H., Mc Verry G.H. (1993) *An Introduction to Seismic Isolation*, John Wiley & Sons Ltd, Chichester, West Sussex, UK.

Smyrou E., Sullivan, T.J., Priestley, M.J.N., Calvi, G.M., (2008) "Dynamic Behaviour of T-Shaped RC Walls Designed with Direct Displacement-Based Design" *14th World Conference on Earthquake Engineering*, Beijing, China, paper No. 05-01-0215.

Suarez, V. and Kowalsky, M.J. (2007) "Direct Displacement-Based Seismic Design of Drilled Shaft Bents with Soil-Structure Interaction" *Journal of Earthquake Engineering*, Vol. 11, No. 6, pp. 1010-1030.

Sullivan, T.J. (2007) "Displacement Considerations for the Seismic Design of Tall RC Frame-Wall Buildings" *8th Pacific Conference of Earthquake Engineering*, Singapore, paper No. 125.

Sullivan T.J. (2009) "Direct Displacement-Based Design of a RC Wall-Steel EBF Dual System with Added Dampers" *Bulletin of the New Zealand Society for Earthquake Engineering*, Vol. 42, No.3, pp.167-178.

Sullivan, T.J. (2010) "Capacity Design Considerations for RC Frame-Wall Structures" *Earthquakes and Structures*, Techno Press, Vol. 1, No. 4, pp. 391-410.

Sullivan, T.J., (2012) "Formulation of a direct displacement-based design procedure for steel eccentrically braced frame structures" *15th World Conference on Earthquake Engineering*, Lisbon, Portugal, paper No.2121.

Sullivan, T.J. and Lago, A. (2012) "Towards a simplified Direct DBD procedure for the seismic design of moment resisting frames with viscous dampers" *Engineering Structures*, Vol. 35 pp. 140-148.

Sullivan, T.J., Priestley, M.J.N., Calvi, G.M., (2004) "Displacement Shapes of Frame-Wall Structures for Direct Displacement Based Design" *Proceedings, Japan-Europe Workshop in Earthquake Engineering*, University of Bristol, Bristol, UK.

Sullivan, T.J., Priestley, M.J.N., Calvi, G.M. (2006) "Seismic Design of Frame-Wall Structures" *Research Report ROSE-2006/02*, IUSS press (www.iusspress.it).

Sullivan, T.J., Salawdeh, S., Pecker, A., Corigliano, M., Calvi, G.M. (2010). "Soil-Foundation Structure Interaction Considerations for Performance-Based Design of RC Wall Structures on Shallow Foundations" In *Soil Foundation Structure Interaction* (R Orense, N Chouw, and M Pender (eds)), CRC Press / Balkema, The Netherlands, pp. 193-200.

Taylor, A.W., Lin, A.N., Martin, J.W. (1992) "Performance of Elastomers in Isolation Bearings: a Literature Review" *Earthquake Spectra*, Vol. 8, No. 2, pp. 279-304.

Tomaževič, M. (2007) "Damage as a Measure for Earthquake-Resistant Design of Masonry Structures: Slovenian Experience", *Can. J. Civ. Eng*, Vol. 34, pp. 1043-1412.

Tremblay, R. (2002). "Inelastic Seismic Response of Steel Bracing Members" *Journal of Constructional Steel Research*, Vol. 58, pp. 665-701.

UNI EN 12512 (2006) *Timber Structures*. Test methods. Cyclic testing of joints made with mechanical fasteners.

Vecchietti, S., Cecconi, M., Pane, V. (2007). "Displacement-Methods for the Design of Earth Retaining

Structures", *4th International Conference on Earthquake Geotechnical Engineering*, Thessaloniki, Greece, pp. 25-28 Giugno 2007, su CD rom.

Vucetic, M. and Dobry, R. (1991) "Effect of Soil Plasticity on Cyclic Response", *Journal of Geotechnical Engineering*, Vol. 117, No. 1, January 1991, pp. 89-107.

Watson-Lamprey, J. and Abrahamson, N. (2006) "Selection of Ground Motion Time Series and Limits to Scaling", *Soil Dynamics and Earthquake Engineering*, Vol. 26, pp. 477-482.

Wijesundara, K. (2009) "Design of concentrically braced steel frame with RHS shape braces" *PhD thesis*, European School for Advanced Studies in Reduction of Seismic Risk (ROSE School), IUSS Pavia, Italy, 345pages.

Wijesundara, K., Nascimbene, R., Sullivan T.J., (2011) "Equivalent Viscous Damping of Steel Concentrically Braced Frame Structures", *Bulletin of Earthquake Engineering*, Vol.9, No. 5, pp. 1535-1558.

Wolf, J.P. (1985) Dynamic Soil-Structure Interaction, *Prentice Hall*, Englewood Cliffs, N. J., U.S.

Zonta, D., Piazza, M., Zanon, P., Giuliani, G. (2006), "An Application of Direct Displacement Based Design to Glulam Timber Portal-Frame Structures", *Department of Civil and Mechanical Structural Systems*, University of Trento, Trento, Italy.

ANNEX 1

A1. APPROXIMATE YIELD CURVATURE VALUES OF COMMON SECTIONS

The following expressions can be used to estimate section yield curvatures for Displacement-Based Design. The expressions are approximate and actual nominal yield curvature values will typically be within +/-10% of the values obtained using the equations below. Note that there is currently uncertainty and some disagreement regarding the best simplified expression for T- and C-shaped sections and designers may be well advised to undertake moment-curvature analyses to verify their design values.

Circular Concrete Columns

$$\phi_y = 2.25\frac{\varepsilon_y}{D} \tag{A1.1}$$

Rectangular Concrete Columns

$$\phi_y = 2.10\frac{\varepsilon_y}{h_c} \tag{A1.2}$$

Rectangular Concrete Walls

$$\phi_y = 2.00\frac{\varepsilon_y}{l_w} \tag{A1.3}$$

Rectangular Masonry Walls

$$\phi_y = 2.10\frac{\varepsilon_y}{l_w} \tag{A1.4}$$

C-Shaped Concrete Walls for bending parallel to web, and bending parallel to flange with web in compression

$$\phi_y = 1.40\frac{\varepsilon_y}{l_w} \tag{A1.5}$$

C-Shaped Concrete Walls for bending parallel to flange with web in tension

$$\phi_y = 1.80\frac{\varepsilon_y}{l_w} \tag{A1.6}$$

T-Shaped Concrete Walls, distributed reinforcement, flange in compression

$$\phi_y = 1.75\frac{\varepsilon_y}{l_w} \tag{A1.7}$$

T-Shaped Concrete Walls, distributed reinforcement, flange in tension

$$\phi_y = 2.15\frac{\varepsilon_y}{l_w} \tag{A1.8}$$

T-Shaped Concrete Beams with strain-hardening

$$\phi_y = 1.9\frac{\varepsilon_y}{h_b} \tag{A1.9}$$

T-Shaped Concrete Beams without strain-hardening

$$\phi_y = 1.7 \frac{\varepsilon_y}{h_b} \qquad\qquad (A1.10)$$

ANNEX 2

A2. RELATIONSHIPS BETWEEN ELASTIC DISPLACEMENT SPECTRA AND INELASTIC DISPLACEMENT DEMANDS

In Section 1 of this document two different sets of expressions are provided to scale the elastic displacement response spectrum to the highly damped response spectrum required for design (as per Section 5). It was explained in the commentary to Section 1.5 that as part of the DDBD procedure, ductility dependent equivalent viscous damping expressions specified in Section 7 are inserted into a damping modification expression in order to scale the elastic design spectrum and identify the inelastic displacement demands for the case in question. It was also stated that damping reduction factors given by the expression in the current version of the EC8 (CEN 2004a), shown below as Eq.(A2.1), possibly provides the most reliable prediction of viscous damping effects on the elastic response spectra of real records, as shown by Faccioli and Villani (2009).

$$R_\xi = (0.10/(0.05+\xi))^{0.5} \qquad (A2.1)$$

However, it was also stated that the results of numerous NLTH analyses have indicated that improved displacement estimates are obtained for structures responding inelastically when the equivalent viscous damping expressions within Section 7 are combined with the damping modification factor expression given in Cl.1.5.1, which is shown here for discussion purposes:

$$R_\xi = (0.07/(0.02+\xi))^{0.5} \qquad (A2.2)$$

In Section 7 a series of expression for the equivalent viscous damping of non-linear systems are presented, with a form typically given by:

$$\xi_{eq} = 0.05 + C\left(\frac{\mu-1}{\mu\pi}\right) \qquad (A2.3)$$

where C is a constant that varies according to the expected hysteretic form of the structure's cyclic load-deformation response.

The expressions included in Section 7 for structures responding non-linearly stem principally from the work of Grant et al. (2005) and Dwairi et al. (2007), who undertook a series of NLTH analyses to calibrate the equivalent viscous damping expressions. In undertaking their independent studies, Grant et al. (2005) and Dwairi et al. (2007) obtained very similar equivalent viscous damping expressions. Interestingly, the Grant et al. (2005) study was undertaken using a set of artificial records, where the elastic spectra at different levels of damping were well predicted by Eq.(A2.2), whereas the study by Dwairi et al. (2007) used a large set of real earthquake records whose highly damped elastic spectra were better predicted through Eq.(A2.1). This observation suggested at the time that damping modification expressions, such as those shown in Eq.(A2.1) and Eq.(A2.2), could be developed for a site independent of the ductility-dependent equivalent viscous damping expression of Eq.(A2.3). However, there remained an anomaly that even though the spectra of real records might scale according to Eq.(A2.1), results of NLTH analyses on different structural typologies suggested that the equivalent viscous damping expressions (Eq.(A2.3)) should be used with the damping modification expression of Eq.(A2.2), and this is the recommendation provided in Priestley et al. (2007).

More recently, Pennucci et al. (2011, 2011a) appear to have shed some light on this aspect. By re-running the analyses of Grant et al. (2005) and also those of Dwairi et al. (2007), and by running a series of additional NLTH analyses with a new set of real records (characterised by linearly increasing spectral displacement demands over the effective period range being considered), they found that the spectral shape and the accelerogram type (artificial or real) both significantly influence the calibration of equivalent viscous damping expressions. Fig. A2.1 shows the calibrated equivalent viscous damping curves obtained by Pennucci et al.

(2011) for two different sets of accelerograms; set 1a is a set of real records with linearly increasing spectral displacement demands, and set 2 is the set of artificial accelerograms used by Grant et al. (2005). Fig. A2.2 shows that the two sets of accelerograms exhibit significantly different spectral reduction and that the damping reduction for set 1a is well predicted by Eq.(A2.1) (the current EC8 expression) whereas set 2 is better predicted by Eq.(A2.2) (the old EC8 expression).
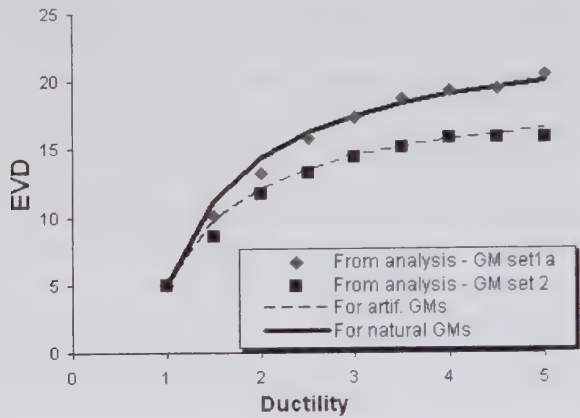

Fig. A2.1: Calibrated equivalent viscous damping curves for the Takeda thin model, obtained from NLTH analyses using real records (GM set 1a) and artificial records (GM set 2) (from Pennucci et al. 2011)
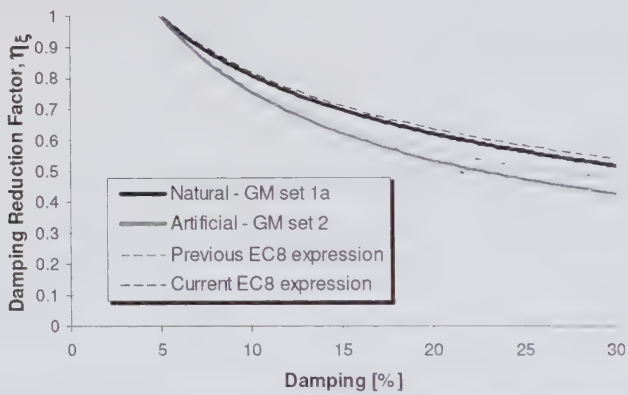

Fig. A2.2: Damping reduction factors obtained for the real record set (GM set 1a) and artificial record set (GM set 2) used in the study by Pennucci et al. (2011).

Unfortunately, the differences in equivalent viscous damping shown in Fig. A2.1, due to record type, were not apparent when the results of Grant et al. (2005) and Dwairi et al. (2007) were initially compared. Pennucci et al. (2011) have shown that this was because differences in both the spectral shape and accelerogram type used in the two studies lead to the same equivalent viscous damping expressions. Furthermore, however, Pennucci et al. (2011) also studied how the inelastic displacement reduction factor, defined according to Eq.(A2.4), is affected by spectral shape and response spectra sensitivity to damping.

$$\eta_{in} = \frac{\Delta_{in}}{\Delta_{el.Te}} \tag{A2.4}$$

where Δ_{in} is the inelastic displacement and $\Delta_{el.Te}$ is the elastic spectral displacement at the effective period of the non-linear system.

The displacement reduction factor (Eq.A2.4) is essentially the same ratio that should be obtained by inserting Eq.(A2.3) into Eq.(A2.2)) as part of the DDBD process. As shown in Fig. A2.3, Pennucci et al. (2011) found that this factor appears to be independent of the record type, and therefore independent to the manner in which spectral displacement demands may be affected by elastic damping (i.e. it is independent of the elastic damping expressions of the type given by Eq.(A2.1) or Eq.(A2.2)).
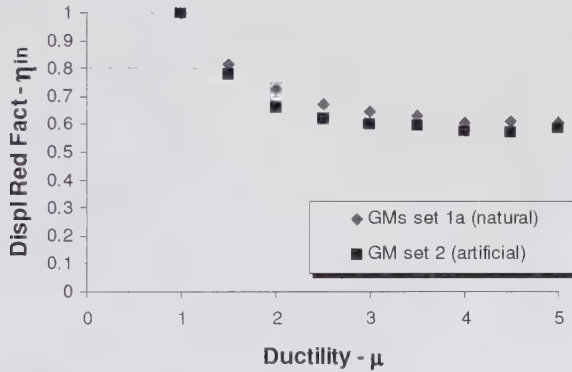

Fig. A2.3: Variation of spectral displacement reduction factors (Eq.A2.4) obtained from NLTH analyses using real records (GM set 1a) and artificial records (GM set 2) (from Pennucci et al. 2011). Note how the displacement reduction factors are essentially the same despite the real and artificial nature of the two record sets.

As a consequence, the findings of Pennucci et al. (2011, 2011a) imply that equivalent viscous damping expressions for non-linear systems, calibrated using NLTH analyses, should be used in combination with the spectral damping reduction expression that characterises the records used for the NLTH analyses. As the damping reduction factors for the records used in the development of the equivalent viscous damping expressions proposed by Priestley et al. (2007) were best described by Eq.(A2.2), this is the damping modification expression that should be used in design. For this reason, in the model code the equivalent viscous damping expressions for non-linear systems presented in Section 7 are combined with the damping modification expression of Eq.(1.2). On the other hand, however, note that when a system is expected to respond elastically with high levels of viscous damping, then the damping modification expression of Eq.(A2.1) appears to be the most appropriate expression. For this reason, Section 1.5 of the model code recommends that Eq.(1.4) be used for highly damped structures responding elastically.

ANNEX 3

A3. PRELIMINARY DIRECT DBD RECOMMENDATIONS FOR CANTILEVER RETAINING SYSTEMS

Cecconi et al. (2007) provide recommendations for the displacement-based seismic design of cantilever diaphragm retaining wall systems. However, very few advanced verification studies have been undertaken to verify the recommendations and hence they are included here as a set of preliminary recommendations.

A3.1 Seismic Masses: Cecconi et al. (2007) recommend that the effective mass of retaining wall systems be set considering the soil volume that is displaced as part of the whole system (soil-structure) mechanism.
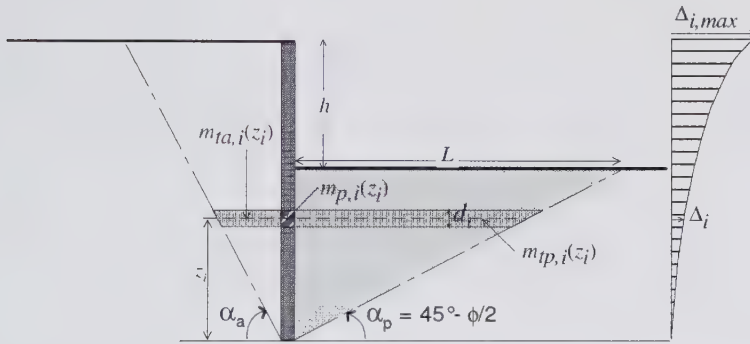

Fig. A3.1: Mass components and design displacement profile of a cantilever diaphragm retaining wall system (Cecconi et al. 2007)

As indicated in Fig. A3.1, the retaining wall system is discretised, into i soil layers of thickness t_i, so that the mass of layer i is given by Eq. (C5.1) (refer Section 5). In other words, for cantilever diaphragm retaining wall systems, Cecconi et al. (2007) recommend that the soil masses participating in the seismic event should be conventionally represented by the active soil wedge behind the wall and the passive wedge in front of it.

The inclination α (α_a and α_p) of the soil wedges is a function of the soil friction angle (ϕ) and the wall roughness (δ). The angles α can be calculated according to the Coulomb limit equilibrium method.

The ith soil mass at a depth (H-z_i) from the ground level is expressed by:

$$m_{as,i}(z_i) = \gamma\, z_i \frac{t_i}{\tan(\alpha_a)} \qquad 0 < z_i < h + d \tag{A3.1}$$

$$m_{ps,i}(z_i) = \gamma\, z_i \frac{t_i}{\tan(\alpha_p)} \qquad 0 < z_i < d \tag{A3.2}$$

where h is the excavation height, d the embedment length, z_i the height of the centre of mass of the ith soil layer of thickness t_i and γ is the soil unit volume weight.

A3.2 Design Displacement Profile: A linear design displacement profile can be adopted for embedded diaphragm retaining walls, as per S.6.14.1.

A3.3 Equivalent Viscous Damping: Cecconi et al. (2007) recommend that the relationship proposed by Vucetic and Dobry (1991) be used to estimate the soil damping in both active and passive states. Vucetic and Dobry (1991) provide a relationship between soil damping and shear strain γ relative to the active and passive soil wedges, which is plotted in the figure below.
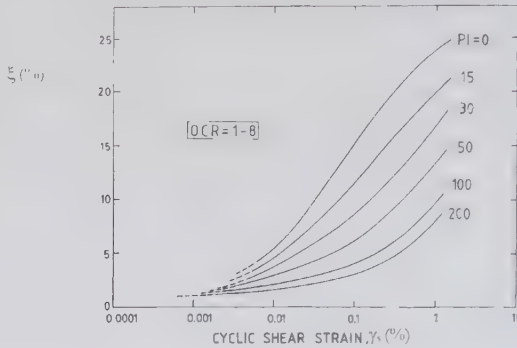

Fig. A3.1: Soil viscous damping as a function of shear strain, γ, (adapted from Vucetic and Dobry, 1991) and plasticity index, **PI** (also referred to as I_p).

The average strain γ_s, for use in the relationships provided by Vucetic and Dobry (1991), can be calculated for the two limit wedges (active and passive) as the ratio between the appropriate design displacement and the related wall height ℓ ($\ell = h+d$ and $\ell = d$ for active and passive limit state, respectively) according to:

$$\gamma_{xs} = \frac{\Delta_{d,xs}}{\ell} \tag{A3.3}$$

where:

$$\Delta_{d,xs} = \frac{\sum_{i=1}^{n}(m_{xs,i}\Delta_i^2)}{\sum_{i=1}^{n}(m_{xs,i}\Delta_i)} \tag{A3.4}$$

where the index "x" changes from "a" (active) to "p" (passive) when ℓ varies from $h+d$ to d.

Cecconi et al. (2007) recommend that the system damping for retaining structures be obtained by "scaling" the soil damping in the active and passive wedges (ξ_{as}, ξ_{ps}) and the wall damping (ξ_w) over the relative masses in accordance with Eq.(7.38).

$$\xi_{eq} = \frac{\xi_{as}\sum_{i=1}^{n}m_{as,i} + \xi_{ps}\sum_{i=1}^{n}m_{ps,i} + \xi_w\sum_{i=1}^{n}m_{w,i}}{\sum_{i=1}^{n}(m_{as,i}+m_{ps,i}+m_{w,i})} \tag{A3.5}$$

Note that this expression does not appear to align well with the work-done approach advocated for combined systems in Section 7.20, but future research may demonstrate that it is sufficient for design purposes.

For **Cantilever diaphragm walls** with cohesionless backfill, by assuming a linear displacement profile and by considering the wall mass negligible, Eq.(A3.5) may be approximated by:

$$\xi_{eq}[\%] = 3.09 \cdot \ln\left[\frac{\Delta_{max}}{H}\right] + 33 \ for \ \frac{\Delta_{max}}{H} > 0.012\% \tag{A3.6a}$$

$$\xi_{eq}[\%] = 5 \quad for \ \frac{\Delta_{max}}{H} \le 0.012\% \tag{A3.6b}$$

with Δ_{max} representing the maximum displacement attained at the top of the wall.

Eq.(A3.6b) was developed through correlation of results obtained for different embedment ratios of diaphragm systems, varying in the range of 1 to 1.5. The two forms of Eq.(A3.6) have been set as a function of the non dimensional deformation ratio Δ_{max}/H as this formulation provides a simple means of quantifying the equivalent damping.

A3.4 Active and Passive Thrusts Derived from Base Shear Force: The base shear force for retaining walls is intended as the design seismic increment representing the sum of the active seismic increment V_{as}, the passive seismic decrement V_{ps} and the diaphragm wall inertia (if the wall mass is not neglected). The force V_{Base} can be distributed to the various discretised masses of the structure according to:

$$V_i = V_{Base} \frac{m_i \Delta_i}{\sum\limits_{i=1}^{n} m_i \Delta_i} \tag{A3.7}$$

where V_i is the design force of the ith mass. In particular, the force V_{Base} shall be distributed into three parts and precisely:
- V_{as}: the seismic increment pertaining to the soil mass in the active wedge;
- V_{ps}: the seismic decrement pertaining to the soil mass in the passive wedge;
- V_w: the lateral inertia force of the wall.
Eq.(A3.7) is useful because it permits the entire distribution of the active/passive seismic forces along the retaining wall to be obtained or, alternatively, the position of their application point to be identified. This is considered one of the advantages of the method with respect to conventional pseudo-static approaches, in which such an application point is unknown.

The active seismic increment is formulated as:

$$V_{as} = \sum\limits_{i=1}^{n} V_{as,i} \tag{A3.8}$$

$$V_{as,i} = V_{Base} \frac{m_{as,i} \Delta_i}{\sum\limits_{i=1}^{n} m_i \Delta_i} \tag{A3.9}$$

Equivalent equations hold for the horizontal forces V_{ps} and V_w, which can be calculated by simply substituting $m_{as,i}$ at the numerator with $m_{ps,i}$ and $m_{w,i}$ respectively.
The lateral seismic force V_{Base} for cantilever retaining structures can be directly calculated according to:

$$V_{Base} = \frac{1}{2}\frac{\gamma}{g}H^2 \cdot \frac{32}{27}\cdot\frac{N^3}{M^2}\cdot\Gamma\cdot\frac{1}{\Delta_{max}}$$ (A3.10)

where

$$N = \left[\frac{1}{\tan\alpha_a} + \left(\frac{d}{H}\right)^3\cdot\frac{1}{\tan\alpha_p}\right]$$ (A3.11)

From Eq. (A3.10) it is possible to derive the seismic active (or passive) increment pertaining to the soil wedges. In the active case, for example, the seismic increment is calculated as follows:

$$V_{as} = \frac{1}{2}\frac{\gamma}{g}H^2\cdot\frac{32}{27}\cdot\left(\frac{N}{M}\right)^2\cdot\Gamma\cdot\frac{1}{\Delta_{max}} = \frac{1}{2}\gamma H^2\cdot\Delta K_{ae}^*\,(\xi_e,\Delta_{max})$$ (A3.12)

with ΔK_{ae}^* the equivalent seismic active earth pressure coefficient.

ANNEX 4

A4. STIFFNESS AND EQUIVALENT VISCOUS DAMPING OF FOUNDATION SYSTEMS

Through a review of experimental data and a series of analytical studies, Paolucci et al. (2009) found that the rotational stiffness and equivalent viscous damping of a shallow foundation vary as indicated in Fig.s A4.1 and A4.2.
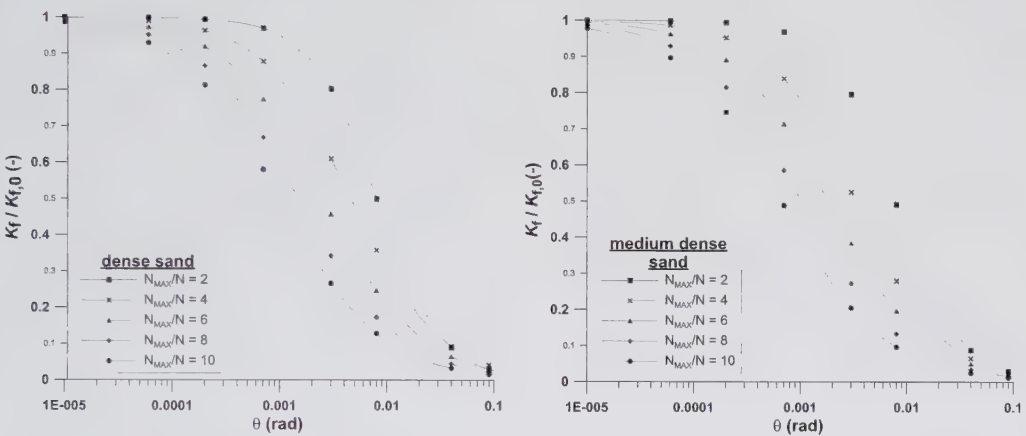

Figure A4.1 – Rotational Stiffness Degradation Curves for dense sand (left) and medium dense sand (right) as a function of foundation rotation for a range of axial compression ratios (N_{MAX}/N = maximum axial resistance/expected axial load).
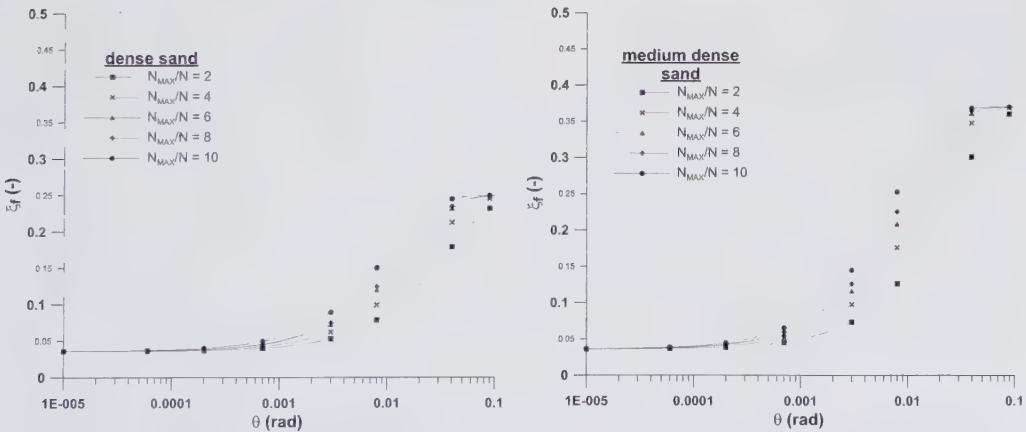

Figure A4.2 – Equivalent Viscous Damping Curves for dense sand (left) and medium dense sand (right) as a function of foundation rotation for a range of axial compression ratios (N_{MAX}/N = maximum axial resistance/expected axial load).

In order to quantify the variation of stiffness and equivalent viscous damping as a function of the foundation rotation, θ_f, Paolucci et al. (2009) developed the following expressions:

$$\frac{K_f}{K_{f,0}} = \frac{1}{1 + a \cdot \theta_f{}^m}$$ (A4.1)

$$\xi_f = \xi_{f,min} + \left(\xi_{f,max} - \xi_{f,min}\right)\left[1 - \exp\left(-\alpha\theta_f\right)\right]$$ (A4.2)

In the previous equations $\xi_{f,min}$, $\xi_{f,max}$, a, m and α are non-dimensional constitutive parameters and vary as a function of the sand relative density and of the static safety factor N_{max}/N. $\xi_{f,min}$ has been suggested to be equal to 0.036 by Paolucci et al. (2009), while the saturation value $\xi_{f,max}$ is equal to 0.25 for dense sands and to 0.37 for medium dense sands. In Table A4.1, from Paolucci et al. (2009), the values of a, m and α both for dense and medium dense sands and for different values of the static safety factor are reported.

TABLE A4.1: Values for parameters a, m and α for use in Equations (A4.1) and (A4.2)

N_{MAX}/N	DENSE SAND			MEDIUM DENSE SAND		
	a	m	α	a	m	α
2	458.36	1.30	27.73	686.26	1.30	39.39
3	281.95	1.11	32.76	386.24	1.11	47.61
4.5	262.90	1.00	43.93	339.87	0.98	67.79
6	292.81	0.94	62.25	352.13	0.92	90.64
7.5	324.76	0.91	66.96	398.44	0.89	104.49
9	378.05	0.89	85.08	433.12	0.86	119.20
10	415.5	0.88	95.60	452.44	0.84	130.85
15	575.36	0.83	164.42	653.02	0.79	210.42
20	1010.99	0.86	233.70	1219.47	0.83	285.15
25	2461.06	0.95	305.97	2461.06	0.89	367.70
30	5192.13	1.02	382.51	5192.13	0.96	442.47

The curves presented in Fig.s A4.1 and A4.2 presently refer to rigid shallow foundations, with a moderate level of embedment, for which a prevailing rotational contribution can be assumed, as supported both by experimental and numerical results. Similar considerations can be extended to deep rigid foundations, such as deep caissons and rafts on densely spaced pile groups, while the interaction with flexible foundation systems (footings on single piles, pile groups with large spacing) is more complicated and may be strongly frequency-dependent.

For stiffness and damping values of different foundation types for small deformation levels, as well as for their frequency-dependence, refer to Gazetas (1991).

ANNEX 5

COMMENTARY

A5. DDBD OF STEEL BRACED FRAME STRUCTURES

This annex contains preliminary requirements for the DDBD of steel braced frame structures. A general simplified procedure for concentrically braced frames is provided in Section A5.1, a refined procedure for concentrically braced frames with flexible beams is provided in Section A5.2, and a general procedure for eccentrically braced frames is provided in Section A5.3.

A5.1 General Procedure for Concentrically Braced Frame Structures: For steel concentrically braced frame (CBF) structures in which tension yielding in braces will be assured prior to exhausting the compression brace deformation capacity, the following design guidelines shall be adopted.

A5.1.1 Design displacement profile: The limit state design displacement profile of a CBF structure, shall be determined by rational structural analysis or, when inelastic response is expected, by direct use of Eq.(A5.1):

$$\Delta_{i,ls} = \theta_c h_i \cdot \frac{(4H_n - h_i)}{(4H_n - h_1)} \qquad (A5.1)$$

Where θ_c shall be set as the minimum of the storey drift limit for non-structural elements (Table 2.1) and the structural storey drift limit, $\theta_{c.CBF}$, obtained from rational analysis or Eq.(A5.2):

$$\theta_{c.CBF} = \frac{2\varepsilon_{LS}}{\sin 2\alpha_{br}} \qquad (A5.2)$$

Where ε_{LS} is the brace strain at the design limit state, set in accordance with Section 2.4, and α_{br} is the angle of inclination of the brace with respect to the horizontal. For the repairable damage and collapse prevention limit states ε_{LS} shall be determined using the brace slenderness at the ground storey of the structure. The designer shall ensure that the structural storey drift capacities above the base level are equal or greater than the storey drift capacity at the ground storey level.

CA5 The guidelines provided here for the Direct DBD of steel braced frame structures are preliminary because they have been subject only to limited verification studies and because it is hoped that the design expressions can be simplified in the future. The different types of braced frame structures covered by this annex are illustrated in Figure A5.1.
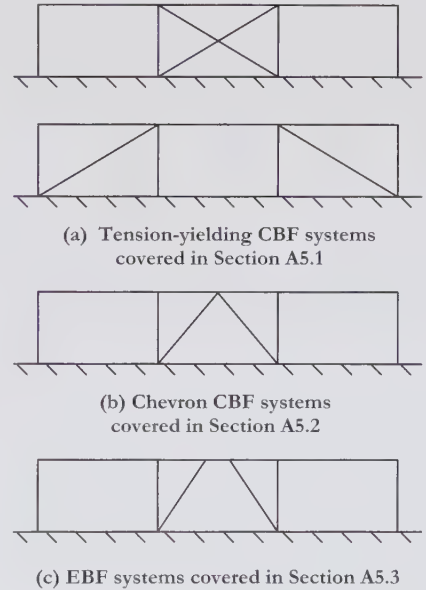

(a) Tension-yielding CBF systems covered in Section A5.1

(b) Chevron CBF systems covered in Section A5.2

(c) EBF systems covered in Section A5.3

Fig. CA5.1: Illustration of different braced frame systems covered by the different sections of this Annex.

CA5.1 The guidelines provided in this section have been formulated on the basis of the research and recommendations of Priestley et al. (2007), Della Corte and Mazzolani (2008), Goggins and Sullivan (2009), Wijesundara (2010), Ackelyan (2011) and Salawdeh (2012).

The clauses of Section A5.1 are applicable to CBF configurations that ensure braces yield in tension prior to the fracture of compression braces. This requirement can typically be assumed satisfied for CBF systems of the type shown in Fig.CA5.1(a), since the tension and compression braces will be subject to similar

ANNEX 5

For CBF structures that are expected to respond elastically for the limit state under consideration, the displaced shape shall correspond to the fundamental mode shape obtained from Eigen-value analyses. The limit state displacement profile shall then be computed by scaling the mode shape to the minimum storey drift capacity associated with either structural (Table 2.3) or non-structural elements (Table 2.1) over the building height.

A5.1.2 Equivalent Viscous Damping: For CBF structures designed to ensure tensile yielding of braces, the equivalent viscous damping shall be defined through rational analysis or using Eq.(7.16) from S.7.8, with the yield displacement approximated as:

$$\Delta_y = 2H_e\left(\frac{\varepsilon_y}{\sin 2\alpha_{br}} + \frac{H_e k_{cols}\varepsilon_y}{L_b}\right) \quad \text{(A5.3)}$$

Where k_{cols} is the average ratio of the design stress (due to DBD seismic forces) to the yield stress in the column sections.

A5.1.3 Equivalent Lateral Force Distribution: In order to identify the required strength of braces within CBF structures with tensile-yielding braces, the structure shall be analysed under a set of equivalent lateral forces in accordance with S.8.1.1 with k = 0.9.
In line with S.6.7.3(8) of EC8, in order to ensure globally distributed dissipation, the ratio of the storey shear resistance to the design storey shear force shall be evaluated for each storey and shall not vary by a factor greater than 1.25. Furthermore, the ratio shall not vary by more than a factor of 1.15 between adjacent storeys.

A5.1.4 Capacity Design Requirements for CBF structures: Capacity design forces for CBF structures shall be calculated assuming a full plastic mechanism may develop with tensile braces developing their maximum plastic overstrength resistance and the following two different scenarios considered for compression braces; (i) compression braces develop their overstrength resistance at first buckling and (ii) the compression brace resistances drop to zero.

COMMENTARY

levels of axial deformation demand. The same is not true for Chevron braced frame configurations of the type shown in Fig. CA5.1(b), in which beam deflections will tend to increase deformation demands on compression braces and reduce deformation demands on tension braces, implying that fracture of compression braces can occur prior to the yielding of tension braces.

C.A5.1.2 The ratio of the design stress to the yield stress in the column sections, k_{cols}, specified in Eq.(A5.3) can be expressed numerically as:

$$k_{cols} = \frac{1}{n}\sum_{i=1}^{n}\frac{N_{E,col,i}}{N_{Rs,col,i}} \quad \text{(CA5.1)}$$

Where $N_{E,col,i}$ is the seismic axial force expected in the column of level i at the design deformation limit state and $N_{Rs,col,i}$ is the section resistance of the column at level i. n is the number of storeys. Note that k_{cols} is a design choice since a designer will choose to provide columns with greater capacity than needed. Buckling checks will typically result in a column axial capacity considerably lower than the column section capacity, and therefore k_{cols} values tend to be low. A reasonable initial estimate might be in the order of 0.25.

C.A5.1.3 The recommendation to provide a relative strength ratio no greater than 1.25 is considered particularly important for CBF and EBF systems as it helps to reduce the possibility that drift concentrates in a single storey.

C.A5.1.4 The capacity design requirement to consider two different compression force scenarios for CBFs recognises that the resistance of compression braces reduces greatly after they buckle. Consequently, while the brace overstrength resistance may be best for estimating maximum column compression forces, the minimum brace resistance is likely to be more critical for elements affected by out-of-balance brace forces (such as beams in Chevron braced systems).

<table>
<tr><td>

ANNEX 5

</td><td>

COMMENTARY

</td></tr>
</table>

A5.2 Procedure for Inverted-V (Chevron) Concentrically Braced Frame Structures: The following clauses are applicable to inverted-V (Chevron) braced frame structures in which beam flexibility is such that tensile yielding of braces is not expected. The frames shall be designed in accordance with good detailing and capacity design procedures to ensure that brace buckling is the only inelastic deformation mechanism that develops in the system.

A5.2.1 Design displacement profile: Both the yielding and the limit state displacement profile shall be defined by rational analysis, or by the following approximate equations:

$$\frac{\Delta_{i,y}}{\Delta_{N,y}} = \alpha_\Delta \left(\frac{i}{N}\right)^2 + (1-\alpha_\Delta)\left(\frac{i}{N}\right) \qquad (A5.4)$$

$$\Delta_{N,y} = \left(\frac{1}{2} k_{c,y} \chi_c \frac{N}{\alpha_\Delta}\right) \varepsilon_y H_n \qquad (A5.5)$$

$$\alpha_\Delta = \left(1 + \frac{1}{N}\left(4\frac{\chi_{br}}{k_{c,y}\chi_c} - 1\right)\right)^{-1} \qquad (A5.6)$$

$$\frac{\Delta_{i,ls}}{\Delta_{N,ls}} = \beta_\Delta \left(\frac{i}{N}\right)^2 + (1-\beta_\Delta)\left(\frac{i}{N}\right) \qquad (A5.7)$$

$$\Delta_{N,ls} = \left(\frac{1}{4} k_{c,d} \chi_c \frac{N}{\beta_\Delta}\right) \varepsilon_y H_n \qquad (A5.8)$$

$$\beta_\Delta = \left(1 + \frac{1}{N}\left(4\frac{\overline{\varepsilon} + \mu_d}{k_{c,d}\chi_c} - 1\right)\right)^{-1} \qquad (A5.9)$$

Column deformations: The average normalized column strains corresponding to yielding (brace buckling) and design displacement ($k_{c,y}$ and $k_{c,d}$) are related to each other by the following approximate relationship:

$$k_{c,d} = k_{c,y} + (1 - k_{c,y})\overline{\varepsilon} \qquad (A5.10)$$

The value of $k_{c,y}$ is selected as a design parameter.

Beam deformations: Beams shall be designed so that the mid-span maximum deflection after brace buckling, at every floor, is not larger than:

C.A5.2 The recommendations provided in Section 5.2 stem from the work of Della Corte and Mazzolani (2009). They have been specifically developed for the case of inverted-V (Chevron) braced frames systems, of the type shown in Figure CA5.1(b), for which beam deformations need to be considered during the design process.

C.A5.2.1 The parameter $k_{c,y}$ is a non dimensional measure of the column axial strain due to earthquake loads, at the buckling displacements. Indeed, it should be equal to $k_{c,y} = \dfrac{\varepsilon_{c,y}^E}{\chi_c \varepsilon_y}$. The real value of this parameter will obviously change from floor to floor. An average value is used to calculate displacements. It is noted that a sensitivity study conducted by Della Corte and Mazzolani (2009) showed that the height-wise variation of $k_{c,y}$ has relatively minor effects on the final displacements.

$k_{c,y}$, $k_{c,d}$, μ_d and $\overline{\varepsilon}$ are design parameters.

k_c indicates the ratio between the column strain at any given state of the structure and the buckling value of the column strain. It will be called "normalized column strain" in the following. Therefore, $k_{c,y}$ and $k_{c,d}$ are the values of k_c at the yielding and design state, respectively. Note that $k_c < 1$ because columns must not buckle.

$\overline{\varepsilon}$ is the ratio between the design strain for the tension brace and the yield strain. The average value over the height of the building can be used for multi-storey structures.

μ_d is the average design value of the compression brace ductility defined as per T. 2.3 and Eq.(2.3). Because columns shall be designed according to capacity design criteria, the assumed value for $k_{c,y}$ should be coherent with those criteria. The larger the forces used for capacity design, the smaller the final value of $k_{c,y}$. Furthermore, it is noted that an accurate calculation of $k_{c,y}$ at the start of the design process is not typically possible because the theoretic cross section properties coming out from the design process will not typically be perfectly matched by real commercial steel

ANNEX 5   COMMENTARY

$$v_{b,\max} = \frac{1}{2}\left(\frac{\mu_d - \bar{\varepsilon}}{\sin 2\alpha_i} - k_{c,y}\chi_c \tan\alpha_i\right) \quad (A5.11)$$

The check must be made using the same forces used for capacity design of beams (set in line with Section 9 and A5.1.4).

profiles. Therefore, only an approximate, but reasonable, value of $k_{c,y}$ must initially be established. Usually, if the initial value of $k_{c,y}$ is realistic, then the design will not need to be later modified by correcting the value of $k_{c,y}$, since only a limited variation of the yielding and design displacement will result. However, it is recommended to check the assumed value of $k_{c,y}$, by comparing it with the real value which can be calculated at the end of the design. At this point displacements, and consequently design forces, can be calculated again to check whether the member cross sections need to be corrected.

In the plastic range of response of the chevron (V-braced) system, beams are subjected to concentrated forces at mid-span because of the unbalanced vertical force resulting from the tension and compression brace unsymmetrical response. Consequently beams vertical deflections have an effect on the frame displacements. This does not appear in the equations proposed for calculating displacements, because it has been implicitly assumed that the beam deflections will not be larger than the value given by Eq. (A5.11). Though increasing the beam flexibility is advantageous from the point of view of the global deformation capacity, it produces an increase of the brace ductility demand in compression. The approach proposed here is considered to be conservative. Future research may suggest that the proposed criterion may be relaxed.

A5.2.2 Equivalent Viscous Damping: The equivalent viscous damping of the CBF system, designed according to the recommendations in this section A5.2, shall be defined through rational analysis, with account for the possibility that tension braces may not have yielded at the design limit state.

A5.2.3 Equivalent Lateral Force Distribution: In the case of concentrically braced frames designed according to the recommendations in Section A5.2, the design of braces shall be carried out at the yielding state (i.e. brace buckling), using the following force vector:

$$F_i = \frac{2\chi_{br}}{\bar{\varepsilon} + \chi_{br}}V_{Base}\left(m_i\Delta_{i,j}\right)/\sum_{i=1}^{n}\left(m_i\Delta_{i,j}\right) \quad (A5.12)$$

The brace axial force due to the earthquake forces given by Eq.(A5.12) shall be added to the brace axial force associated with any gravity loads directly applied to the braces. The braces shall then be designed for buckling under the resulting total axial force.

C.A5.2.3 In the case of Chevron CBF structures with flexible beams, the base shear force is first scaled down from the design displacements to the brace buckling displacements and then distributed in proportion to floor mass and floor displacement at buckling. The design of braces under the combined action of gravity and earthquake loads generally avoids the undesired concentration of damage in a few stories (generally the upper stories). Indeed, the percentage incidence of gravity loads at the upper floors is larger than at lower stories, where the earthquake story shear is much larger. Note that χ_{br} and $\bar{\varepsilon}$ are defined in the list of symbols and in Section C.A5.2.1.

ANNEX 5

A5.3 Eccentrically Braced Frame Structures:
This section provides guidelines for the displacement-based seismic design of eccentrically braced frame (EBF) structures of up to 15 storeys with centrally located links. The EBF structures shall be carefully detailed in accordance with Section 6.8.3 of EC8 (CEN). Deformation limits for either short or long links of eccentrically braced frame structures are provided in Table 2.5. The links shall be detailed and provided with a sufficient number of stiffeners to ensure that the indicated deformations limits can be sustained.

A5.3.1 Design displacement profile: The limit state displacement of an EBF structure at level i, shall be defined by rational analysis, or for by the following equation:

$$\Delta_{i.ls} = \theta_v h_i + \left(\theta_c - \theta_v\right)h_i \cdot \frac{(2H_n - h_i)}{(2H_n - h_1)} \quad \text{(A5.13)}$$

Where h_i is the height of level i above the base, H_n is the total building height, h_1 is the height of the 1st storey, θ_v is the minimum storey yield drift over the height of the structure and θ_c is the critical storey drift limit. When using the displacement profile from Eq.(A5.13) within Eq.(5.3), the ω_θ factor shall be set equal to 1.0 for $n \leq 6$ and as 0.6 for $n > 15$ with linear interpolation permitted for intermediate values of n.

The critical storey drift limit, θ_c, shall be taken as the minimum value of the non-structural or structural storey drift limit, $\theta_{c,str}$, over the height of the EBF structure. The non-structural storey drift limit shall be taken from Table 2.1. The structural storey drift limit shall be evaluated from rational analyses or from Eq.(A5.14):

$$\theta_{c.str,i} = \theta_{i,y} + \theta_{i,p} \quad \text{(A5.14)}$$

Where $\theta_{i,y}$ and $\theta_{i,p}$ are, respectively, the elastic (yield) and plastic storey drift capacities of level i.

The storey drift at yield of EBF structures shall be determined from rational analyses or using Eq.(A5.15):

COMMENTARY

C.A5.3 The guidelines provided in this section for EBF structures have been developed by Sullivan (2012). The guidelines refer to the DDBD of EBFs with short or long links centrally located as shown in Figure CA5.1. The definition of "short" and "long" links is provided in C2.5.

C.A5.3.1 The empirical displaced shape expression of Eq.(5.13) aims to approximate the manner in which the displaced shape of an EBF will change with increasing inelastic deformation demands.

The higher mode drift reduction factors specified for use within Eq.(5.3) for EBFs are considerably lower than those specified for other systems early in Section 5.9. This reflects the relatively long second mode periods of EBF systems and consequently the large drift demands that higher mode excitations can produce in EBF systems.

The term θ_c-θ_y can be considered equivalent to a plastic storey drift. The wording used in Section A5.3.1 recognises the possibility that drift demands can be large at any storey of an EBF even though the design displacement profile of Eq.(A5.13) will indicate lower storey drift demands at the upper levels.

When setting the critical storey drift limit, consideration should also be given to the need to control P-delta effects in line with Section 5.6. To this extent, a maximum P-delta stability coefficient of 0.20 (instead of 0.30) may be suitable here given the manner in which drifts tend to concentrate at localised storeys in EBF systems.

ANNEX 5

$$\theta_{i,y} = \frac{2\delta_{v,i}}{L_b - e_i} + k_{br,i}\varepsilon_y \tan\alpha_{br,i} + \frac{2k_{cols,i-1}\varepsilon_y\left(h_i - h_s\right)}{L_b}$$
$$- (A5.15)$$

Where $k_{br,i}$ is the ratio of the design stress (due to DBD seismic forces) to the yield stress of the brace section at level i, as per Eq.(A5.16), $k_{cols,i-1}$ is the average ratio of the design stress to the yield stress in the column sections up to (but excluding) the level under consideration, as per Eq.(A5.17), and $\delta_{v,i}$ is the vertical displacement of the end of the link at level i due to elastic deformations that shall determined using the relevant form of Eq.(A5.18).

$$k_{br,i} = \frac{N_{E,br,i}}{N_{Rs,br,i}} \tag{A5.16}$$

$$k_{cols,i-1} = \frac{1}{i-1}\sum_{j=1}^{j=i-1}\frac{N_{E,col,j}}{N_{Rs,col,j}} \tag{A5.17}$$

Vertical displacement for Short Links:

$$\delta_{v,i} = 0.577 F_y A_{v,i}\left(\frac{e_i^2(L_b - e_i)}{24EI_i} + \frac{e_i}{2GA_{v,i}}\right) \tag{A5.18a}$$

Vertical displacement for Long Links:

$$\delta_{v,i} = M_{p,i}\left(\frac{e_i(L_b - e_i)}{12EI_i} + \frac{1}{GA_{v,i}}\right) \tag{A5.18b}$$

Where e_i is the link length at level i, L_b is the distance between column centrelines of the EBF, I_i and $A_{v,i}$ are respectively the second moment of inertia and shear area of the link at level i, and $M_{p,i}$ is the plastic section moment resistance of the link at level i.
The plastic storey drift capacity shall be set using rational analyses or by Eq.(A5.19):

$$\theta_{i,p} = \frac{e_i \cdot \gamma_{p,link,i}}{L_b} = \frac{e_i \cdot \left(\gamma_{ls,link,i} - \gamma_{y,link,i}\right)}{L_b} \tag{A5.19}$$

Where the permissible link chord rotation at the design limit state, $\gamma_{ls,link}$, shall be obtained from T.2.5, and $\gamma_{y,link}$ and $\gamma_{p,link}$, are respectively yield and plastic chord rotations of the link.

COMMENTARY

Fig.CA5.2 illustrates the terms used in Eq.(A5.15) that refer to the EBF geometry.
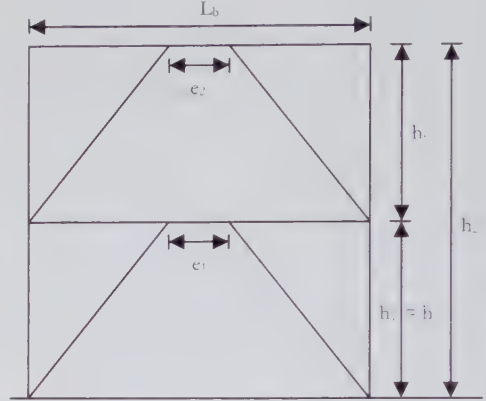

Fig. CA5.2: Illustration of geometrical terms used for the design of EBF systems.

Eq.(A5.15) approximates the yield drift as the sum of drift components due to link beam shear and flexural deformations, and brace and column axial deformations. The column axial deformation drift component refers to the rigid-body drift caused by axial deformations of columns below the storey under consideration (hence $k_{cols,i-1} = 0$ for $i = 1$). Eq.(A5.15) does not include terms to account for other sources of deformation, such as the axial deformations of beams.
Through multiplication of the axial deformation factors from Eq.(A5.16) and Eq.(A5.17) with the steel yield strain within Eq.(A5.15), the average brace and column strains are estimated. Note that the factors in Eq.(A5.16) and Eq.(A5.17) are a design choice since, in line with capacity design principles, a designer will provide braces and columns with greater capacity than needed. Buckling checks will typically result in axial capacities considerably lower than the section capacities, and therefore the factors tend to be small. A reasonable initial estimate might be in the order of 0.25 for both $k_{br,i}$ and $k_{cols,i}$. Some iteration will typically be required in the design process in order to obtain efficient column and brace section sizes that provide the k factors initially input into Eq.(A5.15).

ANNEX 5

COMMENTARY

Eq.(A5.19) stems from the work of Englehart and Popov (1989). Note that the terms $\gamma_{p,link}$ and $\gamma_{y,link}$ do not require evaluation since the total chord rotation at the limit state, $\gamma_{ls,link}$, is set as a function of $\gamma_{y,link}$, according to T.2.5, such that the $\gamma_{y,link}$ terms on the right hand side of Eq.(A5.19) cancel.

A5.3.2 Equivalent Viscous Damping: The equivalent viscous damping of well detailed steel EBF structures shall be obtained from rational analyses or from Eq. (A5.20):

$$\xi_{eq} = 0.07\left(1 + \frac{1.17(\mu - 1)}{1 + \exp\left(\sqrt{\mu - 1}\right)}\right)^2 - 0.02 \quad \text{(A5.20)}$$

Where μ is the EBF displacement ductility demand.

In order to consider the effect of variations in link ductility demands up the building height on the equivalent viscous damping, the yield drift of each storey shall first be calculated according to Eq.(A5.21). Storey ductility demands shall then be obtained according to:

$$\mu_i = \frac{\theta_{i,ls}}{\theta_{t,y}} \quad \text{(A5.21)}$$

The equivalent viscous damping of each storey shall then be found through substitution of the storey ductility demands into Eq.(A5.20). The EBF system damping shall then be obtained by combining the equivalent viscous damping values of each storey according to S.7.20 and Eq.(C7.4).

C.A5.3.2 The equivalent viscous damping expression of Eq.(A5.20) has been derived from the expression for displacement reduction factors developed by Maley (2011) for bi-linear systems with a post-yield stiffness ratio of 0.05. It should be used in combination with the spectral displacement reduction expressions provided in Section 1.5.1.

A5.3.3 Equivalent Lateral Force Distribution: In order to identify the required strength of links within EBF structures, the structure shall be analysed under a set of equivalent lateral forces in accordance with S.8.1.1, with $k = 0.9$ for $n \geq 6$ and $k = 1.0$ for $n < 6$. In line with S.6.8.2(7) of EC8, in order to ensure globally distributed dissipation, the ratio of the storey shear resistance to the design storey shear force shall be evaluated for each storey and shall not vary by a factor greater than 1.25. Furthermore, the ratio shall not vary by more than a factor of 1.15 between adjacent storeys.

C.A5.3.3 The recommendation to provide a relative strength ratio no greater than 1.25 is considered particularly important for CBF and EBF systems as it helps to reduce the possibility that drift concentrates in a single storey. Similarly, the requirement that the provided strength ratio does not vary from one storey to another by a factor greater than 1.15 also aims to reduce the probability of storey drift concentrations.

In lieu of plastic mechanism analyses, the following expression can be used to identify the design shear, $V_{link,i}$ of an EBF link at level i, knowing the design storey shear, V_i resisted by

ANNEX 5

COMMENTARY

the EBF (which will be a portion of the total storey shear when more than one EBF or lateral-load resisting system acts at storey i):

$$V'_{link,i} = \frac{V_i h_s}{L_b}$$ (CA5.2)

and from this the design moment for the link is obtained as:

$$M_{link,i} = \frac{2V'_{link,i}}{e_i}$$ (CA5.3)

Where e, h_s and L_b are the link length, the storey height and the bay length respectively, as shown in Fig.CA5.2.

A5.3.4 Capacity Design Requirements for EBF structures: Capacity design forces for EBF structures shall be obtained assuming a full plastic mechanism may develop with links at their maximum plastic overstrength resistance.

ANNEX 6

COMMENTARY

A6. CAPACITY DESIGN AIDS FOR STRUCTURES WITH SEISMIC ISOLATION

This Annex presents an approximate method that assists in defining capacity design forces for moment-resisting frame structures with seismic isolation. Note that even though these techniques may be used for design, Section 9 requires that non-linear time-history analyses be undertaken to verify the performance of structures with isolation systems.

A6.1 Lateral Force Distributions for Preliminary Design of Base Isolated Moment Resisting Frame Buildings:
For base isolated moment-resisting frame buildings, the lateral force distributions that should be used for capacity design of the structure shall be set considering the actual cyclic mechanical behaviour of the isolation system utilized. The following subsections provide guidelines for specific types of isolation device.

A6.1.1 Visco-Elastic Isolation Systems:
The base shear force shall be distributed to the locations of floor mass of the building in accordance with the relationship:

$$F_i = V_{Base} \frac{m_i \cdot \Delta_i}{\sum m_j \cdot \Delta_i} \cdot Z \qquad (A6.1)$$

where m_i e Δ_i represent the mass and the design displacement of the i-th storey, respectively. The coefficient Z is evaluated through:

$$Z = 1 \qquad\qquad\qquad i \le \frac{N}{2} \qquad (A6.2)$$

$$Z = 1 + \left[\frac{2 \cdot i - N}{N} \cdot \left(Z_{max} - 1 \right) \right] \quad i > \frac{N}{2}$$

where N is the number of storeys of the building while Z_{max} is the maximum value of Z, which is reached at the upper storey of the building. It can be obtained as:

$$Z_{max} = 1 + 0.044 \cdot N \qquad (A6.3)$$

CA6. This Annex focuses on providing a simplified means of setting capacity design forces for base-isolated frame buildings. Note that the draft version of this model code, DBD09, also included guidance for the selection of the isolation system displacement that stemmed from the work of Cardone et al. (2010). For simplicity however, and because the design displacements indicated by Cardone et al. (2010) need not be considered as strict displacement limits but rather as a good design possibility, the guidelines are not included in this version of the model code and instead, interested readers should refer to Cardone et al. (2010).

CA6.1.1 The proposed relationships (Eq.s (A6.1)-(A6.3)) are applicable for regular framed buildings, of up to eight storeys in height, equipped with visco-elastic isolation systems characterised by damping ratios ranging from 10% to 30%.
The coefficient Z increases linearly from 1 to Z_{max} passing from the mid-height to the top of the building.

ANNEX 6

A6.1.2 Isolation Systems with Bi-Linear Hysteretic Response: The base shear force shall be distributed to the locations of floor mass of the building in accordance with the relationship:

$$F_i = V_{Base} \frac{m_i \cdot \Delta_i^*}{\sum m_j \cdot \Delta_j^*} \qquad (A6.4)$$

where m_i e Δ_i^* are the mass and the generalized displacement of the i-th storey, respectively,.
The generalized displacement profile (Δ_i^*) is defined as:

$$\Delta_i^* = \phi_{1i} + a_2 \cdot \phi_{2i} + a_3 \cdot \phi_{3i} \qquad (A6.5)$$

where ϕ_{1i}, ϕ_{2i} and ϕ_{3i} represent the first three modal shapes of the BI-building, which can be evaluated for frame structures with the following approximated expressions:

$$\phi_{1i} = cos\left[\left(\frac{1}{I_r}\right) \cdot \left(1 - \frac{i}{N}\right) \cdot \frac{\pi}{2}\right] \qquad (A6.6)$$

$$\phi_{ji} = cos\left[(2N-2) \cdot \frac{\pi}{2} \cdot \frac{i}{N}\right] \quad j \geq 2 \qquad (A6.7)$$

where $I_r = T_{IS}/T_{fb}$ is the actual isolation ratio of the BI-building and N the number of storeys.
The coefficients a_2 and a_3 are defined by the following relationships:

$$a_2 = m \cdot NL^p \cdot (I_r)^q \qquad (A6.8)$$

$$a_3 = A \cdot a_2^2 + B \cdot a_2 \qquad (A6.9)$$

The values of the parameters m, NL, p, q, A and B depend on the type of the isolation system utilized and its basic mechanical characteristics, as described in the next paragraphs.

COMMENTARY

CA6.1.2 The proposed relationships are valid for regular framed buildings of eight storeys or less, equipped with bilinear isolation systems characterised by post-yield stiffness ratios lower than 25%. The form of the bi-linear system considered is shown in Fig. CA6.1.
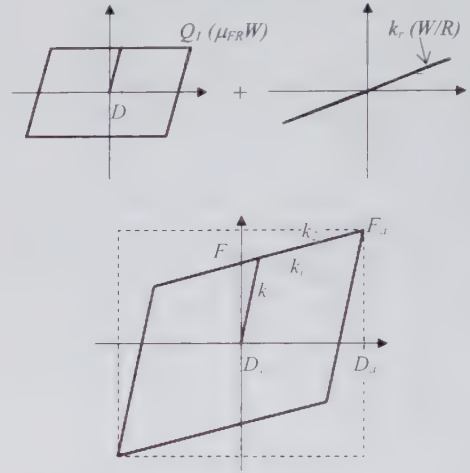

Fig. CA6.1: Bilinear hysteretic model of an isolation system.

The fundamental period of vibration of the fixed-base building (T_{fb}) can be evaluated for use in Eq.(A6.6) with the approximate relationship provided by EC8 (par. 4.3.3.2.2 – Eq.4.6):

$$T_{fb} = C_t \cdot H^{3/4} \qquad (CA6.1)$$

where $C_t = 0.075$ for RC frame buildings and H is the total height of the building (in meters).

The bilinear model (see Fig. A6.1) can be used to describe the cyclic behaviour of several currently used isolation systems, including: (i) Lead-Rubber Bearings (LRB), (ii) Friction Pendulum Bearings (FPB), (iii) Combinations of Flat Sliding Bearings (FSB) and Low-Damping Rubber Bearings (LDRB) (SB+LDRB) and occasionally (in an approximate fashion) (iv) High-Damping Rubber Bearings (HDRB).

ANNEX 6

(i) LRB/HDRB isolation systems

For LRB/HDRB IS's, the NL-factor can be expressed as:

$$NL = \frac{(r-1)\cdot(1-r)}{\mu\cdot[1+r\cdot(\mu-1)]} \qquad (A6.10)$$

where $r = k_2/k_1$ is the post-yielding stiffness ratio and $\mu = D_d/D_y$ the ductility demand on the isolation device at the design displacement.

The parameter m of Eq. (A6.8) shall be computed by the relationships reported in Table A4.3 as a function of the period ratio T_1/T_{fb} and the number of storey of the building (N).

For values of N and T_1/T_{fb} between those considered in Table A6.3 a linear interpolation can be performed.

Table A6.3: Variability of m with number of storeys (N) and T_1/T_{fb}

Storeys	m
$N = 3$	$0.3 - 0.1\ T_1/T_{fb}$ (for $T_1/T_{fb} < 3.0$)
$N = 5$	$0.7 - 0.3\ T_1/T_{fb}$ (for $T_1/T_{fb} < 2.3$)
$N = 8$	$1.0 - 0.5\ T_1/T_{fb}$ (for $T_1/T_{fb} < 2.0$)

The parameters p, q, A e B of Eqs. (A6.8)-(A6.9) can be assumed constant and equal to: $p = 2.5$, $q = 1.5$, $A = 0$ and $B = 0.7$, respectively.

For $NL < 0.15$, both a_2 and a_3 (see Eq. (A6.5)) can be taken equal to zero.

COMMENTARY

The bilinear model exhibits a high stiffness (k_1) before yielding/sliding ($D < D_y$) and a lower stiffness (k_2) during yielding/sliding ($D > D_y$). The ratios $r = k_2/k_1$ and $\mu = D_d/D_y$ are the post-yield stiffness ratio and the design ductility ratio of the IS, respectively.

The NL-factor measures the degree of non-linearity of the IS. It is defined as the ratio of the area of the hysteresis loops (W_d) at the IS design displacement (D_d) to that of the corresponding rectangle:

$$NL = \frac{W_d}{4\cdot D_d \cdot F_d} \qquad (CA6.2)$$

F_d being the IS force at the design displacement D_d. The general expression of the NL factor given in Eq.(CA6.2) shall be specialized to each IS type.

The fundamental period of vibration of regular framed buildings in the fixed-base configuration (T_{fb}) can be evaluated with Eq. (CA.6.1).

The yield displacement (D_y) of LRB IS's typically results between 5mm and 20mm (Skinner et al. 1993). For HDRB IS's, the yield displacement can be conventionally assumed in the range 20-35mm (Naeim and Kelly 1999). The typical values of the post-yielding stiffness ratio of LRB IS's are between 5% and 15% (Skinner et al. 1993). For HDRB IS's, the post-yielding stiffness ratio results in the order of 15%-25% (Naeim and Kelly 1999).

The period T_1 corresponds to the period of vibration of a SDOF system, with lumped mass equal to the total mass of the building and stiffness equal to initial stiffness (k_1) of the bilinear IS.

The equations of Table A6.3 are valid for bilinear IS's with $0.15 \leq NL \leq 0.65$ and BI-buildings with $T_{IS}/T_{fb} \geq 2$ and $T_{IS} \leq 4$. The aforesaid values of NL are expected to cover the ranges of interest for elastomeric-based IS's. Typical values of NL are between 0.25 and 0.3 for HDRB IS's and between 0.3 and 0.47 for LRB IS's (Cardone et al., 2009b).

ANNEX 6

COMMENTARY

(ii) FPB/FSB+LDRB isolation systems

For FPB IS's, the NL-factor can be expressed as:

$$NL = \frac{\mu_{FR}}{\mu_{FR} + \dfrac{D_d}{R}} \qquad (A6.11)$$

in which μ_{FR} is the friction coefficient of the sliding bearings, R is the radius of curvature of FPB, D_d is the IS design displacement and W is the total weight of the superstructure.

For FSB+LDRB IS's, the NL-factor can be expressed as:

$$NL = \frac{\mu_{FR}}{\mu_{FR} + \dfrac{k_r \cdot D_d}{W}} \qquad (A6.12)$$

where k_r is the elastic stiffness of LDRB.

For the IS's under consideration, the parameter m of Eq. (A4.2.8) shall be computed as:

$$m = 0.08 \cdot N + 0.68 \qquad (A6.13)$$

where N is the number of storeys of the building.

For the IS's under consideration, the parameters p, q, A and B of Eq.s (A6.8)-(A6.9) can be assumed constant and equal to: $p = 1.5$, $q = 0.3$, $A = -0.5$ and $B = 0.1$, respectively.

A6.1.3 Isolation Systems with Flag-Shaped Hysteretic Response: For FSB+SMA IS's, the NL-factor can be expressed as:

$$NL = \frac{1}{1 + \dfrac{F_2^*}{\mu_{FR} \cdot W}} \qquad (A6.14)$$

where μ_{FR} is the friction coefficient of the sliding bearings, F_2^* is the force of the non-linear re-centring device (SMA) at the design displacement (D_d) and W is the total weight of the superstructure.

For NL<0.15, the isolation system exhibits a quasi-elastic behaviour. As a consequence the generalized displacement profile is very similar to the first modal shape of the structure.

The bilinear model (see Fig. CA6.1) used to describe the cyclic behaviour of FPB and FSB+LDRB IS's is characterised by yield displacements (D_y) lower than 5 mm and post-yielding stiffness ratio lower than 3%.

Typical values of the NL-factor for FPB IS's are in the range 0.16-0.4, in presence of lubricated steel-PTFE sliding interfaces (μ_{FR} = 2-5%), while in the range 0.4-0.5, in presence of pure steel-PTFE sliding interfaces (μ_{FR} = 10-12%).
For FSB+LDRB IS's, instead, the typical values of the NL-factor are between 0.24 and 0.47, as a function of the state of lubrication of the steel-PTFE interfaces (Cardone et al., 2009b).

CA6.1.3 The flag-shaped model (see Fig. CA6.2) used to describe the cyclic behaviour of FSB+SMA IS's is obtained by combining a rigid-plastic element (modelling the FSB's) with a non-linear elastic element (modelling the re-centring device) whose post-yielding stiffness results in the order of 3-5%.

ANNEX 6

For FSB+SMA isolation devices, the parameter m of Eq. (A6.8) shall be set based on the following expression:

$$m = 30.5 \cdot \left[2.35 - \left(\lambda_{IS} + 1 \right)^{1.15} \right]^{-2.75} \qquad (A6.15)$$

where λ_{IS} is a parameter measuring the supplemental re-centring capacity of the IS:

$$\lambda_{IS} = \frac{F_1^* - \mu_{FR} \cdot W}{F_1^* + \mu_{FR} \cdot W} \qquad (A6.16)$$

The force F_1^* in Eq.(A6.16) represents the activation force of the nonlinear re-centring device.

For the IS's under consideration, the parameters p, q, A and B of Eqs. (A6.8)-(A6.9) can be assumed constant and equal to: $p = 2.0$, $q = 0$, $A = 0$ and $B = 0.5$, respectively.
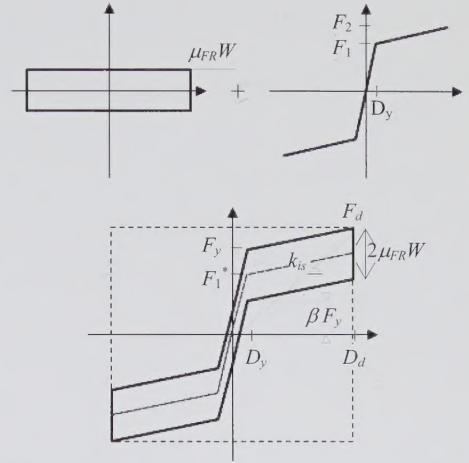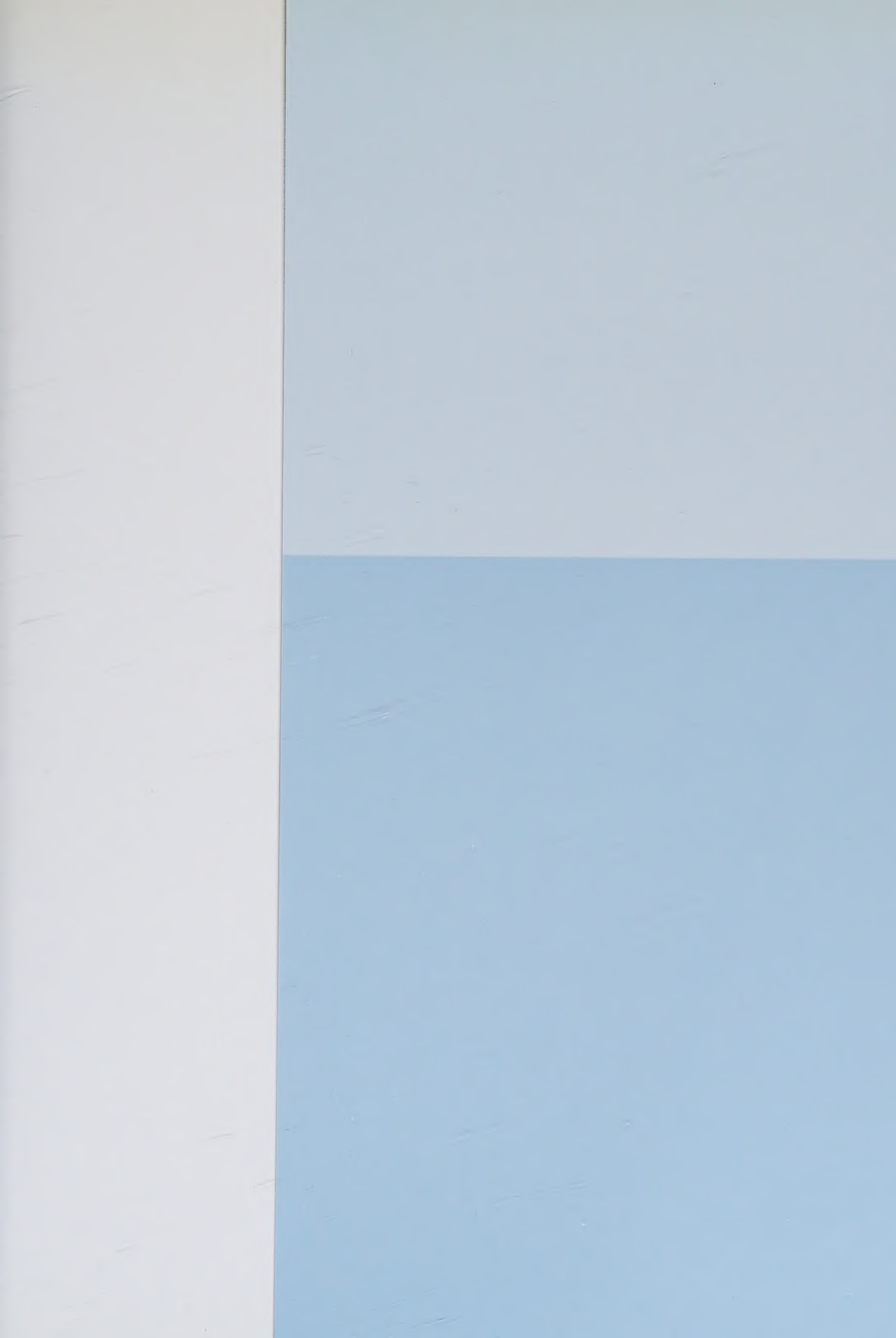
COMMENTARY

Fig. CA6.2: Flag-shaped hysteretic model of an isolation system.

Typical values of the NL-factor for FSB+SMA IS's are between 0.1 and 0.45 in the presence of lubricated steel-PTFE sliding interfaces ($\mu_{FR} = 2$-5%).

The expressions proposed for m, p, q, A and B are considered valid for $-0.6 < \lambda_{IS} < 0.6$.